TURUN YLIOPISTO
UNIVERSITY OF TURKU

Disrupting Immune Evasion and Metabolic Vulnerabilities in Myeloid Malignancies

A Therapeutic Perspective on Clever-1

Arno Ylitalo

TURUN YLIOPISTON JULKAISUJA – ANNALES UNIVERSITATIS TURKUENSIS
SARJA – SER. D OSA – TOM. 1973 | MEDICA – ODONTOLOGICA | TURKU 2026

TURUN
YLIOPISTO
UNIVERSITY
OF TURKU

DISRUPTING IMMUNE EVASION AND METABOLIC VULNERABILITIES IN MYELOID MALIGNANCIES

A Therapeutic Perspective on Clever-1

Arno Ylitalo

TURUN YLIOPISTON JULKAISUJA – ANNALES UNIVERSITATIS TURKUENSIS
SARJA – SER. D OSA – TOM. 1973 | MEDICA – ODONTOLOGICA | TURKU 2026

University of Turku

Faculty of Medicine
Institute of Biomedicine
Immunology
Turku Doctoral Programme of Molecular Medicine

Supervised by

Docent Maija Hollmén, PhD
MediCity Research Laboratory
Institute of Biomedicine
University of Turku
Turku, Finland

Academician Sirpa Jalkanen, MD, PhD
MediCity Research Laboratory
Institute of Biomedicine
University of Turku
Turku, Finland

Reviewed by

Mikko Myllymäki, MD, PhD
Institute for Molecular Medicine Finland (FIMM), University of Helsinki, Finland

Docent Markus Vähä-Koskela, PhD
Institute for Molecular Medicine Finland (FIMM), University of Helsinki, Finland

Opponent

Martin Jädersten, MD, PhD
Department of Hematology
Karolinska University Hospital
Karolinska Institutet
Stockholm, Sweden

The originality of this publication has been checked in accordance with the University of Turku quality assurance system using the Turnitin OriginalityCheck service.

Cover Image: Transmission electron microscopy image showing the ultrastructure of a cell from the KG-1 human acute myeloid leukemia cell line, Arno Ylitalo

ISBN 978-952-02-0703-8 (PRINT)
ISBN 978-952-02-0704-5 (PDF)
ISSN 0355-9483 (Print)
ISSN 2343-3213 (Online)
Painosalama, Turku, Finland 2026

To my grandfather, "Appa" Kale Juva, MD, PhD – my greatest inspiration

UNIVERSITY OF TURKU
Faculty of Medicine
Institute of Biomedicine
Immunology
ARNO YLITALO: Disrupting immune evasion and metabolic vulnerabilities in myeloid malignancies – A Therapeutic Perspective on Clever-1
Doctoral Dissertation, 195 pp.
Turku Doctoral Programme of Molecular Medicine
May 2026

ABSTRACT

Relapse and persistence remain major challenges in acute myeloid leukaemia (AML) and myelodysplastic syndromes (MDS). Malignant cells endure not only through clonal genetics but also through support from the marrow niche, where immune restraint and metabolic adaptation coexist. Mitochondrial respiration and lipid utilisation confer survival advantages under therapeutic stress, while intracellular trafficking links immune signalling to mitochondrial metabolism. Clever-1 (*STAB1*), a scavenger receptor expressed in immunoregulatory myeloid compartments, integrates these processes through endocytic–lysosomal routing.

In this PhD thesis, I examine whether Clever-1 functions solely as a niche-level immunoregulatory receptor or also contributes directly to leukaemic cell fitness through cargo routing, mitochondrial lipid handling and bioenergetic adaptation. I characterise Clever-1 expression across malignant myeloid compartments in AML and MDS, spanning immature progenitors and more differentiated myeloid populations, and relate its distribution to differentiation state and immune context. I then investigate cell-intrinsic consequences of Clever-1 targeting. The findings support a role for Clever-1 in endocytic trafficking to mitochondria and selective effects on respiratory organisation. Blockade alters lipoprotein-derived cargo routing, reshapes mitochondrial lipid composition, and reduces respiratory capacity under metabolic constraint, consistent with impaired adaptive flexibility rather than baseline cytotoxicity.

To bridge the mechanism with therapeutic relevance, I evaluate antibody-mediated Clever-1 blockade (bexmarilimab) in AML and MDS in *ex vivo* systems and in an early-phase clinical combination with azacitidine. In this setting, Clever-1 blockade is not primarily a direct cytotoxic therapy but rather a modulator of myeloid state, with target engagement and variable effects shaped by disease context and immune composition. Together, these findings identify Clever-1 as a state-linked trafficking receptor active in both immune and malignant compartments and help define the therapeutic role of Clever-1–directed strategies in AML and MDS.

KEYWORDS: acute myeloid leukaemia; myelodysplastic syndromes; Clever-1; endocytic trafficking; mitochondrial metabolism; immunotherapy

TURUN YLIOPISTO
Lääketieteellinen tiedekunta
Biolääketieteen laitos
Immunologia
ARNO YLITALO: Immuunivasteen vaimentuminen ja metabolinen alttius myelooisissa verisyövissä – Clever-1 terapeuttisesta näkökulmasta
Väitöskirja, 195 s.
Molekyylilääketieteen tohtoriohjelma (TuDMM)
Toukokuu 2026

TIIVISTELMÄ

Taudin uusiutuminen ja hoitoresistenssi ovat keskeisiä haasteita akuutissa myelooisessa leukemiassa (AML) ja myelodysplastisissa oireyhtymissä (MDS). Pahanlaatuiset solut säilyvät klonaalisen evoluution lisäksi luuytimen mikroympäristön tuella, jossa aineenvaihdunnallinen sopeutuminen ja immuunivasteen vaimeneminen limittyvät. Mitokondrioissa tapahtuva soluhengitys ja lipidien hyödyntäminen tarjoavat leukemiasoluille selviytymisedun hoitopaineen alla, ja solunsisäiset kuljetusreitit kytkevät immuunisäätelyn mitokondrioiden toimintaan. Clever-1 (*STAB1*) on immuunivastetta muokkaavissa myelooisissa soluissa ilmentyvä haaskareseptori, joka yhdistää nämä prosessit endosyyttisen kierron kautta.

Tässä väitöskirjassa tutkin, toimiiko Clever-1 yksinomaan mikroympäristön immuniteetin säätelijänä vai liittyykö se myös leukemiasolujen vastustuskykyyn kuljetusreittien, mitokondrioiden lipidikäsittelyn ja aineenvaihdunnallisen sopeutumisen kautta. Määritän sen ilmentymistä AML- ja MDS-potilaiden soluissa ja suhteutan havainnot taudin kliiniseen ja biologiseen taustaan sekä tutkin Clever-1:n kohdentamisen solunsisäisiä vaikutuksia leukemiasoluissa. Tulokset osoittavat, että Clever-1 osallistuu lipoproteiiniperäisen materiaalin reititykseen mitokondrioihin ja soluhengityksen säätelyyn osana aineenvaihdunnallista sopeutumista. Sen estäminen muuttaa kolesterolin solunsisäistä reititystä, muokkaa mitokondrioiden lipidikoostumusta ja heikentää hengityskapasiteettia aineenvaihdunnallisen kuormituksen aikana, mikä viittaa heikentyneeseen sopeutumiskykyyn eikä suoraan solunjakautumisen estoon.

Mekanismin kliinisen merkityksen arvioimiseksi tutkin myös vasta-ainevälitteistä Clever-1-estämistä AML:ssa ja MDS:ssa sekä *ex vivo* -kokeissa että varhaisvaiheen kliinisessä tutkimuksessa, jossa potilaat saivat yhdistelmähoitoa atsasitidiinin kanssa. Clever-1-estäminen ei näyttäydy ensisijaisesti sytotoksisena hoitona, vaan luuytimen immunologisen tilan kontekstiriippuvaisena säätelijänä. Tulokset osoittavat, että Clever-1 toimii sekä immuuni- että pahanlaatuisissa soluissa ja tarkentaa Clever-1-kohdennettujen hoitojen terapeuttista roolia AML:ssa ja MDS:ssa.

AVAINSANAT: akuutti myelooinen leukemia; myelodysplastiset oireyhtymät; Clever-1; endosyyttinen kuljetus; mitokondriaalinen aineenvaihdunta; immunoterapia

Table of Contents

Abbreviations

acLDL	acetylated low-density lipoprotein
AML	acute myeloid leukaemia
APC	antigen-presenting cell
AP-2	adaptor protein complex 2
ARG1	arginase 1
ASXL1	additional sex combs-like 1
ATAD3	ATPase family AAA domain-containing protein 3
ATP	adenosine triphosphate
BCL2	B-cell lymphoma 2
BEAT-AML	Beat Acute Myeloid Leukemia
BH3	BCL2 homology domain 3
BM	bone marrow
BN-PAGE	Blue Native polyacrylamide gel electrophoresis
CCL3	C-C motif chemokine ligand 3
CCUS	clonal cytopenia of undetermined significance
CD	cluster of differentiation
CD40L	CD40 ligand
CHIP	clonal haematopoiesis of indeterminate potential
CI-M6PR	cation-independent mannose-6-phosphate receptor
CMML	chronic myelomonocytic leukaemia
CO2	carbon dioxide
CPT1A	carnitine palmitoyltransferase 1A
CRAPome	contaminant repository for affinity purification
CXCL	C-X-C motif chemokine ligand
CXCR4	C-X-C motif chemokine receptor 4
DC	dendritic cell
DLT	dose-limiting toxicity
DNMT3A	DNA methyltransferase 3 alpha
EEA1	early endosome antigen 1
EGF	epidermal growth factor
ELISA	enzyme-linked immunosorbent assay

ELN	European LeukemiaNet
ER	endoplasmic reticulum
ETC	electron transport chain
EV	extracellular vesicle
FAB	French–American–British
FABP4	fatty acid-binding protein 4
FAO	fatty acid oxidation
Fc	fragment crystallisable region
FcγR	Fc gamma receptor
FDR	false discovery rate
FLT3	FMS-like tyrosine kinase 3
FoxP3	forkhead box P3
FP-1305	bexmarilimab
FPKM	fragments per kilobase of transcript per million mapped reads
FPKM-UQ	fragments per kilobase of transcript per million mapped reads upper quartile normalised
GAPDH	glyceraldehyde-3-phosphate dehydrogenase
GGA	Golgi-localised γ-ear–containing ARF-binding protein
GM-CSF	granulocyte–macrophage colony-stimulating factor
GSEA	gene set enrichment analysis
HLA	human leukocyte antigen
HMA	hypomethylating agent
HSC	haematopoietic stem cell
HSPC	haematopoietic stem and progenitor cell
IDO1	indoleamine 2,3-dioxygenase 1
IDH	isocitrate dehydrogenase
IFN-γ	interferon gamma
IGF2R	insulin-like growth factor 2 receptor
IgG	immunoglobulin G
IKK	inhibitor of nuclear factor kappa-B kinase
IL	interleukin
IMDM	Iscove's modified Dulbecco's medium
IMPDH2	inosine monophosphate dehydrogenase 2
IP	immunoprecipitation
ITIM	immunoreceptor tyrosine-based inhibitory motif
KG-1	human acute myeloid leukaemia cell line
KMT2A	lysine methyltransferase 2A
LAG-3	lymphocyte activation gene 3

LAMP-1	lysosome-associated membrane protein 1
LC3	microtubule-associated protein 1 light chain 3
LDL	low-density lipoprotein
LSC	leukaemic stem cell
M-CSF	macrophage colony-stimulating factor
MDA-LDL	malondialdehyde-modified low-density lipoprotein
MDS	myelodysplastic syndromes
MDSC	myeloid-derived suppressor cell
MECOM	MDS1 and EVI1 complex locus
MHC	major histocompatibility complex
MPP	multipotent progenitor
mGSH	mitochondrial glutathione
NCI-CTCAE	National Cancer Institute Common Terminology Criteria for Adverse Events
NCT	National Clinical Trial identifier
NF- κB	nuclear factor kappa B
NK	natural killer
NPM1	nucleophosmin 1
NPC	Niemann–Pick disease type C protein
OCR	oxygen consumption rate
OCI-AML2	human acute myeloid leukaemia cell line
ORR	objective response rate
OS	overall survival
OXPHOS	oxidative phosphorylation
PAGE	polyacrylamide gel electrophoresis
PD-1	programmed cell death protein 1
PD-L1	programmed death-ligand 1
PDI	protein disulfide isomerase
PI3K	phosphatidylinositol-3-kinase
Rab	Ras-related in brain (small GTPase family)
RNA	ribonucleic acid
RPKM	reads per kilobase of transcript per million mapped reads
ROS	reactive oxygen species
RPMI	Roswell Park Memorial Institute medium
RP2D	recommended phase II dose
RUNX1	runt-related transcription factor 1
SCAP	SREBP cleavage-activating protein
SDS	sodium dodecyl sulphate
SF3B1	splicing factor 3b subunit 1

SHP	Src homology 2 domain-containing phosphatase
Siglec	sialic acid-binding immunoglobulin-like lectin
SIRPα	signal-regulatory protein alpha
SLC25A10	solute carrier family 25 member 10
SNX17	sorting nexin 17
SPARC	secreted protein acidic and rich in cysteine
SREBF	sterol regulatory element-binding transcription factor
SRSF2	serine and arginine-rich splicing factor 2
STAT3	signal transducer and activator of transcription 3
STARD4	StAR-related lipid transfer domain containing 4
STING	stimulator of interferon genes
TCGA-LAML	The Cancer Genome Atlas Acute Myeloid Leukae-mia
TCA	tricarboxylic acid
TEAE	treatment-emergent adverse event
TET2	ten–eleven translocation 2
TF-1	human erythroleukaemia cell line
TGF-β	transforming growth factor beta
THP-1	human monocytic cell line
TIGIT	T-cell immunoreceptor with Ig and ITIM domains
TIM	T-cell immunoglobulin and mucin-domain con-taining
TLR	toll-like receptor
TNF-α	tumour necrosis factor alpha
TOM22	translocase of outer mitochondrial membrane 22
TP53	tumour protein p53
TREM2	triggering receptor expressed on my-eloid cells 2
Treg	regulatory T cell
U2AF1	U2 small nuclear RNA auxiliary factor 1
UHPLC–MS/MS	ultra-high-performance liquid chromatography–tandem mass spectrometry
VAF	variant allele frequency
v-ATPase	vacuolar H+-ATPase
VISTA	V-domain Ig suppressor of T-cell activation

List of Original Publications

This dissertation is based on the following original publications, which are referred to in the text by their Roman numerals:

I Aakko S, **Ylitalo A**, Kuusanmäki H, Rannikko JH, Björkman M, Mandelin J, Heckman CA, Kontro M, Hollmén M. CLEVER-1 targeting antibody, bexmarilimab, supports HLA-DR expression and alters *ex vivo* responsiveness to azacitidine and venetoclax in myeloid malignancies. *Scientific Reports*. 2025;15:16775. https://doi.org/10.1038/s41598-025-01675-y

II Kontro M, Stein AS, Pyörälä M, Rimpiläinen J, Siitonen T, **Ylitalo A**, Fjällskog M-L, Jalkanen J, Aakko S, Pawlitzky I, Hollmén M*, Daver N*. Bexmarilimab plus azacitidine for high-risk myelodysplastic syndrome and relapsed or refractory acute myeloid leukaemia: results from the dose-escalation part of a multicentre, single-arm, phase ½ trial. *The Lancet Haematology*. 2025;12:e516–e528. https://doi.org/10.1016/S2352-3026(25)00103-6

III **Ylitalo A**, Mickos J, Hakoniemi M, Turpin R, Prince S, Hollmén M. Clever-1 blockade disrupts lipid metabolism and mitochondrial fitness in acute myeloid leukemia. Submitted manuscript, 2026.

1 Introduction

Haematopoiesis is a lifelong regenerative process that sustains oxygen transport, immune defence, and tissue repair. Within the bone marrow, a hierarchically organised system balances stem-cell self-renewal with lineage commitment and differentiation according to systemic demand (Pinho and Frenette, 2019; Comazzetto et al., 2021). This equilibrium requires tight regulation, as excessive proliferation or insufficient renewal compromises functional output. In acute myeloid leukaemia (AML) and myelodysplastic syndromes (MDS), this balance is disrupted as progenitor populations acquire clonal advantage while failing to mature appropriately, leading to impaired blood cell production and persistent disease (Steensma et al., 2015). These disorders therefore develop within existing haematopoietic organisation rather than outside it, and their biology must be considered not only through genetic lesions but also in relation to the marrow environment in which malignant cells persist (Bonnet & Dick, 1997; Shafat et al., 2017).

Despite advances in classification and therapy, relapse and disease persistence remain defining challenges in AML and MDS (Döhner et al., 2017; Hellström-Lindberg & Kröger, 2023). Although remission may be achieved, durable control is often limited by residual malignant populations that survive therapeutic pressure and reemerge (Schuurhuis et al., 2018; Shlush et al., 2017). Recurrent genetic lesions have clarified important aspects of disease biology, but they do not fully explain how malignant cells endure cytotoxic, epigenetic, or immune-mediated stress (Mulherkar & Scadden, 2021; Tettamanti et al., 2022). Durable control therefore depends on factors beyond clone genetics, including both intrinsic properties of malignant cells and the local conditions that sustain them (Mian et al., 2025).

Within the bone marrow, malignant cells remain embedded in a structured niche in which spatial organisation and intercellular signalling influence both immune engagement and metabolic adaptation (Bandyopadhyay et al., 2024; Mian et al., 2025). A prominent feature of this environment is macrophage-dominant regulation, as myeloid-lineage cells shape antigen handling and inflammatory tone and thereby influence the balance between activation and restraint. In AML and MDS, immune dysfunction is not confined to a single compartment but involves coordinated alterations across myeloid and lymphoid populations. The marrow microenvironment may therefore favour restraint over activation and limit immune clearance in ways that

are shaped by differentiation state and prior therapy (Barakos & Hatzimichael, 2022; Maynard et al., 2022; de Jong et al., 2024).

A notable feature of AML and MDS is that the malignant clone arises from the same myeloid lineage responsible for immune regulation. This overlap makes regulatory and malignant programmes difficult to separate, as pathways associated with the microenvironment may also remain active within malignant progenitors or their progeny. Myeloid-directed mechanisms therefore cannot be assumed to act exclusively through non-malignant cells and may support persistence while also restraining immune clearance (Khaldoyanidi et al., 2021; Tettamanti et al., 2022; Bachmann & Ochsenbein, 2025). It remains unclear whether these mechanisms operate solely at the niche level or also influence leukaemic cell–intrinsic behaviour, and this distinction has therapeutic implications.

Persistence is also shaped by metabolic state. Leukaemic stem and progenitor populations frequently depend on mitochondrial oxidative phosphorylation in a state-dependent manner, particularly under therapeutic or environmental stress. This oxidative metabolism can adjust in response to niche-derived cues and thereby support survival under constraint (Moschoi et al., 2016; Farge et al., 2017). Selection for such bioenergetic states may contribute to relapse (Farge et al., 2017). This dependence positions mitochondrial fitness as a potential vulnerability in myeloid malignancy (Lagadinou et al., 2013; Pollyea et al., 2018).

This metabolic dependence is closely linked to lipid handling. Fatty acids provide substrate for oxidative phosphorylation, while cholesterol trafficking influences membrane composition and mitochondrial redox balance (Mishra et al., 2023; Goicoechea et al., 2023). Altered lipid availability may stabilise stress-adapted phenotypes in both malignant and immune compartments (Mishra et al., 2023; Veglia et al., 2019). Lipid utilisation and cholesterol routing thereby link immune regulation with bioenergetic state in myeloid malignancy (Maynard et al., 2022; Li et al., 2021).

These processes also depend on intracellular routing. Endocytic–lysosomal trafficking links antigen processing with metabolic regulation by determining whether internalised material is degraded, recycled, or redistributed. Through this sorting function, trafficking influences immune priming thresholds as well as mitochondrial substrate availability. Perturbations in this machinery may alter immune tone and metabolic adaptability, drawing attention to receptors that connect immune restraint with mitochondrial function (Roche & Furuta, 2015; Settembre et al., 2013; Ledderose et al., 2021).

Clever-1, also known as stabilin-1 (*STAB1*), is a scavenger receptor expressed on subsets of macrophages and endothelial cells and participates in endocytic trafficking of modified lipoproteins and related cargo. Through its role in cargo routing and lysosomal processing, it links antigen handling with lipid redistribution in myeloid

biology (Kzhyshkowska et al., 2010; Zhang et al ., 2009). In malignant diseases of the bone marrow, where immune restraint and metabolic adaptation coexist, such a receptor may influence both immune activity and mitochondrial fitness (Virtakoivu et al., 2021). Whether Clever-1 functions exclusively within non-malignant myeloid compartments or also contributes directly to leukaemic cell–intrinsic biology remains unresolved.

Modulation of Clever-1 in AML and MDS therefore not determined by target expression alone. Functional consequences are likely to depend on differentiation state, immune context, and prior or concurrent therapy. Combination treatment may reshape immune tone and cellular state, thereby altering the setting in which intervention occurs (Vago & Gojo, 2020; Ciantra et al., 2025). In addition, receptor engagement may not correlate directly with baseline surface abundance, given receptor cycling and intracellular pools (Prevo et al., 2004; Kzhyshkowska et al., 2006). Antibody-mediated blockade of Clever-1 should therefore be understood as an intervention whose effects depend on myeloid state, intracellular trafficking, and the therapeutic context in which it is given (Kzhyshkowska et al., 2010; Virtakoivu et al., 2021).

These considerations frame the focus of this thesis. This work examines Clever-1 across immune and malignant compartments in AML and MDS, beginning with its expression patterns and disease associations in relation to differentiation state and immune context within the marrow niche. It evaluates Clever-1 blockade in a therapeutically conditioned setting, recognising that intervention occurs in tissue already shaped by prior and concurrent therapy, and defines leukaemic cell–intrinsic functions with emphasis on intracellular trafficking pathways intersecting with mitochondrial lipid handling and cholesterol-dependent bioenergetic adaptation. Together, these studies link mechanistic investigation with clinical evaluation and place Clever-1 within a broader framework of immune regulation and metabolic adaptation in myeloid malignancy.

.

2 Review of the Literature

2.1 Haematopoietic organisation and disruption in myeloid malignancies

2.1.1 Normal haematopoiesis and marrow cell production

At the apex of the haematopoietic system is a rare population of haematopoietic stem cells (HSCs), with long-term self-renewal capacity and the ability to generate all major blood lineages (Orkin & Zon, 2008). Through progressive differentiation, HSCs give rise to multipotent progenitors (MPPs), which gradually lose self-renewal potential while retaining multilineage differentiation capacity. Subsequent lineage commitment produces progenitors increasingly restricted towards myeloid or lymphoid fates (Pellin et al., 2019; Jacobsen & Nerlov, 2019).

This hierarchy is often depicted as a branching structure in which differentiation potential narrows stepwise (Figure 1A). Single-cell analyses have refined lineage models and demonstrated heterogeneity within immunophenotypically defined compartments; however, the central concept remains that stem and progenitor cells generate mature effector populations through regulated and progressively restricted differentiation (Pellin et al., 2019; Zeng et al., 2025). However, recent lineage-tracing data in mice suggest that, during ageing, platelet production can also arise through a direct HSC-derived pathway that bypasses aspects of the canonical hierarchy (Poscablo et al., 2024). Disruption at defined developmental stages can translate into distinct clinical phenotypes.

The myeloid branch produces several functionally distinct cell types. Erythroid progenitors mature into erythrocytes, which circulate for approximately 120 days and mediate oxygen delivery. Megakaryocytic progenitors generate platelets, anucleate fragments essential for haemostasis and vascular repair. Granulocytic progenitors give rise to neutrophils, the most abundant circulating innate immune cells, providing rapid antimicrobial defence. Monocytic progenitors generate monocytes that circulate transiently before differentiating into macrophages or dendritic cells in tissues. These mononuclear phagocytes contribute to antigen presentation, immune regulation, and tissue homeostasis (Pishesha et al., 2022; Mosser & Edwards, 2008).

The lymphoid branch produces B lymphocytes, T lymphocytes, and natural killer (NK) cells. B cells differentiate into antibody-secreting plasma cells; T cells mediate antigen-specific cellular immunity; and NK cells provide rapid cytotoxic responses against infected or transformed cells. Although frequently described separately, effective immune defence depends on coordinated interaction between myeloid and lymphoid compartments.

Production demands vary according to physiological state. Under steady conditions, output is tightly regulated to match need while limiting excessive proliferation. During infection, bleeding, or other systemic stress, lineage output can shift rapidly. Pro-inflammatory signals and growth factors alter progenitor proliferation and differentiation to increase generation of selected effector populations, a process often referred to as “emergency haematopoiesis” (Passegué et al., 2015; Leimkühler & Schneider, 2019). Following resolution of stress, regulatory mechanisms restore balanced production. The capacity to transition between quiescence, steady-state output, and stress-adapted expansion underlies the resilience of the haematopoietic system (Kokkaliaris & Scadden, 2020; Ciantra et al., 2025).

These processes occur within a structured bone marrow microenvironment. HSCs and progenitors interact with stromal, endothelial, osteolineage, and immune elements that regulate quiescence, proliferation, retention, and differentiation (Hurwitz et al., 2020; Chen et al., 2020; Kim et al., 2020). Current models describe a distributed regulatory network rather than control by a single cell type, with vascular and osteolineage-associated structures frequently highlighted. Marrow macrophages and related immune populations contribute to both steady-state and stress-adapted haematopoiesis, indicating close linkage between blood formation and immune regulation under physiological conditions (Lévesque et al., 2021; de Jong et al., 2024).

The organisation of normal haematopoiesis clarifies the clinical manifestations of myeloid malignancies. Because erythrocytes, platelets and granulocytes arise from this hierarchy, disruption of differentiation commonly results in cytopenias such as anaemia, thrombocytopenia, and neutropenia (Figure 1B). Impairment of granulocytic and monocytic compartments compromises innate immune defence. Somatic alterations affecting HSCs or early progenitors may be carried through multiple downstream lineages. Myeloid malignancies therefore present as disorders of dysregulated blood formation rather than isolated expansions of a single mature cell type (Khwaja et al., 2016; Arber et al., 2022).

A

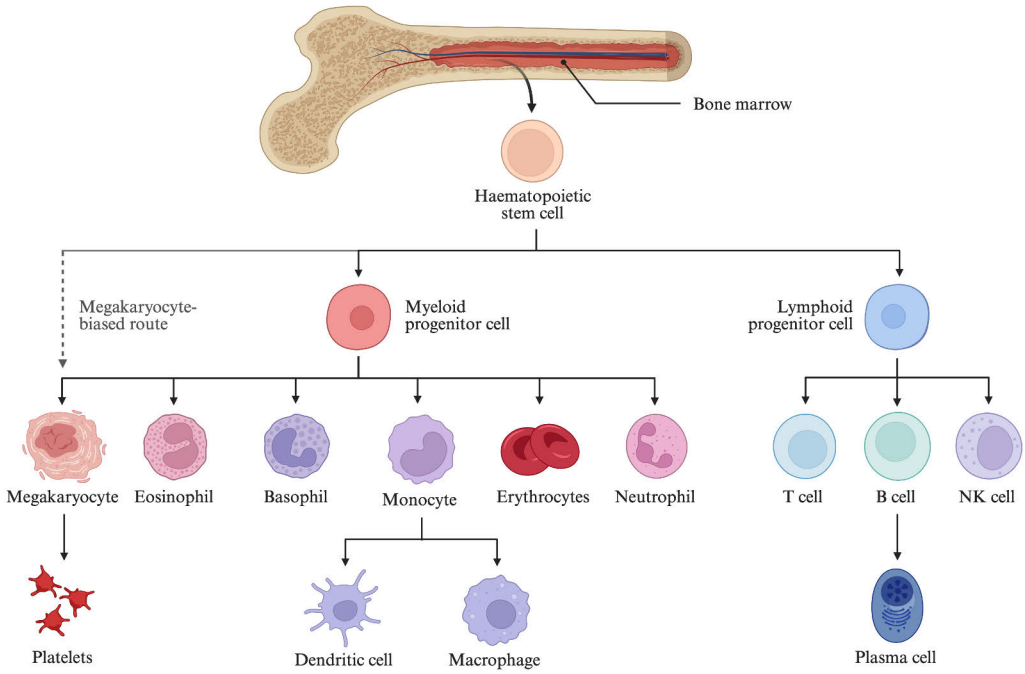
Bone marrow
Haematopoietic stem cell
Megakaryocyte-biased route
Myeloid progenitor cell
Lymphoid progenitor cell
Megakaryocyte
Eosinophil
Basophil
Monocyte
Erythrocytes
Neutrophil
T cell
B cell
NK cell
Platelets
Dendritic cell
Macrophage
Plasma cell

B

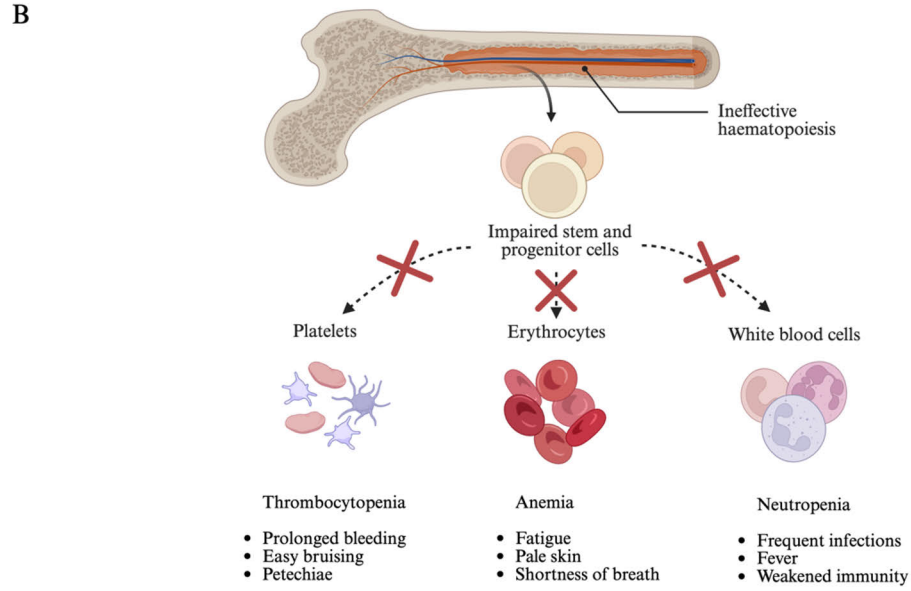
Ineffective haematopoiesis
Impaired stem and progenitor cells
Platelets
Erythrocytes
White blood cells
Thrombocytopenia
• Prolonged bleeding
• Easy bruising
• Petechiae
Anemia
• Fatigue
• Pale skin
• Shortness of breath
Neutropenia
• Frequent infections
• Fever
• Weakened immunity

Figure 1. Organisation of normal haematopoiesis and clinical consequences of its disruption. (A) Schematic representation of adult bone marrow haematopoiesis. Haematopoietic stem cells (HSCs) reside within the marrow and give rise to multipotent progenitors that progressively restrict lineage potential through hierarchical differentiation. The myeloid branch generates erythrocytes, megakaryocytes and platelets, granulocytes, and monocytes (which further differentiate into macrophages and dendritic cells), whereas the lymphoid branch produces B cells, T cells, and natural killer (NK) cells. In addition to the conventional hierarchical pathway, the dashed arrow denotes an early megakaryocyte-biased differentiation route from the haematopoietic stem and progenitor cell compartment. Continuous and tightly regulated lineage output maintains oxygen transport, haemostasis, and immune defence. **(B)** Conceptual illustration of disrupted or ineffective haematopoiesis. Impairment at the level of haematopoietic stem and progenitor cells reduces effective lineage output, resulting in peripheral cytopenias. Decreased erythrocyte production manifests clinically as anaemia; reduced neutrophil production increases susceptibility to infection (neutropenia); and diminished platelet production leads to bleeding tendency (thrombocytopenia). Together, these features characterise myeloid malignancies as disorders of dysregulated blood formation rather than isolated expansion of a single mature cell population. (Illustrations A and B created with BioRender).

Long-term haematopoietic durability depends on genomic integrity and balanced regulatory input within stem and progenitor compartments (Shih et al., 2012; Hunter and Padron, 2021). With ageing, the haematopoietic stem cell compartment undergoes functional attrition, including reduced regenerative capacity and diminished clonal diversity, even as the phenotypic HSC pool may expand (Verovskaya et al., 2019; Symeonidi et al., 2022). With advancing age, cumulative replication, environmental exposure, and inflammatory signalling increase the probability that somatic variants arise in haematopoietic stem and progenitor cells. Many variants remain functionally neutral, whereas others confer a competitive advantage, enabling gradual clonal expansion within otherwise preserved haematopoiesis (Mitchell et al., 2022; Robertson et al., 2022). When such clones are detectable in individuals without overt haematologic malignancy, this state is broadly referred to as clonal haematopoiesis. When mutations in haematologic malignancy-associated genes are present at a variant allele frequency of at least 2% in individuals without diagnostic cytopenias or morphological criteria for a myeloid neoplasm, the condition is termed clonal haematopoiesis of indeterminate potential (CHIP) (Genovese et al., 2014; Jaiswal et al., 2014; Steensma et al., 2015). When persistent unexplained cytopenias coexist with clonal mutations but without definitive features of a myeloid neoplasm, the condition is designated clonal cytopenia of undetermined significance (CCUS) (Valent et al., 2018; Taborda et al., 2024). These premalignant states illustrate that clonal dominance may precede overt malignancy and provide a biological bridge to myeloid neoplasia. The stepwise relationship between age-associated clonal haematopoiesis, molecular evolution, and overt myeloid malignancy is summarised schematically in Figure 2 (Chandra et al., 2024).

Figure 2. Stepwise clonal evolution from normal haematopoiesis to overt myeloid malignancy. Normal polyclonal haematopoiesis may acquire somatic mutations at the level of haematopoietic stem and progenitor cells (HSC/HSPC), leading to clonal haematopoiesis of indeterminate potential (CHIP). Further clonal expansion associated with impaired effective blood production can result in clonal cytopenia of undetermined significance (CCUS). Accumulation of additional transforming events gives rise to overt myeloid neoplasms, represented here by myelodysplastic syndromes (MDS), chronic myelomonocytic leukaemia (CMML), and acute myeloid leukaemia (AML). Early lesions frequently involve epigenetic regulators and RNA-splicing factors. Acquisition of additional transforming lesions affecting signalling pathways, transcription factors, or tumour suppressors is associated with progression to overt malignancy (Sperling et al., 2017). Increasing genomic instability accompanies this transition. Overt myeloid neoplasms consist of genetically distinct subclones derived from a common ancestral clone. Therapeutic pressure promotes selective expansion of resistant subclones, contributing to relapse. The lower gradient indicates increasing clinical impact, including cytopenias and disease-related symptoms, across progression. (Illustration created with BioRender).

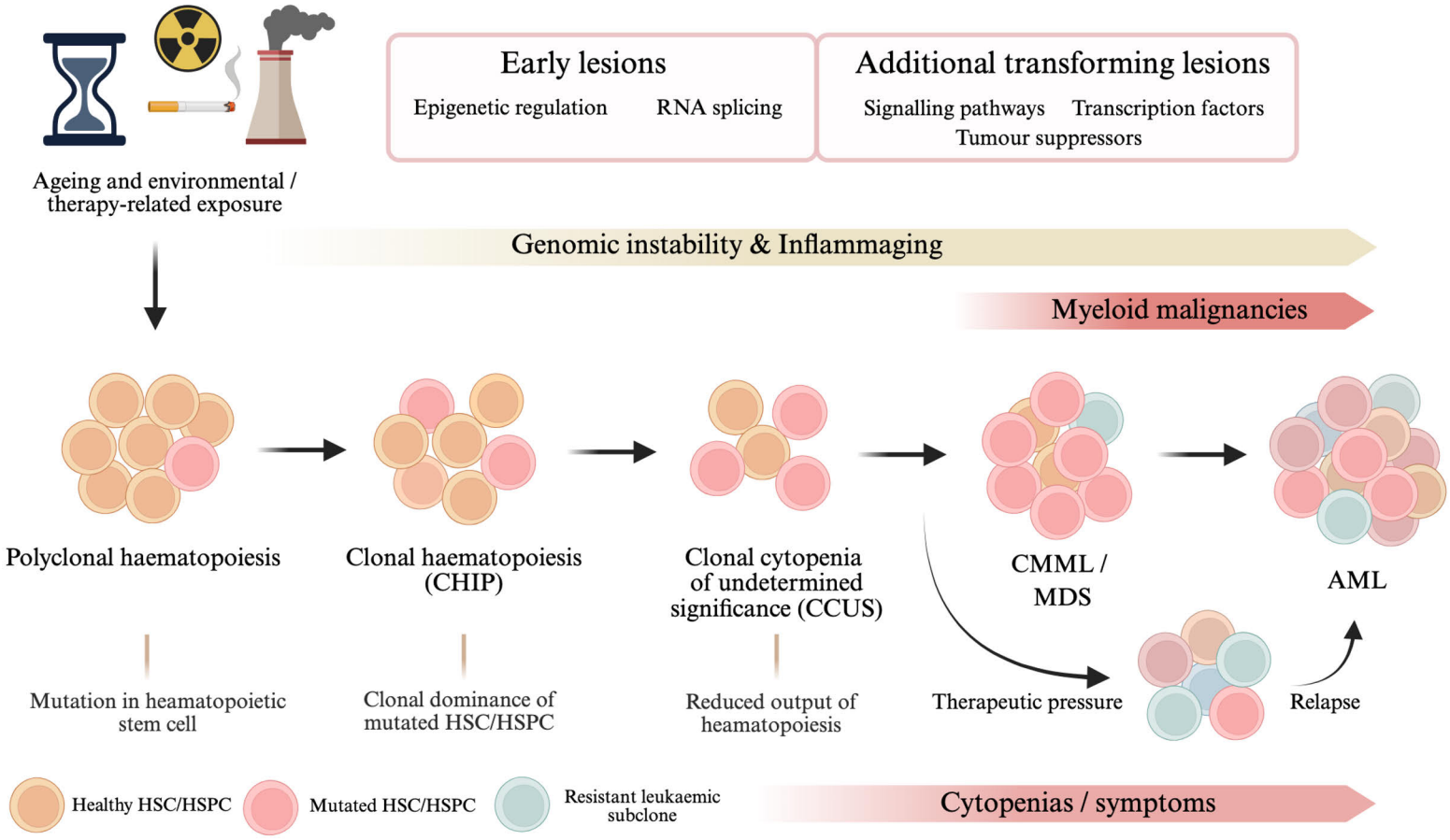
Early lesions
Epigenetic regulation
RNA splicing
Additional transforming lesions
Signalling pathways
Transcription factors
Tumour suppressors
Ageing and environmental / therapy-related exposure
Genomic instability & Inflammaging
Myeloid malignancies
Polyclonal haematopoiesis
Clonal haematopoiesis (CHIP)
Clonal cytopenia of undetermined significance (CCUS)
CMML / MDS
AML
Mutation in heamatopoietic stem cell
Clonal dominance of mutated HSC/HSPC
Reduced output of heamatopoiesis
Therapeutic pressure
Relapse
Healthy HSC/HSPC
Mutated HSC/HSPC
Resistant leukaemic subclone
Cytopenias / symptoms

2.1.2 Myeloid malignancies as disorders of dysregulated haematopoiesis

Myeloid malignancies comprise a broader group of clonal disorders arising from haematopoietic stem and progenitor cells, including AML, MDS, CMML, and myeloproliferative neoplasms (MPNs) such as polycythaemia vera, essential thrombocythaemia, and primary myelofibrosis (Arber et al., 2022). Among these, AML, MDS, and CMML form a biologically related spectrum of myeloid neoplasms characterised predominantly by disrupted differentiation and ineffective haematopoiesis (Figure 2). Although classified as distinct entities, they share key features: recurrent somatic alterations, abnormal differentiation, competitive expansion of malignant clones within the marrow, and suppression of effective blood formation (Adès et al., 2014; DeZern, 2018; Döhner et al., 2022). In these disorders, the marrow serves as a shared regenerative system in Ih malignant and non-malignant populations coexist and compete, shaping clinical manifestations and contributing to persistence of treatment-tolerant clones (Kokkaliaris & Scadden, 2020; Mulherkar & Scadden, 2021).

MDS is characterised primarily by ineffective haematopoiesis, with cytopenias developing despite typically normo- or hypercellular marrow. Morphological dysplasia and variable risk of progression to AML are central features (Adès et al., 2014; Malcovati et al., 2023). Clinical behaviour ranges from relatively indolent cytopenic states to progressive marrow failure and transformation to AML. Contemporary risk models integrate clinical and biological variables to reflect this heterogeneity (Bernard et al., 2022; DeZern, 2018).

AML represents a more advanced failure of haematopoietic regulation. It is characterised by expansion of immature myeloid blasts accompanied by suppression of normal lineage output (Döhner et al., 2022; Newell & Cook, 2023). Clinical consequences reflect both loss of normal marrow function and complications related to blast accumulation. Although remission can be achieved in defined patient subsets, relapse remains frequent (Döhner et al., 2017; Döhner et al., 2022).

CMML occupies an intermediate position, combining dysplastic and proliferative features. It is characterised by persistent monocytosis with variable cytopenias and splenomegaly, and may present either with ineffective haematopoiesis resembling MDS or with a more proliferative myeloid phenotype accompanied by inflammatory features (Patnaik & Tefferi, 2018; Tremblay et al., 2021).

AML, MDS, and CMML are predominantly diseases of older adults, and their clinical burden is shaped by cytopenias, repeated diagnostic assessment, prolonged supportive care, and treatment-related complications. Incidence

increases markedly after the sixth decade of life, with median age at diagnosis typically around 70 years in AML and MDS (Woolthuis & Park, 2016; Zeidan et al., 2019; Döhner et al., 2022; Malcovati et al., 2023). This age dependence is consistent with the cumulative acquisition and selection of somatic alterations within long-lived haematopoietic stem and progenitor compartments, as outlined above (Genovese et al., 2014; Jaiswal et al., 2014; Ogawa, 2019). Additional environmental and iatrogenic exposures, including benzene, ionising radiation, tobacco use, and prior cytotoxic therapy, may further contribute to disease risk, particularly in therapy-related AML and MDS (McNerney et al., 2017; Zeidan et al., 2019). Thus, these myeloid neoplasms arise through interaction between age-associated biological vulnerability, clonal evolution, and external or treatment-related insults.

2.1.3 Recurrently perturbed pathways and founder lesions

Recurrent mutations in myeloid neoplasms cluster in defined functional domains, particularly epigenetic regulation, transcriptional control, RNA splicing, and signal transduction (Bejar et al., 2011; Sperling et al., 2016; Döhner et al., 2022). In AML, frequently altered genes include *FLT3*, *NPM1*, *DNMT3A*, *IDH1/2*, and *RUNX1* (Sperling et al., 2016; Döhner et al., 2022). In MDS and CMML, alterations in *DNMT3A*, *TET2*, *ASXL1*, and spliceosome components such as *SF3B1*, *SRSF2*, and *U2AF1* are common and often detected early in clonal evolution (Papaemmanuil et al., 2016; Sperling et al., 2016; Huber et al., 2022).

Chromosomal alterations are likewise common and biologically consequential in myeloid malignancies. Recurrent cytogenetic abnormalities include complex karyotype, monosomy 5 or del(5q), monosomy 7 or del(7q), trisomy 8, and rearrangements involving *KMT2A*, *MECOM*, or core-binding factor genes, depending on disease context (Döhner et al., 2022; Arber et al., 2022). These lesions contribute to disease classification and risk stratification and, in many settings, are associated with adverse clinical outcome (Bernard et al., 2022; Döhner et al., 2022). In del(5q) MDS, co-occurring *TP53* mutations further refine progression risk, including among patients otherwise classified as lower risk (Jädersten et al., 2011).

Lesions affecting epigenetic regulation are overrepresented among early events in clonal evolution, consistent with altered chromatin and methylation states supporting long-term clonal persistence (Sperling et al., 2016; Döhner et al., 2022). Among recurrent early lesions, *DNMT3A* represents a prototypic founder mutation in clonal haematopoiesis, whereas other alterations show more variable evolutionary timing and disease associations. Longitudinal studies indicate that *DNMT3A*-mutant clones often emerge and expand earlier in adult life, whereas spliceosome mutations tend to show later expansion dynamics and are more closely linked to malignant

progression (Watson et al., 2022; Mitchell et al., 2022). *TET2* and *ASXL1* may also occur as early clonal lesions, but their expansion behaviour appears more context-dependent and can be modified by inherited mechanisms, including *TCL1A*-associated effects described in clonal haematopoiesis (Miller et al., 2023). Individuals with CHIP have a higher risk of subsequent myeloid neoplasia than CHIP-negative individuals, although absolute risk remains low in most cases and rises substantially only in higher-risk genetic and clinical contexts (Weeks et al., 2023; Bolton et al., 2023). Acquisition of additional alterations, including those affecting signalling pathways, transcription factors, or tumour suppressors, is associated with more pronounced disruption of differentiation and increased blast burden or proliferative features (Papaemmanuil et al., 2013; Döhner et al., 2022). Contemporary classification systems identify biologically adverse categories, including *TP53*- and *ASXL1*-mutated disease and spliceosome-associated profiles, which are linked to poor treatment response and rapid progression (Attardi et al., 2023).

In MDS, temporal sequencing studies indicate that early alterations in epigenetic regulation and RNA splicing often precede overt dysplasia, whereas later lesions are enriched in transforming disease (Papaemmanuil et al., 2013; Malcovati et al., 2017). Genetic and cytogenetic context informs, but does not fully determine, phenotype and risk; transcriptomic approaches can provide additional information on disease state, expressed variants, fusions, and therapy-relevant biology in AML (Docking et al., 2021; Döhner et al., 2022). At diagnosis, many patients harbour multiple genetically distinct subclones derived from a shared ancestral population, and clonal architecture may change over the course of disease and treatment. Relapse frequently reflects expansion of pre-existing resistant subclones rather than acquisition of entirely new driver events, indicating that clinically relevant diversity may already be present at initial diagnosis (Hemmati et al., 2017; Döhner et al., 2022). These observations provide a bridge from cell-intrinsic genetic lesions to the marrow context in which subclones are selected, retained, and exposed to therapeutic pressure.

2.1.4 Therapeutic landscape and persistence

Therapeutic strategies in AML and MDS aim to achieve disease control while preserving acceptable haematopoietic function. Current management includes supportive care, disease-modifying non-transplant therapy, immunological approaches, and allogeneic haematopoietic stem-cell transplantation, increasingly guided by genotype-informed stratification (Döhner et al., 2017; Döhner et al., 2022). Relapse remains the principal clinical limitation and reflects persistence of treatment-tolerant malignant populations (Pang et al., 2019; Sarhan et al., 2020; Vago & Gojo, 2020; Ciantra et al., 2025).

Supportive care remains fundamental, particularly in MDS and in older or frail patients, and includes transfusion support, erythropoiesis-stimulating agents in selected

settings, and anti-infective or other symptom-directed measures that may improve quality of life without eliminating the underlying clone (Kaur et al., 2021).

Disease-modifying non-transplant therapy includes both intensive and lower-intensity approaches. Cytarabine- and anthracycline-based induction regimens induce remission in many younger AML patients; relapse is nevertheless common without allogeneic stem-cell transplantation, particularly in older individuals and in adverse-risk disease (Döhner et al., 2017; Arber et al., 2022; Seipel et al., 2023). Liposomal cytarabine–daunorubicin has been incorporated into frontline strategies for selected high-risk categories (Lancet et al., 2018). For older or medically unfit patients, hypomethylating agents form a core platform and are frequently used in combination. Hypomethylating agent–venetoclax regimens have improved initial response rates in AML, but durable control is limited by resistance and relapse, including in adverse-risk genotypes (DiNardo et al., 2019; Lachowiez et al., 2023; Döhner et al., 2024; Nwosu et al., 2024). Targeted inhibitors against *FLT3* or *IDH1/2* alterations provide benefit in molecular subsets; however, resistance remains common. In *FLT3*-ITD AML treated with midostaurin, relapse may occur with disappearance of the *FLT3*-ITD clone in a substantial proportion of cases. In contrast, resistance to more selective *FLT3* inhibition frequently remains associated with *FLT3*-dependent or kinase-pathway lesions rather than simple loss of the original target (Kayser et al., 2021; McMahon et al., 2022). These observations suggest that persistence and relapse are not explained by target presence alone, but reflect broader clonal and microenvironmental mechanisms of survival (Wang et al., 2022; Belt et al., 2024; Huber et al., 2023). Menin inhibitors have recently emerged as an additional targeted strategy, particularly in KMT2A-rearranged and NPM1-mutated AML. Early clinical data support their activity in genetically defined relapsed or refractory disease, and 2024 trial updates have increasingly shifted attention toward rational combinations with venetoclax, hypomethylating agents, and intensive chemotherapy, although their long-term role in combination therapy and resistance management remains under evaluation (FDA, 2024; Cao et al., 2025).

Immunological approaches have thus far demonstrated modest activity in myeloid malignancies. Immune checkpoint blockade has shown limited efficacy as monotherapy and is mainly explored in combination regimens, while bispecific engagers and cellular therapies remain challenged by antigen heterogeneity, overlapping expression on normal haematopoietic cells, and immune suppression within the marrow (Daver et al., 2019; Vago & Gojo, 2020; Haddad & Daver, 2021; Abaza & Zeidan, 2022; Kuen et al., 2023; Shahzad et al., 2023).

Allogeneic haematopoietic stem-cell transplantation remains the only potentially curative approach for AML, MDS, and CMML and is mediated in part by graft-versus-leukaemia effects. Relapse and transplant-related morbidity remain substantial, and outcomes depend on pre-transplant disease biology and residual disease burden (Bejanyan et al., 2015; Jentzsch et al., 2019; Cao et al., 2023). Beyond graft-versus-

leukaemia activity, transplantation also resets haematopoiesis within a profoundly perturbed marrow microenvironment, so post-transplant control depends not only on disease eradication but also on successful re-establishment of donor haematopoiesis within the niche (Cencini et al., 2022).

Current therapies can induce remission and extend survival in defined settings; relapse nevertheless remains common. Persistence under treatment pressure reflects clonal diversity and context-dependent fitness, rather than failure of any single therapeutic class alone (Huber et al., 2023; Kouroukli et al., 2022). The following section therefore considers the bone marrow microenvironment as a setting in which malignant and non-malignant populations interact, immune clearance is constrained, and treatment-tolerant clones may be retained.

2.1.5 Marrow niche constraints in disease

The bone marrow provides the anatomical and cellular context in which relapse and treatment resistance emerge. Haematopoiesis is regulated by local inputs within the marrow microenvironment, and in myeloid malignancies these inputs become integral to disease biology because they influence how malignant and non-malignant populations coexist, compete, and respond to therapeutic stress (Daver et al., 2018; Kouroukli et al., 2022). Thus, disease persistence is shaped not only by cell-intrinsic genetic lesions, but also by the marrow context in which subclones are selected and retained.

Altered intercellular signalling and support programmes are consistently described in AML and related myeloid disorders (Kokkaliaris & Scadden, 2020; Ennis et al., 2023). Changes in cytokine networks, adhesion signals, and stromal responses are associated with marrow environments that protect treatment-tolerant populations under inflammatory or cytotoxic stress, without complete loss of immune or stromal cellularity (Luciano et al., 2022; Ennis et al., 2023). Immune activity may therefore be detectable but insufficient to achieve effective clearance, reflecting functional limitation rather than absence of immune cells (Straube et al., 2024; Chandra et al., 2024).

Spatial organisation also contributes to this functional constraint. Recent proteogenomic and spatial analyses of human bone marrow have shown that malignant and non-malignant populations may occupy distinct niches, and that immune and antigen-presenting cells are unevenly positioned relative to leukaemic compartments (Triana et al., 2021; Bandyopadhyay et al., 2024; Koedijk et al., 2024; Ly et al., 2025). Such localisation may reduce the efficiency of immune engagement (Dolgalev & Tikhonova, 2021; Unger et al., 2025). Notably, paediatric AML may represent a partially distinct immunological context, as multidimensional and spatial

profiling has identified a subset of cases with marked T-cell infiltration and organised immune aggregates within the bone marrow (Koedijk et al., 2024).

Remodelling of myeloid-lineage compartments is frequently reported in myeloid malignancies (Hegde et al., 2021; Jackett et al., 2024). Expanded macrophage populations with immune-restraining phenotypes, together with increased representation of myeloid-derived suppressor cells, have been associated with impaired T-cell activation and broader immune suppression within the marrow of patients with myeloid malignancies (Bauer et al., 2021).

Chronic inflammatory and niche-derived signalling intersect with these changes. Elevated inflammatory mediators have been described in AML and MDS marrow, reflecting contributions from both malignant and non-malignant populations (Ofir et al., 2012; Ogawa, 2019; Luciano et al., 2022). Among the best-characterised support pathways, the *CXCL12–CXCR4* axis is overrepresented in AML relative to healthy bone marrow and contributes to leukaemic-cell retention, survival, and protection within the marrow niche (Korbecki et al., 2024). Sustained exposure to inflammatory and stromal signals may reinforce suppressive immune states and influence progenitor fitness in a genotype-dependent manner (Navada & Silverman, 2016; Lévesque et al., 2021; de Jong et al., 2024; Huber et al., 2023). Although disruption of *CXCL12–CXCR4* signalling can mobilise AML cells and increase treatment sensitivity in some settings, therapeutic targeting of this axis alone may be insufficient because marrow protection is maintained through redundant adhesion, stromal, and inflammatory programmes (Uy et al., 2012; Korbecki et al., 2024). Together, these niche-associated features provide a microenvironmental basis for persistence of malignant populations under immune and therapeutic pressure (Daver et al., 2018; Kouroukli et al., 2022). They also provide the conceptual basis for the following chapter, which focuses on myeloid-lineage immune regulation and introduces Clever-1 as a macrophage-associated scavenger receptor linked to immune organisation within the marrow.

2.2 Niche immunoregulation in myeloid malignancies: macrophage dominance and adaptive paralysis

As described in Chapter 2.1, persistence in myeloid malignancies reflects interaction between clonal properties, therapeutic pressure, and the marrow microenvironment. The following sections focus on the immune dimension of this environment, with emphasis on macrophage-centred regulation and adaptive immune dysfunction.

2.2.1 Disorganised and immunosuppressive bone marrow niches in AML and MDS

The bone marrow is a tissue in which immune cells are positioned, maintained, and instructed within microanatomical contexts (Méndez-Ferrer et al., 2020; Cooper et al., 2025). Marrow immune organisation is therefore not fully captured by peripheral blood measurements. Single-cell profiling indicates that marrow immune-cell composition and cytokine-associated patterns vary with disease status and progression more clearly than can be inferred from peripheral blood alone (Guo et al., 2021).

Building on Chapter 2.1.5, recent proteogenomic, spatial, and single-cell analyses support the view that immune architecture in AML marrow is heterogeneous and clinically relevant (Triana et al., 2021; Bandyopadhyay et al., 2024; Brück et al., 2020; Koedijk et al., 2024; Ly et al., 2025; Unger et al., 2025). Malignant and non-malignant populations may occupy distinct or unevenly distributed niches, and immune and antigen-presenting cells are not uniformly positioned relative to leukaemic compartments (Triana et al., 2021; Bandyopadhyay et al., 2024; Unger et al., 2025). Brück et al. (2020) identified discrete immune architectures that stratified patients by age, T-cell clonality, and outcome. Younger patients more often displayed diverse cytotoxic and memory T-cell populations, whereas older patients exhibited patterns consistent with immunosenescence, including restricted T-cell repertoires and increased representation of suppressive myeloid subsets (Brück et al., 2020; Triana et al., 2021). Thus, immune context varies across patients and is shaped by age and marrow-local factors rather than representing a uniform feature of AML or MDS (Dolgalev & Tikhonova, 2021; Unger et al., 2025).

Across AML and MDS, several immunological features recur despite biological differences. Impaired antigen presentation, expansion of regulatory populations, enrichment of immunosuppressive cytokines, and altered innate and adaptive effector-cell function have been reported, contributing to a milieu in which inflammatory activation is constrained rather than absent (Barakos & Hatzimichael, 2022; Vadakekolathu et al., 2024). In AML, leukaemic blasts can contribute directly to immune remodelling, while stromal and myeloid interactions may stabilise restrained immune states and reduce the tractability of adaptive dysfunction to single-pathway interventions (Vago et al., 2020; Zhao et al., 2012; Mian et al., 2025).

Together, these niche-level features help explain why immune activation in AML and MDS may be detectable yet insufficient for disease control. Macrophage-centred regulation, myeloid-derived suppressor cells, and phagocytic checkpoint pathways are discussed in Chapter 2.2.2, whereas T-cell dysfunction, NK-cell impairment, regulatory T-cell expansion, and defective antigen presentation are considered in Chapter 2.2.3. These processes are summarised schematically in Figure 3 and help explain the limited efficacy of immunotherapies in AML and MDS (Li et al., 2020; Lévesque et al., 2021; de Jong et al., 2024).

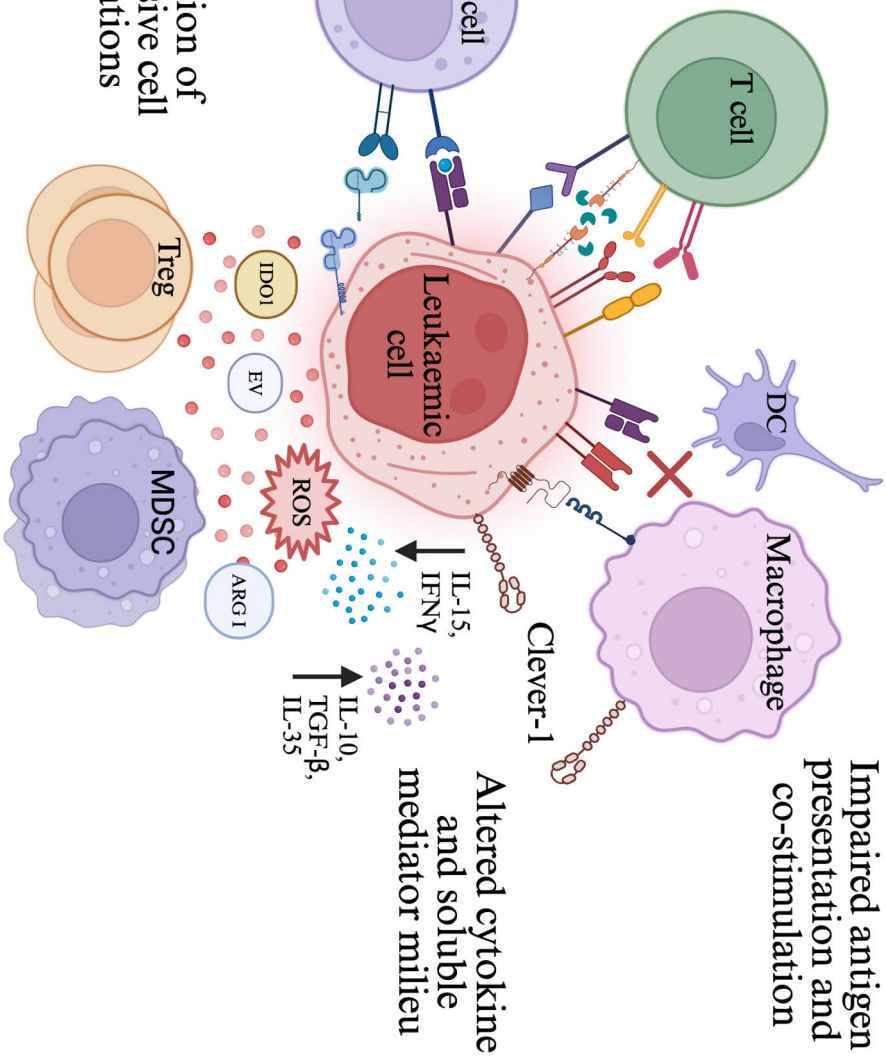
T-cell dysfunction / exhaustion
NK-cell dysfunction / impaired cytotoxicity
Expansion of suppressive cell populations
T cell
NK cell
Leukaemic cell
DC
Macrophage
Clever-1
IL-15, IFNγ
IL-10, TGF-β, IL-35
Impaired antigen presentation and co-stimulation
Altered cytokine and soluble mediator milieu
IDO1
EV
ROS
ARG I
Treg
MDSC

Figure 3. Organisation of immune restraint in the bone marrow niche of myeloid malignancies. Schematic overview of immunoregulatory architecture in the bone marrow niche of acute myeloid leukaemia and related myeloid malignancies. Malignant myeloid cells are embedded within a network of innate and adaptive immune elements that collectively favour immune restraint. Inhibitory surface interactions and soluble mediators attenuate T-cell and NK-cell effector function, while altered antigen handling and reduced co-stimulatory signalling limit effective immune activation. Macrophages, dendritic cells, and myeloid-derived suppressor cells contribute to this restrained immune tone through altered antigen handling, impaired antigen presentation, and production of immunomodulatory mediators, including IL-10, TGF-β, IL-35, reactive oxygen species (ROS), arginase 1 (ARG1), IDO1, and extracellular vesicles (EVs). Scavenger receptors associated with immunoregulatory macrophage states, including Clever-1, are shown as part of this broader endocytic and immunoregulatory programme. Expansion of regulatory T cells and suppressive myeloid populations further stabilises feedback loops that maintain immune dysfunction within the marrow environment. Illustration created with BioRender.

2.2.2 Myeloid dominance and macrophage-centred regulation

Macrophages occupy a spectrum of activation states shaped by cytokines, stromal interactions, and signals derived from malignant and dying cells (Mosser et al., 2008; Siebeler et al., 2023). Classically activated macrophages support inflammatory responses through mediators such as TNF-α and IL-12, whereas immunoregulatory macrophage states are associated with scavenger receptor expression and production of IL-10 and transforming growth factor (TGF)-β (Siebeler et al., 2023). In AML, increased expression of markers associated with immunoregulatory macrophages has been linked to adverse outcomes (de Jong et al., 2024). CD206, the macrophage mannose receptor and a commonly used marker of immunoregulatory or M2-like macrophage states, has been reported to reflect inferred M2 macrophage abundance in AML and to associate with inferior overall and event-free survival, supporting the clinical relevance of macrophage-associated immune polarisation in this disease (Xu et al., 2019).

In AML, Brück et al. (2020) identified spatial immune architectures associated with outcome after intensive therapy. In particular, regulatory populations such as Tregs were linked to inferior survival in independent AML cohorts, whereas M2-like macrophages are more consistently supported as contributors to a leukaemia-supportive and therapy-resistant marrow microenvironment than as a uniformly validated prognostic marker (Brück et al., 2020; Szczepanski et al., 2020; Al-Matary et al., 2021). These findings are consistent with the broader observation that older patients more often exhibit immune architectures characterised by restricted T-cell repertoires and increased representation of suppressive myeloid subsets (Brück et al., 2020; Triana et al., 2021).

A related feature of myeloid dominance is expansion of MDSIwhich can arise under chronic inflammatory cues and accumulate in marrow and peripheral blood in association with disease progression (Hegde et al., 2021; de Jong et al., 2024). Monocytic and granulocytic MDSC subsets suppress effector T-cell activity through multiple mechanisms, including arginase 1–mediated depletion of extracellular L-arginine, production of nitric oxide and reactive oxygen species, and secretion of IL-10 and TGF-β (Kim et al., 2019; Bizymi et al., 2020; Schieber et al., 2020). In higher-risk MDS, inflammatory mediators such as IL-6, TNF-α, and S100A9 have been linked to sustained MDSC expansion and reinforcement of suppressive myeloid states (Christiansson et al., 2013; Pellin et al., 2019). Stromal and myeloid interactions may further support a niche configuration in which immune suppression is maintained through several overlapping mechanisms (Zhao et al., 2012; Mian et al., 2025). Elevated frequencies of MDSCs and Tregs have also been associated with progression from MDS to AML (Kittang et al., 2015), supporting coupling between suppressive myeloid expansion and disease progression in selected settings.

Myeloid regulation further includes inhibitory surface signalling that constrains clearance of malignant cells and limits downstream immune activation. A prototypic example is the CD47–signal-regulatory protein alpha (SIRPα) axis, which provides a ‘do not eat’ signal and suppresses phagocytosis through inhibitory signalling pathways (Veillette & Chen, 2018; Matlung et al., 2017). Increased CD47 expression on leukaemic blasts has been associated with reduced susceptibility to macrophage-mediated clearance and impaired downstream immune engagement (Galli et al., 2015; Swatler et al., 2021). More broadly, receptors regulating phagocytosis, endocytosis, and antigen handling contribute to thresholds for macrophage activation and the availability of antigen for adaptive priming (Cullen & Steinberg, 2018; Gopaldass et al., 2024). Within this category, the scavenger receptor Clever-1 represents a myeloid-lineage molecule associated with immunoregulatory macrophage states and with endocytic programmes relevant to immune restraint (Viitala et al., 2019).

2.2.3 Adaptive immune dysfunction and immune paralysis

Adaptive immune dysfunction in AML and MDS reflects the cumulative effects of chronic antigen exposure, inhibitory signalling, regulatory-cell expansion, and impaired antigen presentation within a myeloid-dominant niche (Hegde et al., 2021; de Jong et al., 2024). Whereas the preceding sections introduced these features as components of the disorganised marrow niche and myeloid-centred regulation, this section focuses on their consequences for adaptive immune function.

Cytotoxic T-cell responses are frequently characterised by reduced effector function together with sustained and combinatorial expression of inhibitory receptors, although these states are heterogeneous and do not uniformly recapitulate the canonical terminal exhaustion described in highly immunogenic solid tumours (Li et al., 2020; Vadakekolathu & Rutella, 2024; Abbas et al., 2021). In AML, marrow-resident $CD8^+$ T-cell subsets expressing PD-1, TIM-3, LAG-3, TIGIT, and related inhibitory programmes have been reported, particularly in relapsing disease, and are associated with impaired cytokine production, restricted proliferative capacity, and adverse clinical features (Noviello et al., 2019; Vadakekolathu & Rutella, 2024). These findings suggest that adaptive dysfunction is shaped by heterogeneous checkpoint combinations and marrow-local immune restraint rather than by a single dominant exhaustion programme. TIM-3 is additionally relevant in AML because it is expressed on leukaemic stem cells, and its detection therefore cannot be interpreted solely as a marker of dysfunctional T cells (Kikushige et al., 2010). $CD4^+$ T-helper populations similarly show enrichment of inhibitory and regulatory features, including diminished co-stimulatory capacity and altered memory formation (Noviello et al., 2019). These changes may be accentuated in older patients through immunosenescence-associated restriction of repertoire diversity, as noted above (Brück et al., 2020; Vadakekolathu & Rutella, 2024).

Natural killer (NK) cells represent a parallel component of immune dysfunction within this suppressive architecture. In MDS, NK cells show reduced cytotoxic capacity, impaired maturation, and altered activating and inhibitory receptor balance, and recent studies suggest that these defects may be reinforced by both the marrow microenvironment and disease-associated mutations such as *TET2* (Arellano-Ballestero et al., 2023; Boy et al., 2023). More recent single-cell work further suggests that functionally impaired NK cells can contribute to immune escape already at early disease stages, supporting the view that defective innate cytotoxic surveillance is not merely secondary to advanced marrow remodelling (Rodriguez-Sevilla et al., 2025).

Expansion of Tregs provides an additional stabilising mechanism of immune restraint (Hegde et al., 2021; Jackett et al., 2024). Increased marrow Treg frequencies have been associated with adverse clinical outcome and disease progression (Kordasti et al., 2007; Alfinito et al., 2009; Han et al., 2018). In AML, leukaemic blasts may also contribute directly to this regulatory state. For example, interferon-γ–driven activation of indoleamine 2,3-dioxygenase 1 (*IDO1*) has been associated with expansion of regulatory T cells, linking malignant-cell signalling to suppression of cytotoxic T-cell function (Vago et al., 2020; Corradi et al., 2022). Stromal and myeloid interactions can reinforce this state. Mesenchymal stromal cells have been reported to promote differentiation of naïve $CD4^+$ T cells into FoxP3-positive Tregs (Zhao et al., 2012), supporting a niche configuration that limits effector activation and reduces the tractability of adaptive dysfunction to single-pathway interventions (Mian et al., 2025).

Defects in antigen presentation further compound adaptive failure. Dendritic cells (DCs) coordinate antigen processing and T-cell priming, yet are quantitatively and functionally altered in AML and MDS. Plasmacytoid DCs exhibit impaired maturation and reduced expression of co-stimulatory molecules required for naïve T-cell activation (Zalmaï et al., 2021). Differentiation and function of myeloid DCs can be suppressed by cytokines including IL-10 and TGF-β, thus limiting antigen processing and cross-priming (Wang et al., 2013; Maher et al., 2021). In MDS, reduced expression of CD80, CD86, and human leukocyte antigen–DR (HLA-DR) on DCs has been associated with impaired T-cell stimulation and immune escape (Krevvata et al., 2018). Because *CIITA* is the central transcriptional regulator of MHC class II expression, reduced *CIITA*-dependent antigen-presentation capacity in APCs would be expected to impair CD4 T-cell activation rather than imply a general defect in HLA class I expression (Machado et al., 2021). Contact-dependent disruption of immune synapse formation has been described as an additional route by which interactions between AML blasts and T cells may limit effective T-cell activation. In parallel, altered CD40–CD40L co-stimulatory signalling is biologically relevant in AML, although CD40 engagement may have context-dependent effects on both antigen-presenting cells and CD40-positive AML blasts (Le Dieu et al., 2009; Zhang et al., 2013; Aldinucci et al., 2002). Together, these alterations reduce the likelihood

that antigen exposure within the niche translates into durable effector responses (Li et al., 2020).

The combination of heterogeneous checkpoint-associated T-cell states, impaired NK-cell function, regulatory expansion, and defective antigen presentation supports the concept of immune paralysis as a property of the marrow environment rather than a defect in a single immune compartment (Lévesque et al., 2021; de Jong et al., 2024). Within this architecture, immune organisation introduces additional selection pressures by determining whether antigen exposure is coupled to productive immune engagement or diverted towards tolerance (Mian et al., 2025). Immune restraint therefore contributes to disease persistence as part of the broader structure of the marrow niche (Lévesque et al., 2021; Jackett et al., 2024).

2.3 Metabolic organisation and mitochondrial fitness in AML and related myeloid malignancies

As described in Chapter 2.2, immune restraint in AML and MDS is organised at the level of the bone marrow niche, with macrophage-dominant regulation and adaptive dysfunction emerging as structural features of diseased tissue. These immune states are not independent of intracellular bioenergetics. Mitochondrial metabolism influences survival, differentiation state, apoptotic priming, and treatment tolerance in leukaemic and myeloid-lineage cells, and may thereby reinforce persistence within the marrow environment (de Jong et al., 2024; Mishra et al., 2023).

Across myeloid malignancies, mitochondrial respiration has emerged as a recurrent axis of vulnerability and adaptation (de Beauchamp et al., 2022; Shi et al., 2024). Oxidative phosphorylation (OXPHOS) refers to ATP generation through the mitochondrial electron transport chain (ETC), in which electron flow across respiratory complexes drives proton pumping and ATP synthesis (Cogliati et al., 2021). Functionally, OXPHOS dependence denotes a requirement for intact mitochondrial respiration to sustain ATP levels and cellular viability, and is reflected experimentally by impaired oxygen consumption, ATP maintenance, or survival following respiratory-chain perturbation (Lagadinou et al., 2013; Farge et al., 2017; Saito et al., 2021). This chapter focuses on mitochondrial respiration, lipid utilisation, and cholesterol handling as interlinked but mechanistically distinct contributors to AML persistence and as background for the findings of Manuscript III.

2.3.1 Mitochondrial respiration and state-dependent fitness in AML

AML is genetically heterogeneous, yet recurrent patterns of mitochondrial reliance have been described across biologically diverse disease states. Within this landscape, leukaemic stem-like cells (LSCs) represent a relapse-relevant compartment sustained by distinct bioenergetic programmes (de Beauchamp et al., 2022; Rattigan et al., 2023). Several studies indicate that primitive and quiescent AML populations display disproportionate reliance on mitochondrial OXPHOS, distinguishing them from more proliferative or glycolysis-biased blast populations and conferring relative survival advantage under metabolic and therapeutic stress (Ye et al., 2016; Patel et al., 2022; Egan & Schimmer, 2023; Shi et al., 2024). Heightened mitochondrial respiration in these compartments has been associated with persistence following cytotoxic exposure and with features linked to relapse risk (Farge et al., 2017; Panuzzo et al., 2020).

This association between mitochondrial respiration and survival wiring is further illustrated by the sensitivity of quiescent LSC-enriched populations to perturbation of anti-apoptotic control at the level of the mitochondrion (Lagadinou et al., 2013). In this setting, mitochondrial bioenergetics and apoptotic priming appear closely aligned, such that disruption of mitochondrial function can destabilise survival programmes in stem-like compartments (de Beauchamp et al., 2022; Rattigan et al., 2023). However, this vulnerability is not uniform across AML states. Developmental plasticity and differentiation-state transitions can reconfigure mitochondrial dependencies. Pei et al. (2020) demonstrated that sensitivity to mitochondrial disruption tracks with developmental state, and that resistance may emerge in more differentiated, monocytic-like subclones with alternative survival requirements. OXPHOS reliance is therefore enriched in selected primitive or quiescent AML states, but it is not a fixed property of AML as a whole.

Therapeutic and cytokine-derived pressures further modify mitochondrial configuration. In a chemotherapy regression–regrowth model, Nóbrega-Pereira et al. (2018) reported that AML cells recovered at terminal regrowth exhibited altered metabolic characteristics compared with untreated disease, including changes in lipid content, cellular energy state, and mitochondrial features. Stromal support has also been linked to enhanced mitochondrial metabolism in AML cells through an IL-6/STAT3/OXPHOS axis, indicating that inflammatory and niche-derived signals can reinforce oxidative metabolism (Hou et al., 2020). In addition, organelle-level adaptation may preserve respiratory competence under stress. Saito et al. (2021) showed that exogenous mitochondrial transfer and endogenous mitochondrial fission contribute to resistance to OXPHOS inhibition, while Fu et al. (2024) reported chemotherapy-associated connexin-43-linked mitochondrial transfer from bone marrow stromal cells into stem-like AML cells. These observations support the interpretation

that mitochondrial fitness is a selectable phenotype shaped by differentiation state, cytokine exposure, treatment pressure, and marrow-derived support.

This dynamic framing has therapeutic implications. OXPHOS-directed strategies are biologically attractive because mitochondrial respiration supports survival in selected stem-like and therapy-tolerant AML states. However, inhibition of mitochondrial respiration can induce compensatory ATP production through glycolysis, and resistance may arise through differentiation-state switching, stromal support, mitochondrial transfer, or altered substrate utilisation (Sabnis et al., 2016; Egan & Schimmer, 2023; Rattigan et al., 2023). Mitochondrial dependence should therefore be viewed as a context-dependent vulnerability rather than a universal metabolic hallmark. This is also relevant to BH3 mimetics, including venetoclax-based regimens, because mitochondrial bioenergetics and apoptotic priming are closely linked in AML (Bhatt et al., 2020; Nwosu et al., 2024). Changes in mitochondrial state, differentiation programme, and lipid composition can alter sensitivity to both OXPHOS-directed approaches and apoptosis-targeting therapies.

2.3.2 Fatty-acid utilisation as a component of mitochondrial support in AML

Building on the mitochondrial dependencies outlined in Section 2.3.1, lipid utilisation represents a complementary route by which AML cells can sustain respiratory ATP production under stress. Fatty-acid oxidation (FAO) provides reducing equivalents that support electron flow through the respiratory chain and can therefore preserve mitochondrial output when alternative substrates are constrained (Mishra et al., 2023). In AML, FAO is best treated as a state-enriched programme rather than a universal feature of blasts, with evidence suggesting preferential deployment within quiescent, stem-like, and stress-adapted compartments (de Beauchamp et al., 2022; Shi et al., 2024; Singh et al., 2024; Dembitz et al., 2025).

A key entry point to this axis is uptake of exogenous fatty acids from the marrow environment, which should be distinguished from *de novo* fatty-acid synthesis and desaturation within leukaemic cells. The fatty-acid transporter CD36 has been linked to stem-like, therapy-protected leukaemic populations. Ye et al. (2016) showed that CD36-positive leukaemic cells preferentially utilise fatty acids to support FAO and mitochondrial respiration, and that this lipid-fuelled configuration is associated with persistence in protective tissue niches and reduced sensitivity to chemotherapy. This supports the broader principle that mitochondrial fitness in AML depends not only on intrinsic bioenergetic wiring but also on access to niche-derived substrates (Ye et al., 2016; Tabe et al., 2020).

Marrow architecture may amplify this substrate dependence through adipocyte-rich compartments. Bone marrow adipocytes are increasingly recognised as

metabolically active niche components capable of shaping local haematopoietic and malignant-cell states (Bandyopadhyay et al., 2024; Frenz-Wiessner et al., 2024; Dembitz et al., 2025). In co-culture and niche-modelling studies, leukaemic blasts have been reported to induce adipocyte lipolysis and to utilise adipocyte-derived fatty acids through lipid chaperones such as fatty acid-binding protein 4 (*FABP4*), reinforcing FAO-linked mitochondrial metabolism and survival signalling (Shafat et al., 2017; Tabe et al., 2017). These findings are consistent with selection for AML states with higher fatty-acid uptake and oxidative capacity in adipocyte-enriched niches (Bandyopadhyay et al., 2024; Singh et al., 2024).

Lipid metabolism also influences therapy sensitivity by modifying mitochondrial function and apoptotic priming. FAO-linked programmes can support respiratory ATP production, whereas changes in lipid composition, including sphingolipid and cholesterol-related alterations, can affect mitochondrial membrane function, OXPHOS performance, and sensitivity to OXPHOS inhibition or BH3 mimetics (Ribas et al., 2016; García-Ruiz et al., 2021; Fisher-Wellman et al., 2021; Egan & Schimmer, 2023). Thus, lipid metabolism should not be viewed only as a source of oxidisable substrates, but also as a determinant of the physical and functional mitochondrial state in which respiration and apoptosis occur.

Therapeutic strategies aimed at lipid metabolism should likewise distinguish between interference with fatty-acid uptake or oxidation and interference with *de novo* lipid synthesis, desaturation, or intracellular lipid distribution. FAO-directed strategies and *CPT1A*-linked approaches have been explored in experimental models, although interpretation of pharmacological FAO inhibition requires caution because commonly used agents may have off-target effects (Raud et al., 2018). In parallel, inhibition of lipid synthesis or desaturation, including stearoyl-CoA desaturase-associated strategies, and broader agents such as metformin have been investigated as ways to perturb AML lipid handling and oxidation-linked vulnerabilities (Dembitz et al., 2024; Dembitz et al., 2025; Sternadt et al., 2026). These approaches remain biologically relevant because lipid metabolism can influence fuel availability, mitochondrial state, apoptotic sensitivity, and treatment tolerance.

2.3.3 Cholesterol handling as a distinct mitochondrial regulatory pathway

While fatty acids can support mitochondrial respiration through oxidation, sterol handling influences mitochondrial performance through distinct mechanisms (García-Ruiz et al., 2021; Tabe et al., 2020). Cholesterol is not a bioenergetic substrate in non-steroidogenic cells; instead, its distribution across intracellular membranes affects mitochondrial function by shaping membrane material properties, redox homeostasis, and organisation of respiratory machinery (Ribas et al., 2016; Mari et al., 2013; García-Ruiz et al., 2021). In this view, mitochondrial cholesterol content

becomes a regulatory variable expressed through membrane order, metabolite transport, stress tolerance, and apoptotic priming rather than through ATP generation by direct substrate oxidation (Tatsuta et al., 2014).

Experimental work in non-haematological systems has shown that excess mitochondrial cholesterol can impair mitochondrial function. Cholesterol enrichment increases membrane order and decreases membrane fluidity, which can disturb transport processes and the activity of membrane-associated proteins (Fernández et al., 2009). It has also been linked to depletion of mitochondrial glutathione (mGSH), impaired redox homeostasis, and weaker respiratory performance (Marí et al., 2006; Barbero-Camps et al., 2013; Torres et al., 2017; Solsona-Vilarrasa et al., 2019). Because mGSH is important for buffering mitochondrial oxidative injury, impaired glutathione import provides one route by which altered cholesterol distribution can increase vulnerability to redox stress and compromise mitochondrial fitness (Coll et al., 2003; Marí et al., 2009). Although most of this evidence comes from outside haematological malignancies, it supports the general principle that mitochondrial lipid composition can influence respiratory fitness under stress.

Sterol enrichment has also been linked to altered organisation of the ETC. In liver models, mitochondrial cholesterol accumulation disrupts assembly of respiratory supercomplexes and impairs OXPHOS (Solsona-Vilarrasa et al., 2019). These observations sit alongside broader evidence that respiratory supercomplex organisation is sensitive to membrane lipid composition and contributes to respiratory efficiency while constraining reactive oxygen species production from complex I (Maranzana et al., 2013). Together, these findings support the broader proposition that mitochondrial lipid state can regulate OXPHOS through higher-order membrane and protein-assembly effects.

In AML, relevance of this sterol-centred pathway is suggested by evidence that cholesterol programmes are engaged during cytotoxic stress and that mitochondrial cholesterol trafficking can occur through regulated transport mechanisms (Banker et al., 2004; Rattigan et al., 2023; García-Ruiz et al., 2021). In cancer models, sterol-transfer pathways linked to mitochondrial cholesterol accumulation have been associated with chemoresistance and altered apoptotic priming (Montero et al., 2008; Yue et al., 2022). These observations support the plausibility that sterol routing to mitochondrial membranes may contribute to therapy tolerance by modifying bioenergetic resilience, although direct mechanistic evidence in AML remains limited. In MDS and CMML, support is more indirect and derives mainly from broader evidence of mitochondrial dysfunction, oxidative stress, and altered energy metabolism rather than direct demonstration of sterol trafficking to mitochondria (Mózes et al., 2021).

Intracellular cargo routing provides a focused mechanistic link between scavenger receptor function and lipid-associated mitochondrial phenotypes. Scavenger receptors internalise extracellular material and route cargo through endosomal and

lysosomal compartments, where lipids, proteins, and other ligands can be degraded, recycled, or redirected to intracellular membranes (Hsu et al., 2012; Seaman, 2021). For this thesis, this pathway is relevant primarily because Clever-1 is an endocytic scavenger receptor expressed in myeloid-lineage cells, and altered cargo handling may influence cholesterol availability, membrane composition, and mitochondrial function. Cargo routing is therefore considered here not as a separate cell-biological topic, but as a mechanism that may connect Clever-1 targeting to lipid trafficking and mitochondrial metabolism in Manuscript III.

In summary, cholesterol handling is positioned as a mitochondrial regulatory pathway intersecting with respiratory competence through membrane and redox mechanisms (Ribas et al., 2016; García-Ruiz et al., 2021). This differs from FAO as a fuel module (Tabe et al., 2020) and provides a conceptual bridge to lipid-associated immune modulation, in which lipid availability and intracellular lipid handling can also shape antigen processing and durability of suppressive-cell states within the marrow niche (Veglia et al., 2021) (Section 2.3.4, Figure 4).

Figure 4. Lipid-conditioned mitochondrial fitness in the bone marrow niche of AML. Schematic overview of how marrow-derived lipids may influence mitochondrial performance in leukaemic cells. In adipocyte-rich and stromally supported marrow niches, exogenous fatty acids may become available through lipolysis and can be taken up by leukaemic cells. Within the cell, fatty acids can be routed towards mitochondrial β-oxidation, generating acetyl-CoA and reducing equivalents that support the tricarboxylic acid (TCA) cycle, oxidative phosphorylation (OXPHOS), and ATP production. In parallel, cholesterol is depicted as a regulatory lipid that can be trafficked to mitochondria. Unlike fatty acids, cholesterol does not serve as a direct bioenergetic substrate, but may influence mitochondrial function through effects on membrane properties, redox buffering, respiratory-chain organisation, and apoptotic sensitivity. These lipid-fuel and lipid-regulatory modules converge on mitochondrial fitness, which is shaped by differentiation state, cytokine signalling, therapeutic pressure, and niche-derived substrate availability. The figure summarises lipid utilisation and cholesterol handling as complementary determinants of respiratory competence and persistence in AML, rather than as static or uniform metabolic hallmarks. Illustration created with BioRender.

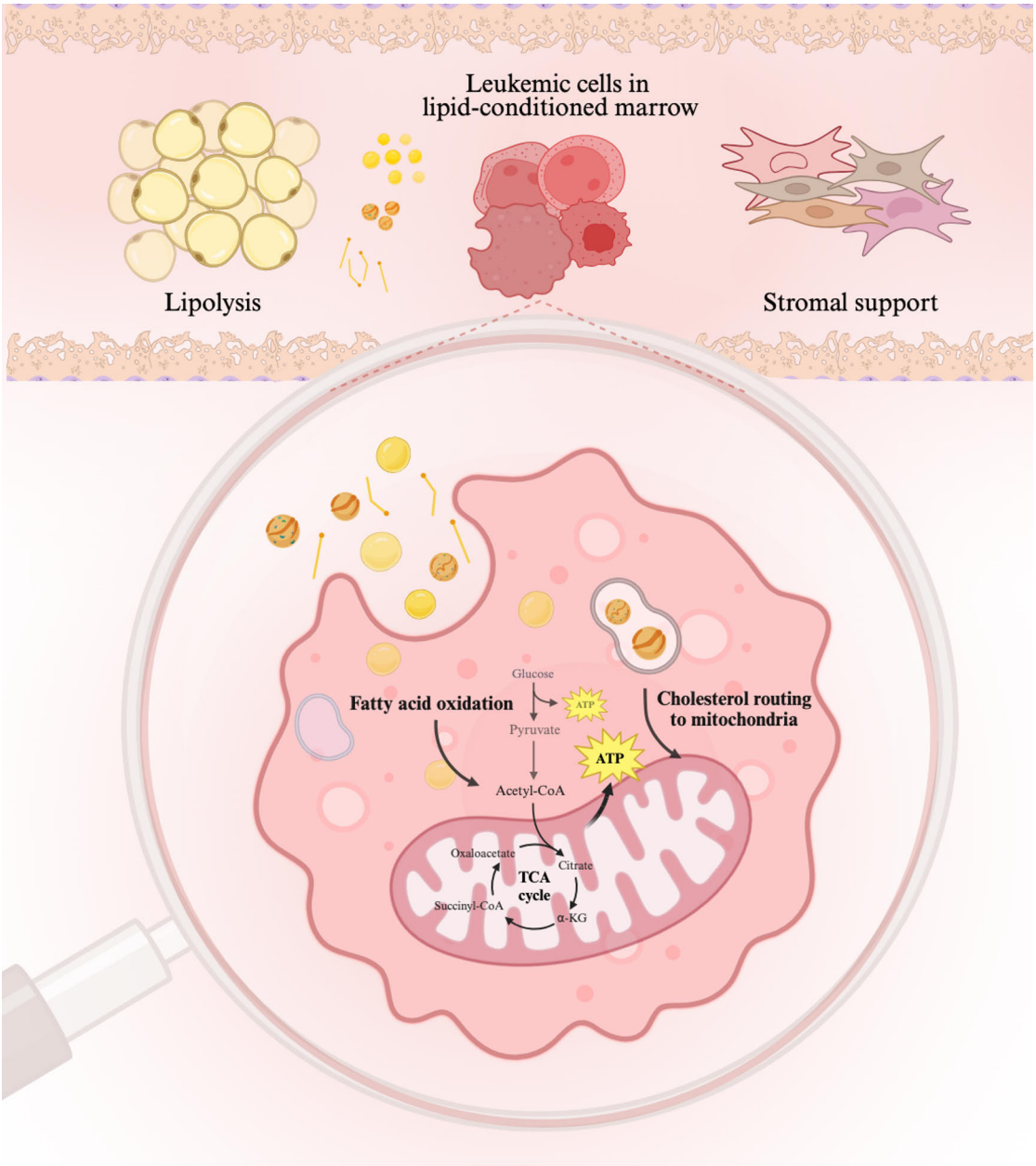
Leukemic cells in
lipid-conditioned marrow
Lipolysis
Stromal support
Glucose
ATP
Fatty acid oxidation
Pyruvate
Cholesterol routing
to mitochondria
ATP
Acetyl-CoA
Oxaloacetate
Citrate
TCA
cycle
Succinyl-CoA
α-KG

2.3.4 Lipid metabolism and suppressive immune organisation in the marrow

As described in the preceding sections, immune restraint in AML and MDS emerges from layered tissue organisation, in which myeloid-lineage populations condition antigen availability and inflammatory thresholds, and adaptive effector dysfunction consolidates over time (Hegde et al., 2021; de Jong et al., 2024). Metabolic organisation can contribute to this structure by stabilising suppressive phenotypes and constraining antigen-presenting competence. Lipid availability is therefore not only a resource for malignant-cell fitness (Figure 4), but also an environmental variable that may reinforce tolerogenic immune states through intracellular lipid handling and mitochondrial programme selection (Tabe et al., 2020).

In AML, immunosuppression is frequently associated with expansion of suppressive myeloid populations and production of soluble mediators that impair T-cell activation and promote regulatory immune states (Mussai et al., 2013; Pyzer et al., 2017). These interactions occur within a marrow environment in which leukaemic and non-malignant myeloid cells coexist under persistent inflammatory and therapeutic stress (Al-Sabah et al., 2020). Under such conditions, metabolic programmes that support cell survival may also help stabilise suppressive immune phenotypes (Hegde et al., 2021). Lipid availability and intracellular lipid routing are therefore relevant candidate mechanisms, as they may support oxidative states associated with persistence and myeloid suppressive function (Hollmén et al., 2020).

One line of evidence concerns antigen-presenting cells and the relationship between lipid accumulation and antigen-processing capacity. In tumour-bearing hosts and patient-derived material, dendritic cells have been shown to accumulate neutral lipids, predominantly triglycerides, driven by increased uptake of extracellular lipids, in part via scavenger-receptor-linked pathways. This lipid loading has been associated with impaired antigen processing and reduced capacity to stimulate T cells, providing a route by which the extracellular lipid environment may reduce adaptive immune priming even when antigen is present (Herber et al., 2010). Relevance to AML follows from the dependence of T-cell recognition on effective presentation of tumour antigens through human leukocyte antigen (HLA) molecules, and from observations that disease progression and relapse have been linked to reduced expression of antigen-presentation machinery, particularly HLA class II pathways (Toffalori et al., 2019; Dufva et al., 2020). Together, these findings support a model in which lipid

accumulation can constrain antigen-presenting competence upstream of classical inhibitory receptor signalling.

A second line of evidence relates to suppressive myeloid populations and their metabolic dependencies. MDSCs, already implicated in AML immune evasion, have been shown in tumour models to upregulate fatty-acid utilisation and oxidative programmes, and pharmacological inhibition of FAO has been reported to attenuate suppressive activity and improve anti-tumour immune responses (Hossain et al., 2015; Yan et al., 2019). However, interpretation of FAO-directed perturbation requires caution, as commonly used tools such as etomoxir can exert effects independent of CPT1A in T-cell systems and may confound attribution of phenotype strictly to FAO blockade (Raud et al., 2018). In a marrow context, these observations support a principle rather than a closed causal chain: oxidative lipid programmes can form part of the functional scaffold of suppressive myeloid states, and lipid availability may influence immune behaviour by sustaining these metabolic configurations.

These observations are relevant to the broader organisation described in Chapter 2, but they should be interpreted as mechanisms that may reinforce suppressive immune states rather than as a single explanatory pathway. In this context, lipid accumulation in antigen-presenting cells may limit priming capacity, whereas oxidative lipid utilisation in suppressive myeloid populations may support persistence under stress. This framing is also relevant to Clever-1, as the receptor is linked to myeloid scavenging and intracellular cargo handling, processes that may influence how cells handle lipid-rich material within the marrow environment (Hsu et al., 2012; Seaman, 2021). Taken together, the available evidence supports a model in which lipid handling contributes to immune restraint at several levels, including antigen presentation and maintenance of suppressive myeloid states, without implying that these associations alone establish direct causality in AML or MDS (Tabe et al., 2020; Zhang et al., 2022; Egan & Schimmer, 2023).

2.4 Myeloid regulatory receptors and cargo routing in the marrow niche

Because antigen presentation depends not only on antigen availability but also on intracellular processing, routing decisions within endolysosomal compartments can influence whether internalised material is fully degraded, partially preserved, or directed into pathways compatible with presentation (Harding & Geuze, 1992; Roche et al., 1993; Alloatti et al., 2015). Cargo routing is therefore relevant not only to clearance efficiency but also to adaptive priming and lipid handling in myeloid cells engaged in continuous scavenging. For the purposes of this thesis, the key distinction is between receptor systems that primarily regulate whether engulfment occurs and receptors that may also influence post-endocytic cargo fate.

Among receptor systems that shape myeloid interactions with extracellular material, the CD47–signal regulatory protein α (SIRPα) axis provides a well characterised example of phagocytic threshold control. Engagement of SIRPα by CD47 expressed on target cells leads to phosphorylation of cytoplasmic immunoreceptor tyrosine-based inhibitory motifs (ITIMs) and recruitment of SHP-family phosphatases, thereby inhibiting actin reorganisation required for phagocytosis (Matozaki et al., 2009). In acute myeloid leukaemia, increased CD47 expression has been associated with reduced macrophage-mediated clearance and adverse outcome, and therapeutic disruption of CD47–SIRPα signalling can enhance phagocytosis of malignant cells (Majeti et al., 2009; Chao et al., 2020). This supports the interpretation that CD47–SIRPα primarily regulates the engulfment threshold, rather than post-endocytic cargo routing, and provides a useful contrast to receptors such as Clever-1.

Antigen presence within tissue does not guarantee its presentation. After uptake, internalised cargo enters endosomal and lysosomal compartments that determine whether material is degraded, recycled, or retained in a form compatible with antigen presentation (Neefjes et al., 2011; Alloatti et al., 2015; Blander, 2018). In classical MHC class II presentation, extracellular proteins undergo proteolysis within endolysosomal compartments before peptide loading, whereas cross-presentation to MHC class I requires preservation of antigenic fragments and avoidance of complete degradation (Harding & Geuze, 1992; Roche et al., 1993; Alloatti et al., 2015). Thus, the proteolytic character and maturation state of endolysosomal compartments influence whether internalised material is destroyed or retained in a form compatible with presentation.

These routing decisions are also relevant to lipid handling. Lipoprotein- and membrane-derived cargo is processed within lysosomes, where cholesteryl esters are hydrolysed and free cholesterol can be redistributed through pathways involving *NPC1* and *NPC2* (Ikonen, 2008; Meng et al., 2020). Perturbation of endosomal trafficking or lysosomal maturation can therefore alter intracellular sterol distribution and downstream cellular responses. This link between cargo routing and sterol handling is particularly relevant in the context of Manuscript III, where Clever-1 targeting is examined in relation to cholesterol trafficking and mitochondrial metabolism.

Within the marrow niche, macrophages and sinusoidal endothelial cells operate under continuous exposure to apoptotic debris, lipid-rich particles, and circulating macromolecules (Méndez-Ferrer et al., 2020). Efficient receptor recycling and regulated endolysosomal maturation help sustain clearance while preserving control over antigen processing, lipid handling, and inflammatory activation (Kinchen & Ravichandran, 2008; Boada-Romero et al., 2020). Among receptors whose regulatory influence is exerted through cargo routing rather than classical kinase-mediated signalling, Clever-1 is of particular interest because it links scavenger activity, endolysosomal maturation, and immune regulation. This provides the conceptual basis for the following chapter, which examines Clever-1 as a myeloid regulatory receptor with

relevance to antigen handling, cholesterol trafficking, and mitochondrial phenotypes explored in Manuscript III.

2.5 Clever-1 as a trafficking scavenger receptor in immune regulation and cancer

Clever-1 (*STAB1*; Stabilin-1) is a type I transmembrane scavenger receptor expressed in selected myeloid and endothelial compartments. In the marrow niche, its relevance lies in its position at the intersection of ligand uptake, endolysosomal trafficking, and immune regulation. The following sections ex-amine its relation to macrophage state, lipid handling, antigen persistence, adaptive immune priming, and tumour-associated immune restraint.

2.5.1 Clever-1 within the myeloid and endothelial regulatory architecture

Clever-1 belongs to the class H scavenger receptor family and shares structural homology with Stabilin-2. Its extracellular region contains fasciclin-like and EGF-like domains together with a Link module, while the short cytoplasmic tail contains internalisation motifs but lacks intrinsic kinase domains (Politz et al., 2002; Kzhyshkowska et al., 2004; Prevo et al., 2004). This architecture is consistent with a primary role in ligand uptake and intracellular trafficking rather than classical signal transduction (Kzhyshkowska, 2010; Gurung et al., 2025).

Clever-1 undergoes constitutive cycling between the plasma membrane and intracellular compartments in macrophages and specialised endothelial cells. Internalisation proceeds predominantly through clathrin-mediated endocytosis and connects surface uptake to endosomal and trans-Golgi trafficking routes (Prevo et al., 2004; Zhang et al., 2009). Recycling is regulated in part by SNX17, which limits lysosomal degradation and helps maintain receptor availability during sustained scavenger activity (Adachi & Tsujimoto, 2010).

The receptor binds structurally diverse ligands, including acetylated and oxidatively modified low-density lipoproteins, matricellular proteins such as SPARC, and phosphatidylserine-exposed membranes associated with apoptotic-cell clearance (Kzhyshkowska et al., 2005; Park et al., 2009; Rantakari et al., 2016). Ligand internalisation depends on phosphatidylinositol-3-kinase activity, consistent with regulated endosomal maturation after receptor engagement (Langemeyer et al., 2018; Borchers et al., 2021).

Beyond ligand uptake, Clever-1 has been linked to endolysosomal organisation in primary human macrophages, where receptor perturbation affects vesicular

maturation and degradative routing (Virtakoivu et al., 2021). These findings support the view that Clever-1 functions not only as an uptake receptor, but also as part of the machinery connecting scavenging to intracellular cargo processing.

In endothelial compartments, Clever-1 is expressed on sinusoidal and lymphatic endothelium, where it participates in leukocyte adhesion and transmigration across vascular interfaces (Salmi et al., 2004; Karikoski et al., 2009). Genetic deletion studies further indicate altered dendritic-cell activation and migration in the absence of endothelial Clever-1, suggesting a role in immune-cell positioning and conditioning at vascular boundaries in addition to intracellular cargo handling (Tadayon et al., 2021).

Within the marrow niche, Clever-1 is best understood as part of the endocytic machinery that coordinates ligand uptake, vesicular maturation, and immune-cell positioning. Its effects appear to arise primarily through cargo routing and compartmental processing rather than through intrinsic kinase-mediated signalling (Kzhyshkowska & Krusell, 2009; Gurung et al., 2025).

2.5.2 Clever-1 in immune-regulatory macrophage states

Clever-1 expression in myeloid compartments is associated with macrophage differentiation states characterised by high scavenging capacity and attenuated interferon priming (Canton et al., 2013; Siebeler et al., 2023). In human monocyte-derived macrophages, *STAB1* expression is induced under differentiation conditions driven by macrophage colony-stimulating factor (M-CSF), IL-4, and glucocorticoids, whereas classical pro-inflammatory stimuli such as IFN-γ or Toll-like receptor ligands reduce its expression (Kzhyshkowska, 2006; Palani et al., 2016). Expression thus aligns with macrophage phenotypes commonly described as immunoregulatory or alternatively activated, although functional output varies by tissue context (Gordon, 2010; Siebeler et al., 2023).

Transcriptomic analyses of *STAB1*-high macrophage populations demonstrate enrichment of gene programmes linked to scavenging, lipid handling, and extracellular-matrix interaction, together with comparatively lower baseline expression of interferon-stimulated genes (Palani et al., 2016; Timperi et al., 2022; Siebeler et al., 2023). In peripheral-blood monocytes, Clever-1-high subsets exhibit reduced inflammatory priming and diminished Th1-skewing capacity in co-culture systems (Palani et al., 2016). Together, these findings associate Clever-1 with macrophage states in which inflammatory signalling is moderated rather than absent (Fleming, 2011; Siebeler et al., 2023).

Perturbation studies support this interpretation. In primary human macro-phages, suppression or antibody-mediated inhibition of Clever-1 has been as-sociated with

increased surface expression of antigen-presentation and co-stimulatory molecules, including HLA-DR and CD86, together with induction of interferon-responsive gene programmes (Viitala et al., 2019; Virtakoivu et al., 2021; Hollmén et al., 2022). These changes have been observed in parallel with altered endolysosomal organisation and reduced degradative routing, suggesting that vesicular processing may influence both inflammatory set point and antigen persistence, although the causal relationship between trafficking alterations and transcriptional reprogramming remains incompletely defined (Pauwels et al., 2017; Virtakoivu et al., 2021).

In vivo observations are consistent with a role for Clever-1 in maintaining reg-ulated inflammatory set points under selected physiological conditions. In models of sterile tissue injury and chronic liver damage, genetic deletion of Clever-1 has been associated with enhanced inflammatory cell infiltration and delayed resolution, supporting a context-dependent contribution of Clever-1-expressing macrophages to the limitation of inflammatory escalation during tissue repair (Rantakari et al., 2016; Siebeler et al., 2023). A similar inter-pretation has been proposed for specialised tolerogenic settings such as preg-nancy, where reduced *STAB1* expression in placental macrophages from pre-eclamptic pregnancies has been associated with increased inflammatory signa-tures (Palani et al., 2011).

2.5.3 Clever-1, lipid handling, and endolysosomal organisation

Clever-1 mediates uptake of lipid-associated cargo, including modified lipoproteins and apoptotic membranes enriched in phospholipids and sterol-containing components (Kzhyshkowska et al., 2005; Park et al., 2009; Rantakari et al., 2016). In this way, it contributes to entry of extracellular lipid material into the endolysosomal system of macrophages and sinusoidal endothelial cells (Kzhyshkowska, 2010; Gurung et al., 2025).

This is relevant to sterol handling because lysosomal networks are major sites of lipid hydrolysis, sterol liberation, and subsequent redistribution (Ikonen, 2008; García-Ruiz et al., 2021). Clever-1 is not a sterol-transfer protein, but a receptor that influences which cargo enters these compartments and how it is routed after internalisation (Kzhyshkowska, 2010; Cullen & Steinberg, 2018; Gopaldass et al., 2024). Its metabolic relevance therefore lies in substrate delivery and exposure to lysosomal processing rather than in direct mediation of cholesterol transport.

Experimental perturbation of Clever-1 alters endolysosomal maturation dynamics (Virtakoivu et al., 2021). Because lipid hydrolysis and sterol mobilisation depend on lysosomal organisation, such changes in vesicular routing could secondarily affect intracellular sterol distribution (Ikonen, 2008; Ballabio & Bonifacino, 2020; García-Ruiz et al., 2021). However, direct quantitative evidence linking Clever-1

modulation to altered cholesterol flux in primary macrophages remains limited. Current data therefore place Clever-1 within the endocytic pathway rather than as a defined regulator of sterol-transfer machinery (Kzhyshkowska, 2010; Gurung et al., 2025).

These lipid-handling associations should be interpreted cautiously. As noted above, *STAB1* expression marks macrophage states enriched for scavenging and lipid-associated programmes, but whether Clever-1 actively drives these configurations or is preferentially expressed in cells adapted to sustained uptake remains unresolved (Palani et al., 2016; Timperi et al., 2022; Siebeler et al., 2023).

The endolysosomal position of Clever-1 is also relevant to antigen handling. In macrophages lacking Clever-1, reduced lysosomal acidification and diminished recruitment of the v-ATPase subunit *ATP6V0A1* have been documented, together with increased intracellular persistence of internalised antigen (Virtakoivu et al., 2021). Functional assays using model antigens such as ovalbumin showed enhanced cross-presentation on MHC class I molecules under these conditions, indicating that altered endolysosomal maturation can affect antigen routing and adaptive priming, although the extent to which this generalises across physiological antigen classes remains uncertain (Virtakoivu et al., 2021; Pauwels et al., 2017).

Taken together, these findings place Clever-1 at the level of cargo entry and endolysosomal routing. In the marrow niche, its relevance to metabolic organi-sation is therefore best understood through effects on substrate availability, degradative processing, and antigen persistence rather than through direct control of intracellular sterol-transfer systems (Hegde et al., 2021; de Jong et al., 2024).

2.5.4 Soluble Clever-1

In addition to its membrane-anchored form, Clever-1 exists as a soluble circulating variant (sClever-1). Biochemical and proteomic analyses indicate that this species consists predominantly of an extracellular fragment generated by proteolytic cleavage of the full-length receptor, supporting ectodomain shedding rather than secretion of an independently translated isoform (Prince et al., 2025).

Available data suggest that sClever-1 formation is linked to receptor turnover during intracellular trafficking. Inhibition of serine proteases and vacuolar H+-ATPase activity reduces accumulation of sClever-1 in macrophage and endothelial-cell culture supernatants, consistent with regulated cleavage in acidic endosomal or lysosomal compartments (Prince et al., 2025; Blander, 2018; Hollmén et al., 2020). The predominant circulating form corresponds to an extracellular fragment of approximately 200 kDa (Prince et al., 2025).

Because sClever-1 can be measured in plasma using dual-epitope immunoassays, it provides a practical readout of receptor turnover across myeloid and endothelial compartments (Prince et al., 2025). In healthy individuals, circulating levels fall within a relatively narrow range, whereas increased concentrations have been reported in settings characterised by chronic immune activation or myeloid skewing, including solid tumours and inflammatory diseases (Prince et al., 2025).

The soluble receptor retains extracellular ligand-binding domains and can bind circulating glycoproteins, apoptotic material, and phosphatidylserine-containing membranes *in vitro* (Prince et al., 2025). Experimental studies have also reported transient binding to activated T cells and interaction with IGF2R/CI-M6PR, but the *in vivo* significance of these observations remains unresolved (Prince et al., 2025).

Overall, sClever-1 is best regarded as a circulating component of the broader Clever-1 system and as a marker of receptor turnover rather than as an independently established signalling receptor. In the context of this thesis, its main relevance lies in biomarker and pharmacodynamic interpretation rather than in a distinct mechanistic role.

2.5.5 Functional consequences of Clever-1 perturbation for innate and adaptive immunity

Across experimental systems, perturbation of Clever-1 has been associated with enhanced inflammatory gene expression and broader immune activation rather than with direct lymphocyte-intrinsic checkpoint release (Canton et al., 2013; Siebeler et al., 2023). The observed effects involve antigen persistence, dendritic-cell conditioning, cytokine milieu, and tissue architecture down-stream of myeloid and endothelial perturbation.

In primary human macrophages, antibody-mediated blockade has been associated with induction of interferon-stimulated genes and chemokines such as *CXCL10*, together with increased surface expression of antigen-presentation and co-stimulatory molecules, including HLA-DR and CD86 (Viitala et al., 2019; Virtakoivu et al., 2021; Hollmén et al., 2022). Together with altered antigen persistence and cross-presentation described above, these findings indicate a shift towards a phenotype more permissive for T-cell priming, without demonstrating direct lymphocyte-intrinsic checkpoint release (Siebeler et al., 2023).

Endothelial Clever-1 adds a further layer of immune regulation. In lymphatic endothelium, it supports leukocyte migration within lymphatic vessels and entry into inflamed tissues (Karikoski et al., 2009). In hepatic sinusoidal endothelium, it has been reported to preferentially support recruitment of $FoxP3^{+}$ regulatory T cells *in vitro* and *ex vivo* (Shetty et al., 2011). In lymphatic endothelial–dendritic cell co-culture

systems, knockdown of endothelial Clever-1 has been associated with increased MHC class II and co-stimulatory molecule expression on dendritic cells together with enhanced $CD4^+$ T-cell proliferation (Tadayon et al., 2021). *In vivo*, Clever-1-deficient mice mount more robust antigen-specific $CD4^+$ T-cell responses following immunisation, despite only modest changes in dendritic-cell migration, supporting an effect on dendritic-cell activation state rather than primary control of migration (Tadayon et al., 2021).

Clever-1 also contributes to tissue-level immune organisation. Its genetic absence has been associated with reduced endothelial *CXCL13* expression, altered localisation of B cells and T follicular helper cells, and disruption of follicular structure in splenic compartments (Tadayon et al., 2019). These structural changes coincide with interferon-inducible transcriptional features in stromal compartments (Unger et al., 2025). Consistent with the macrophage-state associations described above, loss or inhibition of Clever-1 has been linked to increased inflammatory mediator production and Th1-associated signalling in experimental systems (Palani et al., 2016; Rantakari et al., 2016; Virtakoivu et al., 2021). The adaptive consequence is therefore indirect and mediated through altered cytokine context and antigen-handling conditions rather than through direct receptor engagement on T cells (Kzhyshkowska & Krusell, 2009).

Humoral responses also appear to be influenced indirectly. Clever-1-deficient mice exhibit elevated baseline immunoglobulin levels and enhanced antibody responses to thymus-dependent and thymus-independent antigens, with conditional deletion studies identifying macrophages as a principal regulatory compartment and endothelial Clever-1 contributing to splenic microanatomy and *CXCL13*-dependent follicular organisation (Dunkel et al., 2018; Tadayon et al., 2019). An emerging line of work further suggests that stabilin receptors may interact with antigen-associated cargo: Schoufour et al. (2025) identified *STAB1/STAB2* as conformation-dependent interactors of HLA-E and demonstrated enhanced uptake of HLA-E-coated microbeads in a monocyte model, although the physiological relevance of this interaction *in vivo* remains unresolved.

Taken together, these studies indicate that perturbation of Clever-1 can influ-ence innate and adaptive immunity through compartment-specific changes in inflammatory set point, antigen routing, dendritic-cell conditioning, cytokine milieu, and tissue organisation rather than through direct receptor signalling in lymphocytes. For soluble Clever-1, evidence for *in vivo* immunoregulatory signalling remains limited.

2.5.6 Clever-1 in immune evasion contexts

In tumour settings, Clever-1 is expressed in macrophage and endothelial compartments that contribute to immune organisation within malignant tissue

(Kzhyshkowska, 2010; Hollmén et al., 2020). Immunohistochemical analyses have identified increased densities of Clever-1-positive tumour-associated macrophages in several solid cancers, where higher numbers correlate with adverse clinical outcome in cohort-level analyses (Ålgars et al., 2012; Boström et al., 2015; Tervahartiala et al., 2017; Kwon et al., 2019; Yin et al., 2020).

Single-cell and spatial datasets identify *STAB1*-high macrophage clusters enriched for lipid-handling, iron metabolism, and phagocytic gene programmes, with comparatively reduced antigen-presentation signatures (Timperi et al., 2022; Chang et al., 2025; Schoufour et al., 2025). These macrophages frequently localise to immune-excluded tumour regions, placing *STAB1*-associated macrophage states within malignant tissues characterised by restrained adaptive activation and immune exclusion.

Functional evidence from tumour models is broadly consistent with this context. In murine systems, genetic deletion or antibody-mediated inhibition of Clever-1 has been associated with reduced tumour growth and metastatic dissemination in selected settings, together with increased macrophage antigen-presentation features and enhanced $CD8^+$ T-cell infiltration (Karikoski et al., 2014; Viitala et al., 2019; Hollmén et al., 2022). Endothelial Clever-1 adds a further structural layer, as it is expressed on vascular and lymphatic endothelium and participates in leukocyte adhesion and transmigration; in some tumour types, elevated endothelial expression has been associated with increased lymph node metastasis, whereas in others stage-dependent associations have been reported (Irjala et al., 2003a; Karikoski et al., 2014; Ålgars et al., 2012; Ålgars et al., 2021). The impact therefore appears to vary by tumour type and stage.

Across tumour contexts, *STAB1* expression is enriched in macrophage and endothelial programmes associated with moderated inflammatory transcriptional profiles, constrained antigen-presentation signatures, and regulated leukocyte trafficking. This broader cancer-associated biology provides the basis for considering whether Clever-1-associated programmes are also relevant in marrow-based myeloid malignancies.

2.5.7 Relevance to Myeloid Malignancies and Marrow Niche Disease

Although much of the experimental evaluation of Clever-1 modulation has been conducted in solid-tumour systems, several features support its relevance to AML, MDS, and CMML. These diseases develop within a myeloid-rich marrow environment characterised by macrophage-associated immune regulation, altered antigen presentation, and treatment-tolerant niche organisation. In this context, a receptor linked to scavenging, endolysosomal routing, and macrophage conditioning is

biologically relevant, even if its expression and functional contribution are not expected to be uniform across patients.

Public and experimental datasets indicate that *STAB1*-associated programmes are detectable in AML and related myeloid malignancy contexts, with reported associations between higher *STAB1* expression and adverse clinical or immunological features in selected cohorts (Lin et al., 2019; Yin et al., 2025). These observations should be interpreted cautiously, as many analyses derive from bulk marrow material or model systems and do not fully resolve the cellular source of *STAB1* expression within malignant, macrophage, stromal, or endothelial compartments.

Variation across disease subtypes and differentiation states further suggests that Clever-1-associated biology is unlikely to represent a uniform feature of all AML or MDS. Assessment of *STAB1* expression may therefore contribute to characterisation of immune and stromal organisation within the bone-marrow environment rather than serve as a validated predictive biomarker. At present, such stratification approaches remain exploratory. This provides the rationale for evaluating Clever-1 modulation in myeloid malignancies while keeping interpretation anchored to cohort structure, sampling context, and pharmacodynamic endpoints.

2.6 Therapeutic Targeting of Clever-1: Preclinical Rationale and Translational Development

The biological features outlined above provide the basis for therapeutic targeting of Clever-1. Across experimental systems, genetic deletion or antibody-mediated inhibition of Clever-1 has been associated with changes in macrophage phenotype, antigen handling, interferon-responsive programmes, tissue immune organisation, and increased $CD8^+$ T-cell infiltration in selected tumour models, rather than by direct effects on lymphocyte checkpoint pathways (Karikoski et al., 2014; Viitala et al., 2019; Virtakoivu et al., 2021; Hollmén et al., 2022; Siebeler et al., 2023). These observations support the evaluation of Clever-1 blockade as a strategy to modulate myeloid and endothelial programmes associated with immune restraint, while aiming to preserve essential physiological clearance functions. Clinical translation of this strategy has proceeded primarily through antibody-mediated inhibition, with bexmarilimab (FP-1305) as the principal clinical agent.

2.6.1 Bexmarilimab (FP-1305): Agent Design, Mechanism, Biomarkers, and Clinical Optimisation

Bexmarilimab (FP-1305) is the lead clinical antibody developed to inhibit Clever-1, with pharmacodynamic effects characterised primarily in macrophage compartments while avoiding target cell depletion (Hollmén et al., 2022). The antibody is derived

from the murine anti-Clever-1 clone 3-372, which inhibited receptor-mediated endocytosis in preclinical systems. For clinical use, it was engineered as an IgG4 antibody incorporating an L248E mutation in the Fc domain (Hollmén et al., 2022; Rannikko et al., 2023). This design reduces interaction with activating Fcγ receptors and C1q, thereby limiting antibody-dependent cellular cytotoxicity and complement activation while preserving neonatal Fc receptor engagement required for physiological antibody half-life. The aim was functional modulation of Clever-1-expressing macrophages rather than depletion of the cells themselves (Gurung et al., 2025).

In macrophage systems, bexmarilimab binds surface Clever-1 and inhibits scavenger-receptor activity. Treatment has been associated with increased antigen-presentation and co-stimulatory markers together with induction of interferon-responsive gene signatures, which have served as pharmacodynamic readouts of pathway perturbation (Virtakoivu et al., 2021; Hollmén et al., 2022; Rannikko et al., 2023).

Circulating soluble Clever-1 (sClever-1), which reflects receptor turnover, can be quantified as a biomarker (Prince et al., 2025). In clinical pharmacodynamic analyses, bexmarilimab treatment has been associated with reduced circulating sClever-1 levels and with activation-associated changes in peripheral $CD8^+$ T-cell and natural killer cell subsets in sampled cohorts (Rannikko et al., 2023; Rannikko et al., 2025). At present, sClever-1 is best interpreted as a marker of target engagement rather than as a mechanistic effector or surrogate efficacy endpoint.

Dose and schedule optimisation in the development programme has incorporated pharmacodynamic and immune-correlate readouts in addition to conventional exposure metrics. A non-linear, bell-shaped relationship between dose and immune activation has been proposed, motivating evaluation of biologically active dose ranges rather than simple escalation to the highest tolerated level (Karthikeyan et al., 2026). Combination strategies have correspondingly been considered in which myeloid modulation is used as a priming component alongside other therapies (Karthikeyan et al., 2026).

Nonclinical safety profiling has supported this development strategy. In *ex vivo* whole-blood assays from healthy donors, bexmarilimab did not induce canonical pro-inflammatory cytokines such as IL-6, IL-8, TNF-α, or IFN-γ (Rannikko et al., 2023). Nonclinical characterisation likewise showed limited Fc-mediated effector activity and no systemic cytokine release signatures under tested conditions (Hollmén et al., 2022). Taken together, available mechanistic and translational data support measurable pharmacodynamic modulation of Clever-1-associated myeloid programmes, with biomarker-led optimisation incorporated into ongoing development.

2.6.2 Clinical Translation: Study Settings, Endpoints, Safety, and Immune Correlates

Clinical evaluation of Clever-1 blockade has thus far proceeded through early-phase studies designed primarily to assess safety, tolerability, pharmacokinetics, and pharmacodynamic effects rather than to establish definitive efficacy.

First-in-human development of bexmarilimab was undertaken in the phase I/II MATINS study (NCT03733990) in patients with advanced solid tumours (Rannikko et al., 2023). The enrolled population consisted largely of heavily pretreated patients with metastatic disease across multiple tumour types. Primary objectives included safety and tolerability during dose escalation and expansion, together with exploratory pharmacokinetic and pharmacodynamic analyses in peripheral blood and tumour tissue.

Within the evaluated dose range, no dose-limiting toxicities were reported and a maximum tolerated dose was not reached. Adverse events were mainly low-grade infusion-related reactions and transient laboratory abnormalities, and cytokine release syndrome was not reported in the published cohorts (Hollmén et al., 2022; Rannikko et al., 2023). Peripheral-blood and tumour-biopsy analyses showed pharmacodynamic changes consistent with myeloid activation and altered immune composition, including reduced circulating sClever-1 and activation-associated changes in $CD8^+$ T-cell and natural killer-cell subsets in sampled cohorts (Hollmén et al., 2022; Rannikko et al., 2023; Rannikko et al., 2025).

Objective responses and disease control were described in subsets of patients within expansion cohorts, but interpretation is limited by small cohort sizes, tumour heterogeneity, and the exploratory design of the study (Rannikko et al., 2023).

Clinical evaluation in haematological malignancies began in 2022 with the phase I/II BEXMAB study (FP2CLI004), an open-label trial of bexmarilimab in combination with standard-of-care regimens in higher-risk MDS, CMML, and AML. Principal cohorts have evaluated azacitidine plus bexmarilimab, with early exploration of azacitidine and venetoclax in newly diagnosed AML patients considered unfit for intensive induction therapy. Subsequent emphasis has centred on the azacitidine–bexmarilimab doublet.

The study evaluates safety, tolerability, recommended phase II dose, pharmacokinetics, and exploratory pharmacodynamic endpoints. Immune monitoring includes peripheral-blood and bone-marrow profiling of macrophage-associated markers, cellular immune subsets, and circulating sClever-1. Clinical responses and marrow-based immune correlates from azacitidine–bexmarilimab cohorts are detailed in Manuscript II of this dissertation.

Further clinical development is expected to include combination strategies in solid tumours, including pairing bexmarilimab with immune checkpoint inhibitors or cytotoxic chemotherapy. At present, available clinical data define safety and pharmacodynamic activity in solid tumours and myeloid malignancies, whereas disease-specific efficacy and therapeutic positioning will require larger and more controlled studies.

2.6.3 Combination Strategies and Positioning Within Immuno-Oncology Approaches

Combination strategies involving Clever-1 blockade have been explored in settings where myeloid regulatory programmes are implicated in immune exclusion or attenuated therapeutic responses. In these approaches, blockade has been administered alongside established modalities, with tumour growth or clinical endpoints assessed together with exploratory immune measurements.

In experimental tumour models, antibody-mediated Clever-1 inhibition has frequently been paired with lymphocyte-directed checkpoint blockade. Such modulation has been associated with altered tumour-associated macrophage phenotype and increased intratumoural $CD8^+$ T-cell abundance relative to control conditions (Viitala et al., 2019; Virtakoivu et al., 2021). In selected systems, addition of PD-1-directed therapy to Clever-1 blockade resulted in greater tumour growth control than monotherapy within those models (Viitala et al., 2019; Virtakoivu et al., 2021).

Clinical combination programmes have been built on the premise that myeloid reprogramming may improve the activity of concurrent systemic therapy. Early studies have therefore focused on the feasibility of combining Clever-1 blockade with established treatment backbones while incorporating safety, pharmacokinetic, and exploratory pharmacodynamic endpoints similar to those used in monotherapy development (Rannikko et al., 2023; Rannikko et al., 2025). Immune correlates in peripheral blood and tumour tissue have been analysed under concurrent treatment conditions.

In myeloid malignancies, this combination logic is reflected in the evaluation of bexmarilimab with azacitidine-based therapy. Detailed response analyses and marrow-based immune correlates from these cohorts are presented in Manuscript II and are therefore not repeated here. At the current stage of reporting, Clever-1 blockade in myeloid malignancies remains under clinical investigation, and interpretation should remain anchored to defined study endpoints, cohort structure, and sampling frameworks rather than extrapolated directly from solid-tumour models.

3 Aims

Clever-1 (*STAB1*) has been primarily characterized as a scavenger receptor expressed by alternatively activated, immunoregulatory myeloid cells, where it contributes to immune homeostasis and tumour-associated immune suppression in solid cancers. Accumulating preclinical and early clinical observations have positioned Clever-1 as a myeloid-directed immunotherapeutic target. However, its role in myeloid malignancies—where the malignant clone itself arises from the myeloid compartment—has remained largely undefined.

Emerging transcriptomic data and preliminary observations suggested that Clever-1 may be expressed within malignant myeloid populations in acute myeloid leukaemia (AML) and myelodysplastic syndromes (MDS), raising fundamental questions. Does Clever-1 in myeloid malignancies function solely as an immunoregulatory checkpoint molecule within the bone marrow microenvironment, or might it also contribute directly to leukaemia cell biology? How does therapeutic Clever-1 targeting reshape immune and malignant compartments in patients? And what cellular programs are influenced by Clever-1 in leukaemic cells?

Therefore, the aims of this thesis were to:

• Define the expression pattern and disease associations of Clever-1 in AML and MDS, and determine how its expression relates to myeloid differentiation state, genetic features, and bone marrow immune context.

• Evaluate the biological and therapeutic relevance of Clever-1 blockade in myeloid malignancies, including its effects on antigen presentation, immune modulation, drug responsiveness, and early-phase clinical activity in combination with azacitidine.

• Elucidate the cell-intrinsic functions of Clever-1 in leukaemic cells, with particular focus on intracellular trafficking, mitochondrial organization, lipid handling, and bioenergetic fitness.

4 Materials and Methods

The results presented in this dissertation are based on three original publications (I–III). The experimental procedures and analytical methods used to generate the data are described in detail in the respective original articles and their supplementary materials. In this chapter, I provide a structured overview of the methodological framework of the thesis and describe selected methods in sufficient detail to allow the chapter to be read independently, with emphasis on procedures that are critical for interpretation of the Results and on analyses performed locally. Table 1 is included as a navigation tool linking key assays and analyses to the corresponding publication(s).

Table 1. Overview of primary methods used in the original publications

METHOD	PURPOSE	PUBLICATION
Ex vivo primary AML/MDS profiling	Treatment-induced immunophenotypic and viability changes	I
Cytokine multiplex assay	Secreted immune mediator profiling	I
NF-κB reporter assay	Functional signalling effects of Clever-1 targeting	I
Cell line viability assays	Proliferation and drug response under antibody treatment	I
Public RNA-seq dataset analysis	Contextualisation of *STAB1* expression in AML cohorts	I
Clinical trial framework and response criteria	Safety, dose determination and survival analysis	II
Soluble Clever-1 ELISA	Systemic target engagement biomarker	II
Trial flow cytometry	Bone marrow immune subset and Clever-1 modulation	II
Bulk RNA sequencing	Transcriptional effects of Clever-1 targeting	III

Gene set enrichment analysis	Pathway-level interpretation of transcriptional changes	III
Advanced microscopy	Subcellular localisation and mitochondrial association of Clever-1	III
Mitochondrial enrichment and biochemical validation	Respiratory complex assembly and fraction purity assessment	III

4.1 Study material and ethical approvals

All studies included in this dissertation were conducted in accordance with the Declaration of Helsinki and applicable Finnish and international regulations governing biomedical research. Detailed regulatory documentation is provided in Publications I–III; the elements essential for interpretation of the present work are summarised below.

Primary human bone marrow (BM) samples from patients with acute myeloid leukaemia (AML) and myelodysplastic syndrome (MDS) analysed in Publication I were obtained from the Finnish Hematology Registry and Biobank. Samples were collected under approved biobank governance with written informed consent and processed according to standardised operating procedures. Mononuclear cells were isolated prior to cryopreservation and stored in vapour-phase liquid nitrogen until use. *Ex vivo* functional and immunophenotypic analyses were performed on thawed samples as described in Publication I, with paired baseline and 48-hour treatment conditions. Clinical metadata were provided by the biobank under approved data access agreements, and analyses were conducted using pseudonymised identifiers.

Clinical data and biological samples analysed in Publication II originated from a multicentre, single-arm ph½ 1/2 clinical trial evaluating bexmarilimab in combination with azacitidine in patients with MDS, chronic myelomonocytic leukaemia, or relapsed/refractory AML (ClinicalTrials.gov NCT05428969; EudraCT 2021-002104-12). The study was approved by a centralised institutional review board in Finland and by institutional review boards at participating US and UK sites, and all participants provided written informed consent prior to study procedures. For the purposes of this thesis, laboratory analyses performed at Medicity, University of Turku, included measurement of soluble Clever-1 concentrations by enzyme-linked immunosorbent assay (ELISA) and confirmatory flow cytometric assessment of blast and myeloid cell populations and their surface Clever-1 expression. Additional protocol-defined biomarker and immuno-phenotyping analyses were conducted at a designated central laboratory and are described in detail in Publication II. All clinical data were analysed in coded, de-identified form in accordance with approved trial governance procedures.

4.2 Reagents and experimental models

This section summarises the principal biological materials, antibodies, and experimental systems used across Publications I–III. Detailed reagent lists and panel compositions are provided in the original articles and accompanying tables; only parameters essential for interpretation are described here.

Therapeutic and detection antibodies

Bexmarilimab (FP-1305), a humanised IgG4 monoclonal antibody, was used as the central experimental perturbation *in vitro* and *ex vivo* (Publications I and III) and as the investigational medicinal product in the clinical study (Publication II). Across experimental systems, bexmarilimab was typically used at 50 µg/mL (24–48 hours for mechanistic assays; 48 hours *ex vivo*), and titrated (0.1–60 µg/mL) in 72-hour viability assays. Clinical dosing is described in Section 4.5.

As a non-targeting control, a recombinant human IgG4 isotype antibody containing the same Fc mutations (S228P, L235E, P329G) as bexmarilimab was used at equivalent concentrations (RecombiMAb human IgG4 SPLEPG isotype control, anti-hen egg lysozyme; BioXCell, Cat. #CP148). The S228P substitution prevents Fab-arm exchange, and the combined SPLEPG mutations reduce Fcγ receptor–mediated effector functions. The control differs from bexmarilimab only in antigen specificity.

Detection of Clever-1 in flow cytometry, microscopy, immunoprecipitation, and immunoblotting was performed using application-specific antibodies, primarily clone 9-11 (and clone 4G9 for immunoelectron microscopy). Appropriate species-matched isotype controls were included in all assay formats. In imaging experiments, fluorophore-conjugated antibodies were used to assess internalisation and subcellular localisation, and in immunoelectron microscopy gold-conjugated secondary antibodies were applied. For co-immunoprecipitation, biotinylated antibodies were coupled to streptavidin-coated magnetic beads with matched isotype controls.

Primary AML/MDS sample culture conditions

Primary AML and MDS BM mononuclear cells were obtained through the Finnish Hematology Registry and Biobank and cryopreserved following Ficoll-based isolation. These samples served as the ex vivo primary-cell material in Publication I. Detailed culture conditions and treatment workflows are described in Section 4.3 and in the original publication.

AML cell lines and culture conditions

AML cell lines used across Publications I and III comprised HL-60, MOLM-13, MV4-11, TF-1, Kasumi-1, KG-1, GDM1, HEL, HNT34, CMK, F36P, SKM1, and OCI-AML2, with specific subsets employed in individual experiments as detailed in the respective publications. Cells were maintained at 37°C in a humidified 5% CO_2 atmosphere in RPMI-1640, IMDM, or AlphaMEM supplemented with 10–20% fetal bovine serum and antibiotics, with additional growth factors where required (e.g., GM-CSF for TF-1 and F36P). KG-1 cells were cultured in IMDM with 20% serum. For Seahorse extracellular flux assays, cells were transferred to bicarbonate-free assay medium supplemented with glucose, glutamine, and pyruvate prior to measurement. Cell lines were maintained under standard sterile conditions and routinely monitored for mycoplasma contamination.

Key kits and reagents

Commercial assay kits were used according to manufacturers' instructions unless otherwise stated. Viability and proliferation assays included ATP-based luminescence (CellTiter-Glo) and resazurin-based (AlamarBlue) readouts. NF-κB reporter activity was measured using a luciferase-based detection system. Bulk RNA extraction for transcriptomic analyses was performed using column-based purification kits with quality control prior to sequencing. Mitochondrial isolation in Publication III utilised translocase of the outer mitochondrial membrane 22 (TOM22)-based magnetic enrichment, followed by biochemical, proteomic, and lipidomic analyses. Blue Native polyacrylamide gel electrophoresis (BN-PAGE), immunoblotting, liquid chromatography–tandem mass spectrometry (LC–MS/MS), and ultra-high-performance liquid chromatography–tandem mass spectrometry (UHPLC–MS/MS) workflows were conducted as detailed in the respective publications.

4.3 *Ex vivo* and *in vitro* functional assays (Publication I)

This section summarises the *ex vivo* analyses performed on primary AML and MDS BM samples in Publication I, together with supporting *in vitro* assays. Detailed panel compositions and reagent lists are provided in the original publication; only parameters required for interpretation of the Results are outlined here.

Primary sample workflow

Thawed BM mononuclear cells were analysed either immediately at baseline (0 h) or after 48 hours of culture under defined treatment conditions. Bexmarilimab was applied at 50 µg/mL, with an irrelevant human IgG4 antibody at an equivalent

concentration as control. Where indicated, azacitidine (300 nM or 1 μM) and/or venetoclax (50 nM) were added as specified in Publication I.

Short-term cultures were performed at two sites using harmonised analytical principles but distinct supportive conditions. At Medicity, cells were maintained in IMDM supplemented with 1% serum, whereas at FIMM cultures were established in RPMI-based medium containing 10% serum and Hs-5–derived conditioned medium to support *ex vivo* viability. These differences are relevant when interpreting site-specific comparisons but did not alter the core exposure conditions.

Flow cytometry and gating principles

Flow cytometric profiling was performed at baseline and after 48-hour treatment to characterise blast, monocyte-like, and lymphoid populations and to quantify Clever-1 and HLA-DR expression. Viable cells were identified using fixable viability dyes, and gating strategies were harmonised across sites. Leukocytes were defined by CD45 expression and scatter characteristics. Within $CD45^+$ cells, blasts were identified by CD34 expression, and monocyte-like populations by CD14 and/or CD16, with additional markers as detailed in Publication I.

To ensure robust quantification, analyses of Clever-1 and HLA-DR expression were restricted to populations representing more than 5% of the parent population and/or containing more than 100 recorded events in the corresponding IgG4-treated control well. Marker expression was reported as median or geometric mean fluorescence intensity as appropriate. Relative viability of gated populations was calculated by normalising the number of viable cells in treated wells to the matched IgG4 control within the same sample. These thresholds and normalisation principles are central to interpretation of treatment-induced immunophenotypic changes.

Cytokine and reporter assays

Soluble immune mediators in conditioned media from primary BM cultures were quantified using a multiplex bead-based cytokine assay (Publication I), with concentrations derived from assay-specific standard curves. This provided a complementary soluble readout of treatment-associated immune modulation.

NF-κB pathway activity was assessed using THP1-Lucia™ NF-κB reporter cells. Cells were exposed to bexmarilimab or IgG4 control (10 μg/mL) for 18–24 hours, and luciferase activity in culture supernatants was measured using a luminescence-based detection system. Where indicated, a recombinant CLEVER-1 fragment was used to assess specificity. Luminescence intensity reflected NF-κB promoter activity as described in Publication I.

Supporting viability assays

To complement primary sample analyses, AML cell lines were subjected to short-term ATP-based viability assays and longer-term metabolic readouts. For 72-hour assays, cells were treated with increasing concentrations of bexmarilimab (0.1–60 µg/mL), with or without azacitidine (1 µM) and/or venetoclax (50 nM), and viability was quantified using a luminescence-based ATP assay. In extended 7-day cultures of KG-1 cells, bexmarilimab (50 µg/mL) or IgG4 control was applied, with additional agents added at defined intervals, and viability was assessed using a resazurin-based assay. These *in vitro* systems provided controlled conditions to support interpretation of the *ex vivo* findings in primary samples.

4.4 Clinical trial procedures (Publication II)

This section summarises the clinical framework underlying Publication II, focusing on elements required to interpret safety, response outcomes, and biomarker findings presented in this thesis. Full protocol details are provided in the original publication and its supplementary materials.

Study design and dosing framework

Publication II reports the phase 1 dose-escalation component of a multicentre, single-arm ph½ 1/2 study evaluating bexmarilimab in combination with azacitidine in patients with higher-risk MDS, CMML, or relapsed/refractory AML. Dose escalation followed a prespecified phase 1 design across three intravenous dose levels of bexmarilimab (1, 3, and 6 mg/kg). Bexmarilimab was administered once weekly in 28-day cycles in combination with standard-dose azacitidine. Azacitidine was administered as per label at 75 mg/m² subcutaneously (or intravenously in the USA) on days 1–7 of each cycle, or on days 1–5 and 8–9 according to local practice. Dose-limiting toxicities were evaluated during cycle 1 according to prespecified criteria, and the primary objective of the phase 1 component was safety.

Response and safety assessment

Treatment-emergent adverse events were graded according to NCI-CTCAE version 5.0. Dose-limiting toxicity was defined as a clinically significant grade ≥4 adverse event during the first cycle not attributable to underlying disease.

Response assessments were performed using disease-specific criteria: European LeukemiaNet (ELN) 2017 recommendations for AML and International Working Group (IWG) 2018 criteria for MDS. Bone marrow evaluations were conducted at protocol-defined intervals. Objective response rate and time-to-event endpoints,

including duration of response and overall survival, were analysed using Kaplan–Meier methodology as specified in Publication II

Thesis-relevant laboratory analyses

For the purposes of this dissertation, laboratory analyses performed at Medicity, University of Turku are described in greater detail. Soluble Clever-1 concentrations in peripheral blood and bone marrow were quantified by ELISA at predefined on-treatment timepoints to assess systemic target engagement.

In addition, confirmatory flow cytometric analyses of bone marrow aspirates were conducted locally to evaluate blast and myeloid cell populations and their surface Clever-1 expression. Populations were identified using standard CD45-based gating with lineage markers, and fluorescence intensity was quantified relative to isotype controls.

Comprehensive immune phenotyping and additional biomarker analyses were performed at a designated central laboratory according to the study protocol and are reported in detail in Publication II but are not reiterated here.

4.5 Mechanistic and mitochondrial studies (Publication III)

This section summarises the mechanistic *in vitro* experiments performed in Publication III to investigate Clever-1 subcellular localisation, mitochondrial function, lipid trafficking, and associated protein interactions in AML cell lines. Only parameters required to interpret the mechanistic conclusions are described; full technical details are provided in the original publication.

Imaging and intracellular localisation

Intracellular localisation of Clever-1 was examined in KG-1 cells using fluorescence microscopy following incubation with fluorophore-conjugated bexmarilimab or IgG4 control. Cells were fixed, permeabilised where appropriate, and co-stained with antibodies against Clever-1 and mitochondrial markers. Super-resolution Airyscan imaging was used to acquire z-stacks for three-dimensional analysis. Colocalisation was quantified in Fiji using object-based segmentation (DiANA plugin), with exclusion of border-touching structures to avoid partial-volume artefacts. Quantification was performed at the single-cell level from three-dimensional image stacks, with the unit of analysis defined as in Publication III.

Ultrastructural validation was performed by immunoelectron microscopy using anti–Clever-1 antibodies and gold-conjugated secondary antibodies. Gold particles

localised to mitochondrial structures were manually quantified, supporting the fluorescence-based localisation findings.

Mitochondrial isolation and validation

Mitochondria were enriched from AML cell lines using magnetic isolation based on TOM22, an outer mitochondrial membrane protein. Following cell homogenisation, TOM22-conjugated magnetic microbeads were used to selectively capture mitochondria, which were recovered by magnetic separation. This enrichment strategy enabled downstream biochemical, proteomic, and lipidomic analyses on mitochondrial fractions.

Fraction purity was assessed by immunoblotting for compartment-specific marker proteins to confirm mitochondrial enrichment and exclude significant cytosolic or endoplasmic reticulum contamination. Assembly of respiratory chain complexes and supercomplexes was evaluated by BN-PAGE followed by immunoblotting using established migration patterns for complex identification.

Proteomic analyses and filtering logic

To characterise Clever-1–associated protein complexes, KG-1 cells were treated for 24 hours with bexmarilimab or IgG4 control and subjected to co-immunoprecipitation using biotinylated anti–Clever-1 antibodies immobilised on streptavidin-coated magnetic beads, with matched isotype controls. Bound proteins were digested on-bead and analysed by LC–MS/MS.

For each identified protein, abundance in the Clever-1 pulldown was normalised to the corresponding isotype control to generate a quotient ratio. Proteins with a quotient value below 4 were excluded to reduce non-specific background, as defined in Publication III. In addition, CRAPome database scores were used to flag commonly observed contaminants. Only proteins passing these filtering criteria were included in downstream comparative analyses between bexmarilimab- and IgG4-treated samples. This filtering strategy is central to interpretation of the reported Clever-1 interactome.

Metabolic and functional assays

Lipid trafficking was assessed using fluorescently labelled acetylated LDL (acLDL). AML cells were pretreated with bexmarilimab or IgG4 for 24 hours and then pulsed with acLDL for 2 hours. In whole-cell analyses, extracellular fluorescence was quenched prior to acquisition. For mitochondrial analyses, mitochondria were isolated following acLDL exposure and analysed separately. Uptake was quantified as

the percentage of acLDL-positive events and by fluorescence intensity, enabling comparison of lipid accumulation in total cells and mitochondrial fractions.

Mitochondrial function under metabolic stress was further evaluated using membrane potential– and mass-dependent dyes and by extracellular flux analysis. Oxygen consumption rate (OCR) was measured using a mitochondrial stress test following 48-hour antibody treatment. Sequential addition of respiratory inhibitors enabled calculation of basal and maximal respiration parameters, and OCR values were normalised to cell number determined by nuclear staining at the end of the assay. This normalisation principle is essential for interpreting treatment-associated differences in respiratory capacity.

Mitochondrial lipid composition was analysed after 24-hour treatment by extracting lipids from isolated mitochondrial fractions and performing UHPLC–MS/MS–based profiling. Relative lipid abundances were compared between treatment conditions as described in Publication III.

Together, these imaging, biochemical, proteomic, and metabolic approaches provided complementary evidence linking Clever-1 targeting to altered mitochondrial lipid handling and respiratory function in AML cells.

4.6 Computational analyses

This section summarises the computational approaches applied to transcriptomic and multi-omic datasets in Publications I and III. Only parameters required for interpretation of the Results are described here; detailed workflows are provided in the original publications.

Public RNA-seq datasets (BEAT-AML, TCGA-LAML)

To contextualise *STAB1* (Clever-1) expression in AML, publicly available RNA sequencing datasets were analysed in Publication I. Conditional quantile normalised log2RPKM expression data and associated metadata were obtained from the BEAT-AML dataset. Only bone marrow aspirate samples annotated as AML or related precursor neoplasms and flagged for inclusion in RNA analyses were retained

For TCGA-LAML, FPKM-UQ normalised expression data and corresponding clinical annotations were downloaded from the Genomic Data Commons. Expression values were log2-transformed, and normal tissue samples were excluded. To align with the immunophenotypic primary cohorts, analyses were restricted to FAB subtypes M0–M2 and M4–M5. Group comparisons were performed in R using non-parametric tests as appropriate.

Bulk RNA-seq (Publication III)

In Publication III, bulk RNA sequencing was performed on AML cell lines (KG-1, HL-60, MOLM-13) following 24–48 hour treatment with bexmarilimab (50 µg/mL) or IgG4 control. Differential gene expression analysis was conducted using standard RNA-seq statistical modelling by an external sequencing provider, with p-values adjusted for multiple testing using the Benjamini–Hochberg false discovery rate procedure.

Gene set enrichment analysis

Gene set enrichment analysis was applied to preranked gene lists derived from differential expression analyses in Publication III using the Broad Institute implementation and Hallmark gene sets. Enrichment was assessed using permutation-based testing, and normalised enrichment scores and enrichment plots were used to interpret treatment-associated transcriptional programmes.

Software environments

Public dataset analyses were conducted in R. Flow cytometry data were analysed using FlowJo or Forecyt software, and statistical analyses of functional assays were performed in GraphPad Prism. Image processing and colocalisation analyses were conducted in Zen and Fiji, including the DiANA plugin. Proteomic data were processed using standard database-search pipelines as described in Publication III. Further study-specific details are provided in the respective publications.

4.7 Statistical analysis

Replicates and normalisation principles

Unless otherwise specified, n denotes biological replicates. Technical replicates within a single experiment were averaged prior to statistical analysis.

In primary bone marrow experiments (Publication I), each patient sample was treated as an independent biological replicate. Paired baseline (0 h) and 48-hour treatment conditions were analysed within the same sample unless otherwise specified. In AML cell line studies (Publications I and III), independent cultures initiated on separate occasions were considered biological replicates. Imaging-based quantifications were performed at the single-cell or field level as defined in the corresponding figure legends, and proteomic or lipidomic experiments used independent preparations where stated. In the clinical trial (Publication II), analyses were conducted at the patient level, with all treated patients included in safety analyses and evaluable patients included in efficacy analyses.

Normalisation procedures were assay-specific and are described in detail in the respective publications. In primary sample flow cytometry, relative viability of gated populations was calculated by normalising treated wells to the matched IgG4 control within each sample, and populations were analysed only if they exceeded predefined thresholds (>5% of the parent population and/or >100 events in the control condition). In cell line assays, luminescence or fluorescence readouts were normalised to control-treated conditions within each experiment. Seahorse OCR measurements were normalised to cell number determined at the end of the assay. Public RNA-seq datasets were analysed using normalised expression values as provided.

Statistical testing framework and reporting conventions

Statistical tests appropriate to data distribution and experimental design were applied as detailed in Publications I–III. For primary sample experiments, paired analyses were used for within-sample comparisons. In the clinical trial, time-to-event endpoints were analysed using Kaplan–Meier methodology. For bulk RNA-seq analyses, p-values were adjusted using the Benjamini–Hochberg false discovery rate procedure.

Across all studies, statistical significance was defined as a two-sided p-value < 0.05 unless otherwise specified. Data are presented as mean ± standard deviation or mean ± standard error of the mean as indicated in the corresponding figure legends, and adjusted p-values are reported where applicable.

4.8 Key reagents and controls by application

Table 2 summarises the primary antibodies and essential detection reagents used across the original publications, including clone information where relevant, suppliers, and the methods in which they were applied.

Table 2. Key antibodies and detection reagents used across Publications I–III

REACTIVITY	CLONE	COMPANY	METHOD
CD45 PerCP-Cy5.5	HI30	BD Biosciences	Flow cytometry
CD45 BV786	HI30	BD Biosciences	Flow cytometry
CD11b BV650	D12	BD Biosciences	Flow cytometry
CD14 Pacific Blue	M5E2	BD Biosciences	Flow cytometry
CD14 FITC	MφP9	BD Biosciences	Flow cytometry
CD16 BV786	3G8	BD Biosciences	Flow cytometry
CD16 BV605	3G8	BD Biosciences	Flow cytometry
CD34 PE	561	BioLegend	Flow cytometry
CD34 PE	581	BD Biosciences	Flow cytometry
HLA-DR, DP, DQ FITC	Tu39	BD Biosciences	Flow cytometry
HLA-DR PE-Cy7	G46-6	BD Biosciences	Flow cytometry
HLA-DR BV421	G46-6	BD Biosciences	Flow cytometry
PD-L1 APC	29E.2A3	BioLegend	Flow cytometry
Clever-1	9-11	InVivo Biotech	Flow cytometry
Clever-1	FP-1305; bexmarilimab	Abzena	Flow cytometry
hIgG4 isotype control	SPLEPG	BioXCell	Flow cytometry
Rat IgG2a isotype control	G155-178	BD Biosciences	Flow cytometry
CD3 PerCP-Cy5.5	SK7	BD Biosciences	Flow cytometry
CD8 APC	RPA-T8	BD Biosciences	Flow cytometry
CD4 PE-Cy7	RPA-T4	BD Biosciences	Flow cytometry
CD25 BV650	M-A251	BD Biosciences	Flow cytometry
CXCR3 BV510	1C6	BD Biosciences	Flow cytometry
CD45RO APC-Cy7	UCHL1	BD Biosciences	Flow cytometry
FoxP3 PE	PCH101	Invitrogen	Flow cytometry
Ki67 Pacific Blue	Ki-67	BioLegend	Flow cytometry
PD-1 FITC	EH12.2H7	BD Biosciences	Flow cytometry
Clever-1	4G9	Santa Cruz Biotechnology	Western blot
SLC25A10	Polyclonal	Proteintech	Immunofluorescence

IMPDH2	Polyclonal	Proteintech	Western blot
ATAD3A or ATAD3B	Polyclonal	Proteintech	Western blot
ATP6V0A2	Polyclonal	Invitrogen	Western blot
PDI	1D3	Enzo	Western blot
GAPDH	6C5	Hytest	Western blot
OXPHOS antibody cocktail	Multiple clones	Abcam	Western blot
Goat anti-rabbit IgG HRP	Polyclonal	DAKO	Western blot
Anti-mouse IgG HRP for IP	Polyclonal	Abcam	Western blot
TrueBlot anti-mouse IgG HRP	Polyclonal	Rockland	Western blot
CD45 PerCP-Cy5.5	HI30	BD Biosciences	Flow cytometry
CD45 BV786	HI30	BD Biosciences	Flow cytometry
CD11b BV650	D12	BD Biosciences	Flow cytometry
CD14 Pacific Blue	M5E2	BD Biosciences	Flow cytometry
CD14 FITC	MφP9	BD Biosciences	Flow cytometry
CD16 BV786	3G8	BD Biosciences	Flow cytometry
CD16 BV605	3G8	BD Biosciences	Flow cytometry
CD34 PE	561	BioLegend	Flow cytometry
CD34 PE	581	BD Biosciences	Flow cytometry
HLA-DR, DP, DQ FITC	Tu39	BD Biosciences	Flow cytometry
HLA-DR PE-Cy7	G46-6	BD Biosciences	Flow cytometry
HLA-DR BV421	G46-6	BD Biosciences	Flow cytometry
PD-L1 APC	29E.2A3	BioLegend	Flow cytometry
Clever-1	9-11	InVivo Biotech	Flow cytometry
Clever-1	FP-1305; bexmarilimab	Abzena	Flow cytometry
hIgG4 isotype control	SPLEPG	BioXCell	Flow cytometry
Rat IgG2a isotype control	G155-178	BD Biosciences	Flow cytometry
CD3 PerCP-Cy5.5	SK7	BD Biosciences	Flow cytometry

5 Results

5.1 Clever-1 Is Expressed on Malignant Myeloid Cells and Modulates Antigen Presentation and Drug Responsiveness in AML and MDS (I)

5.1.1 Malignant Myeloid Cells in AML and MDS Express Clever-1

STAB1 mRNA showed variable expression across AML cell lines in publicly available transcriptomic datasets, and transcript levels corresponded with Clever-1 surface protein expression in selected lines, supporting concordance between mRNA and protein abundance in this setting (I: Fig. 1A; Fig. S2A–B).

In primary human bulk transcriptomic data, Hemap analysis showed generally high *STAB1* expression across AML samples and detectable expression in a subset of MDS samples, with broader heterogeneity across other haematological malignancies (I: Fig. 1B).

Flow cytometric analyses of primary bone marrow samples from patients with AML and MDS, performed in two independent laboratories, confirmed Clever-1 protein expression on malignant myeloid cells, including leukaemic blasts and $CD34^+$ progenitor populations (I: Fig. 1C). Expression was most prominent in monocyte-like compartments, whereas lymphocyte and granulocyte populations showed low or absent staining based on CD45/SSC gating. Within monocyte subsets, classical ($CD14^+CD16^-$) and intermediate ($CD14^+CD16^+$) monocytes displayed the highest Clever-1 levels (I: Fig. 1D).

Clever-1 distribution varied between cell populations within individual samples, being largely confined to monocyte-like cells in some cases and extending to blast populations in others. Comparable results were obtained with surface and intracellular staining, supporting both surface and intracellular localisation in malignant myeloid cells (I: Fig. 1C).

5.1.2 Clever-1 Expression Is Highest in AML with Monocytic Differentiation

Clever-1 protein expression was significantly higher in myelomonocytic and monocytic AML (FAB M4–M5) than in less differentiated AML (FAB M0–M2) and MDS across the analysed primary bone marrow cohorts (I: Fig. 2A; Fig. S2C). Total CLEVER-1 levels were quantified within $CD45^+$ cells and normalised to the cohort median, demonstrating consistent enrichment in FAB M4–M5 despite inter-individual variability within groups.

In independent bulk RNA transcriptomic datasets, *STAB1* mRNA expression was likewise higher in FAB M4–M5 than in FAB M0–M2 AML in both the BEAT-AML (n = 192) and TCGA-LAML (n = 132) cohorts (I: Fig. 2B). Although heterogeneity was present within FAB subtypes, the relative enrichment of *STAB1* in monocytic AML was reproducible across cohorts.

Collectively, protein-level analyses in primary samples and transcript-level analyses in independent AML cohorts consistently identified AML with monocytic differentiation (FAB M4–M5) as the subgroup with the highest Clever-1/*STAB1* expression relative to less differentiated AML and MDS (I: Fig. 2A–B; Fig. S2C).

5.1.3 Clever-1 Expression Associates with Genetic and Immune Contextual Features

Clever-1 protein levels showed exploratory associations with recurrent genetic alterations in primary AML samples. Levels trended higher in cases harbouring *FLT3* and/or *NPM1* mutations than in samples carrying other frequent mutations, including *IDH1/2*, *RUNX1* and *SRSF2*, with substantial inter-individual variability within each category (I: Fig. 2C).

In public transcriptomic cohorts, *STAB1* mRNA expression was higher in *FLT3*-mutated than in *FLT3* wild-type AML in TCGA-LAML, whereas no statistically significant difference was observed in BEAT-AML, indicating dataset-dependent support for this association (I: Fig. 2D).

Clever-1 expression also related to bone marrow immune composition. Total Clever-1 protein levels correlated negatively with the proportion of lymphocytes in bone marrow samples, independent of blast percentage and across FAB subtypes; no positive correlation with lymphocyte abundance was detected (I: Fig. 2E).

5.1.4 *Ex Vivo* Clever-1 Blockade Increases HLA-DR Expression in Antigen-Presenting Cells

Bexmarilimab did not reduce AML cell line viability under the tested conditions. Increasing concentrations for up to 72 hours produced no decrease in cell viability compared with IgG4 control (I: Fig. 3A).

Primary AML and MDS bone marrow samples treated *ex vivo* for 48 hours likewise showed no consistent reduction in viability of blasts, monocyte-like cells, or lymphocytes across cohorts, although responses varied between individual samples (I: Fig. 3B–C).

HLA-DR expression increased in antigen-presenting compartments following bexmarilimab exposure. HLA-DR was significantly upregulated in monocyte-like cells in approximately one-third to two-thirds of samples with evaluable monocyte populations across cohorts, with average increases of approximately 1.2- to 2-fold; HLA-DR also increased on blasts in a minority of cases (I: Fig. 3D; Fig. S3A). Samples with low baseline HLA-DR showed the most pronounced induction (I: Fig. 3D).

Blast Clever-1 expression showed a negative, non-significant correlation with post-treatment HLA-DR levels in antigen-presenting populations (I: Fig. 3E). IFNγ concentrations increased in several, but not all, *ex vivo*–treated primary AML samples (I: Fig. S4A). In an NF-κB reporter AML cell line, bexmarilimab induced dose-dependent NF-κB activation that was reduced by a competing recombinant Clever-1 fragment (I: Fig. S4B–C).

5.1.5 Clever-1 Blockade Modulates *Ex Vivo* Sensitivity to Azacitidine and Venetoclax

To examine whether Clever-1 blockade could modify short-term drug responsiveness in primary AML/MDS samples, *ex vivo* combination experiments were performed with azacitidine and venetoclax. These assays were designed to test whether bexmarilimab might enhance early phenotypic or viability responses to standard agents, particularly in monocyte-like and blast populations. Because the exposure period was brief and the *ex vivo* setting captures only part of the marrow microenvironment, the experiments were not primarily expected to show uniform cytotoxic synergy, but rather to identify signals of sensitisation or immunophenotypic modulation that could justify longer-term and more physiologically complex models.

Azacitidine modestly increased HLA-DR expression in a subset of primary AML/MDS samples, with further enhancement by bexmarilimab in a proportion of cases. In the FIMM cohort treated *ex vivo* for 48 h with azacitidine (300 nM), HLA-

DR upregulation in monocyte-like cells was observed in a minority of samples; in 5/15 samples (33%), addition of bexmarilimab further increased HLA-DR compared with azacitidine alone, although comparisons of treatment-group means did not reach statistical significance (I: Fig. 4A).

At higher-dose azacitidine (1 μM), blast viability was reduced by at least 20% in 12/22 evaluable primary samples, and bexmarilimab produced an additional reduction in a limited subset. Specifically, 2/12 azacitidine-sensitive samples showed further blast reduction with the combination, and in 3 samples azacitidine-associated increases in blast viability were counteracted by bexmarilimab (I: Fig. 4B). Monocyte-like cells were more sensitive than blasts, with 12/16 samples showing at least 20% reduction, but bexmarilimab did not consistently enhance cytotoxicity in this compartment. Lymphocyte viability was variably affected, with only minor additional reductions in isolated samples (I: Fig. 4B).

In AML cell lines, short-term azacitidine exposure (1 μM, 72 h) reduced viability in 4/11 lines, and bexmarilimab did not consistently enhance cytotoxicity across lines. In contrast, in a 7-day KG-1 culture system, the bexmarilimab–azacitidine combination significantly reduced viability compared with azacitidine alone (I: Fig. 4C–D; Fig. 4E), supporting the interpretation that longer exposure may be required for measurable combinatorial effects to emerge.

To assess whether Clever-1 blockade could also influence short-term responsiveness to BCL2-directed therapy, venetoclax was next tested alone and together with azacitidine in AML cell lines and primary AML/MDS samples. In this setting, the aim was not broad direct cytotoxic synergy, but rather identification of selected cases in which bexmarilimab might modify drug sensitivity or counteract treatment-associated immunophenotypic suppression.

Venetoclax (50 nM) reduced viability in most AML cell lines, and bexmarilimab did not enhance venetoclax monotherapy in the short-term setting. However, in pooled analysis of venetoclax/azacitidine-resistant cell lines, defined by greater than 50% residual viability, the triplet combination including bexmarilimab significantly reduced cell viability. In 7-day KG-1 cultures, the venetoclax/azacitidine/bexmarilimab triplet also reduced viability compared with IgG4 control, although differences between IgG4- and bexmarilimab-containing combinations were not significant in all comparisons (I: Fig. 5A–B; Fig. 5C).

In primary AML/MDS samples, 5/18 AML and 2/4 MDS cases were *ex vivo* resistant to venetoclax, and 3 samples were resistant to venetoclax/azacitidine. Bexmarilimab sensitised blasts in 2/5 venetoclax-resistant AML samples and in 1/3 venetoclax/azacitidine-resistant samples, while further reducing blast viability in a minority of venetoclax-sensitive cases. Monocyte-like and lymphocyte populations again showed

variable responses, and treatment-group comparisons did not demonstrate consistent significant differences (I: Fig. 5D–E).

Finally, low-dose venetoclax (5 nM) reduced HLA-DR expression in 3/15 samples, whereas venetoclax plus bexmarilimab increased HLA-DR expression in 4/15 samples, including one sample with marked venetoclax-induced downregulation (I: Fig. 5F). Taken together, these data indicate that short-term Clever-1 blockade did not produce broad direct enhancement of cytotoxic drug responses *ex vivo*, but in selected samples it modified antigen-presentation markers and was associated with limited sensitisation to azacitidine- or venetoclax-containing treatment.

5.2 Bexmarilimab in Combination with Azacitidine in AML and MDS (II)

5.2.1 Patient Characteristics and Treatment Exposure

Patients with relapsed or refractory AML, frontline high-risk MDS, or MDS with no response to hypomethylating agent treatment were enrolled in the phase I dose-escalation part of the study of bexmarilimab in combination with azacitidine, with baseline demographic and disease characteristics summarised in Manuscript II (II: Table 1).

Treatment was delivered in 28-day cycles of standard-dose azacitidine with intravenous bexmarilimab at escalating dose levels of 1.0, 3.0, or 6.0 mg/kg; treatment exposure varied, with early discontinuation in some patients and ongoing multi-cycle treatment at the time of data cut-off in others (II: Fig. 1; Fig. 2).

All treated patients were included in the safety population, and all 33 enrolled patients were evaluable for response in the reported analysis, whereas pharmacokinetic and pharmacodynamic analyses were conducted according to sample availability, as specified in the manuscript (II: Table 2; Fig. 2; Fig. 4).

5.2.2 Bexmarilimab Plus Azacitidine Demonstrates a Manageable Safety Profile

Treatment-emergent adverse events (TEAEs) were recorded and graded according to standard criteria in all treated patients (II: Table 2).

No dose-limiting toxicities were observed during dose escalation at any evaluated dose level. TEAEs were common and were largely consistent with underlying

disease and azacitidine-based therapy, with predominantly haematological and infectious events, including cytopenias and infections of varying severity (II: Table 2).

Grade 3 and grade 4 TEAEs were frequent and mainly reflected haematological toxicity and infectious complications, whereas severe non-haematological events were less common. A limited number of immune-related or infusion-related events were reported, including rash, capillary leak syndrome, cryptogenic organising pneumonia, infusion-related reaction, and one fatal haemophagocytic lymphohistiocytosis event (II: Table 2; Table S3).

Serious adverse events were reported across dose levels and included infectious complications, cytopenia-related events, and selected immune-related events. Treatment discontinuations occurred due to adverse events in some patients and due to disease progression, physician decision, patient decision, or allogeneic HSCT in others. Three treatment-emergent deaths were reported, due to sepsis, neutropenic infection, and haemophagocytic lymphohistiocytosis; the haemophagocytic lymphohistiocytosis event was assessed as treatment-related and led to death (II: Fig. 1; Table 2; Table S3).

5.2.3 Dose Escalation Identifies 6.0 mg/kg as the Recommended Expansion Dose

Dose escalation proceeded sequentially with bexmarilimab at 1.0, 3.0, and 6.0 mg/kg in combination with standard-dose azacitidine, with safety review prior to escalation according to the predefined design (II: Fig. S1).

No dose-limiting toxicities were observed at any dose level. TEAEs occurred across cohorts, without an obvious descriptive increase in severe events (II: Table 2; Table S3).

Pharmacokinetic analyses showed increasing systemic exposure with dose escalation, with minimal accumulation between cycles. Pharmacodynamic analysis showed soluble Clever-1 target engagement in blood across all dose levels, with more sustained engagement at 3.0 and 6.0 mg/kg than at 1.0 mg/kg (II: Fig. 4A–C).

On the basis of the absence of dose-limiting toxicities, the overall safety profile, pharmacokinetic/pharmacodynamic data, and the highest remission rate observed at 6.0 mg/kg, this dose was selected as the recommended expansion dose for patients with MDS with no response to hypomethylating agents (II).

5.2.4 Clinical Responses Are Observed Across Dose Levels

Best overall responses were assessed according to standard criteria and are shown in the patient-level swimmer plot and response summary (II: Fig. 2; Fig. S4).

Clinical activity was observed across dose levels, but responses were concentrated in the MDS cohorts, whereas relapsed or refractory AML showed mainly stable disease and only infrequent objective responses. Because the phase 1 study did not include an azacitidine-only control arm, these responses cannot be attributed to bexmarilimab on the basis of clinical response assessment alone. In high-risk MDS, responses included complete remission, marrow complete remission, partial remission, and haematological improvement. In relapsed or refractory AML, objective responses were infrequent and comprised one complete remission with incomplete haematological recovery and one partial remission, while stable disease was the most common best response (II: Fig. 2; Fig. S4).

Responses occurred at 1.0, 3.0, and 6.0 mg/kg without a clear dose-dependent pattern in conventional response categories. This distribution is consistent with the small cohort sizes and the expectation that any contribution of bexmarilimab would be more likely to appear through pharmacodynamic and immunological changes than through a simple dose–response relationship in remission frequencies in phase 1. Both responding and non-responding patients were present at each dose level, and responses were documented in patients with high-risk mutational features and prior treatment exposure (II: Table 1; Fig. 2; Table S2).

Interpretation of these clinical responses therefore relies not only on formal response categories but also on longitudinal on-treatment biomarker changes. As described below, soluble Clever-1 target engagement provides direct pharmacodynamic evidence of bexmarilimab activity, while increased HLA-DR expression and changes in bone marrow T-cell representation support on-treatment immune modulation during combination therapy despite the absence of a 0 mg/kg comparator. Response duration varied. Some responses were transient, whereas others were maintained over multiple cycles; stable disease was noted in a subset without meeting formal response criteria, and progressive disease occurred in others despite treatment (II: Fig. 2; Fig. S4).

5.2.5 Pharmacodynamic Evidence of Target Engagement

Pharmacodynamic analyses demonstrated binding of bexmarilimab to soluble Clever-1 in blood and bone marrow. In blood, soluble Clever-1 target engagement peaked shortly after the first administration and remained more sustained at the 3.0 and 6.0 mg/kg dose levels than at 1.0 mg/kg by the end of cycle 1. In bone marrow,

binding to soluble Clever-1 was also detected at C1D28 across dose levels (II: Fig. 4C; Fig. S2B).

Relative Clever-1 expression on bone marrow monocytes and blasts did not change significantly during treatment (II: Fig. S3).

5.2.6 Modulation of Antigen Presentation in Bone Marrow

Paired baseline and on-treatment bone marrow samples from a subset of patients were analysed by flow cytometry at predefined time points to assess myeloid marker expression during bexmarilimab plus azacitidine treatment (II: Fig. S3; Fig. S5).

Consistent with the ex vivo findings in primary AML and MDS samples, HLA-DR expression on bone marrow–derived monocyte-like cells showed treatment-associated modulation, although the magnitude and timing of this change varied between patients (I: Fig. 3; Fig. 4A; II: Fig. S3D). In the main article, HLA-DR upregulation was reported in 14 of 19 evaluable patients. The increase in monocyte HLA-DR expression at C1D28 was significantly higher among responders than non-responders, supporting an association between early antigen-presentation changes and clinical response in this exploratory dataset (II: Fig. S3D; Fig. S5A–C).

HLA-DR upregulation was detected at multiple bexmarilimab dose levels, including both lower doses and the recommended expansion dose. However, owing to limited sample availability and small dose-level subgroups, these analyses were not powered to establish definitive dose-dependent pharmacodynamic effects (II: Fig. S3; Fig. S5).

5.2.7 Changes in Bone Marrow Immune Composition

Bone marrow immune composition was further assessed by flow cytometry in samples collected at screening and predefined on-treatment time points (II: Fig. S3; Fig. S5). Clever-1 expression on bone marrow monocytes and blasts showed inter-patient variability and did not demonstrate a uniform treatment-associated directional change across all analysed patients (II: Fig. S3A–C).

Bone marrow lymphocyte analyses showed changes in $CD4^+$ and $CD8^+$ T-cell populations during treatment. $CD4^+$ T-cell representation increased in some patients, particularly at higher dose levels, and $CD8^+$ T-cell increases were more pronounced at 6.0 mg/kg than at 1.0 mg/kg. These lymphocyte changes did not correlate clearly with monocyte HLA-DR upregulation, suggesting that myeloid antigen-presentation changes and T-cell compartment changes reflected partially distinct exploratory pharmacodynamic readouts (II: Fig. S5).

Responders had higher baseline bone marrow $CD3^+$ T-cell numbers than non-responders, indicating that the pre-existing immune composition of the marrow may have influenced treatment responsiveness. Overall, the exploratory flow-cytometry analyses support on-treatment modulation of the bone marrow immune compartment, particularly involving monocyte HLA-DR expression and T-cell representation, but interpretation is limited by small sample numbers and inter-patient heterogeneity (II: Fig. S5).

5.2.8 Exploratory Associations with Clinical Response

Exploratory analyses linking immune phenotyping to best overall response were descriptive and restricted to patients with evaluable paired samples, with interpretation limited by sample size and material availability (II: Fig. S3–S5).

HLA-DR expression on bone marrow monocytes increased in a subset of patients and was significantly higher at C1D28 in responders than non-responders, although the small sample size and inter-patient variability preclude defining a reproducible response threshold (II: Fig. S3D; Fig. S5C).

Changes in bone marrow lymphocyte populations were heterogeneous and did not correlate clearly with monocyte HLA-DR upregulation. Nevertheless, responders showed higher baseline bone marrow $CD3^+$ T-cell numbers than non-responders, indicating that the pre-existing immune composition of the marrow may have contributed to treatment responsiveness in this exploratory analysis (II: Fig. S5). Because paired sample availability was limited and the study did not include a pre-treatment observation phase, these findings should be interpreted as hypothesis-generating rather than as definitive evidence of treatment-induced immune remodelling.

5.3 Clever-1 is associated with mitochondrial lipid handling and respiratory fitness in AML cells (III)

5.3.1 Clever-1 Is Expressed in AML Cell Lines and Supports Bexmarilimab Internalisation

Clever-1 expression was heterogeneous across AML cell lines at both surface and total protein levels, with KG-1 displaying the highest overall abundance in the analysed models (I: Fig. 1A; III: Fig. 1A). Together with the findings from Manuscript I, this supported the selection of KG-1 cells as the principal model for mechanistic studies in Manuscript III.

Bexmarilimab bound surface Clever-1 and showed temperature-dependent internalisation in KG-1 cells. At 4 °C, antibody staining remained confined to the plasma membrane, whereas after a shift to 37 °C for 30 min the signal redistributed to intracellular compartments, consistent with receptor-mediated uptake (III: Fig. 1B).

Clever-1 blockade induced early transcriptional reprogramming. Bulk RNA sequencing of KG-1 cells exposed to bexmarilimab for 24 h identified 41 differentially expressed transcripts (adjusted $p < 0.05$), including upregulation of genes encoding mitochondrial import, translation, and respiratory chain components (*TOMM7*, *MRPL12*, *HSPE1*, *NDUFB2*, *COX6A1*, *ATP5IF1*) (III: Fig. 1C). Gene set enrichment analysis demonstrated enrichment of oxidative phosphorylation, hypoxia, and adipogenesis pathways at this timepoint (III: Fig. 1C).

At 48 h, few individual transcripts remained significantly altered; however, pathway-level analysis revealed downregulation of oxidative phosphorylation, fatty acid metabolism, and reactive oxygen species signatures (III: Fig. 1D), suggesting a time-dependent shift from early enrichment of oxidative phosphorylation-related programmes at 24 h to later suppression of oxidative and lipid metabolic signatures at 48 h.

5.3.2 Clever-1 Associates with Mitochondrial Compartments and Protein Complexes in AML Cells

The rationale for examining mitochondrial association was not based on transcriptional changes alone. In KG-1 cells, Clever-1 was internalised after antibody engagement, and bexmarilimab treatment produced early changes in mitochondrial transcriptional programmes. In addition, subsequent protein-interaction analyses identified mitochondrial-associated candidates among Clever-1-linked proteins. Mitochondrial association was therefore interpreted as a specific, model-based finding in KG-1 cells rather than as a presumed canonical localisation pattern of Clever-1.

Super-resolution Airyscan microscopy demonstrated partial spatial overlap between Clever-1 and mitochondrial structures in KG-1 cells. Clever-1 appeared as discrete intracellular puncta, a subset of which colocalised with the inner mitochondrial membrane marker SLC25A10 (III: Fig. 2A).

Three-dimensional segmentation and proximity analysis showed that approximately one-third of mitochondria contained at least one Clever-1-positive punctum, whereas such overlap was infrequent in isotype control samples; this difference was consistent across imaging replicates (III: Fig. 2B). These findings indicate partial association of Clever-1-positive intracellular structures with mitochondria in KG-1 cells rather than uniform redistribution of total cellular Clever-1 to mitochondria.

Immunoelectron microscopy provided ultrastructural support for this association. Gold-labelled Clever-1 signal was detected adjacent to or in association with mitochondria, and quantitative analysis across transmission electron microscopy fields demonstrated a higher proportion of mitochondria associated with Clever-1 labelling compared with control antibody staining (III: Fig. 2C).

Respiratory chain organisation was selectively altered following bexmarilimab treatment. Conventional SDS–PAGE of enriched mitochondrial fractions showed no detectable changes in steady-state levels of individual oxidative phosphorylation subunits across duplicate experiments, whereas Blue Native PAGE revealed a subtle but reproducible reduction in respiratory chain complex IV assembly and its dimeric form (IV_2); other complexes did not show uniform alterations (III: Fig. 2D–E).

Together, these imaging, ultrastructural, and mitochondrial fractionation findings support a partial association between Clever-1-positive intracellular structures and mitochondrial organisation in KG-1 cells, accompanied by selective alteration of respiratory chain complex IV assembly following bexmarilimab treatment.

5.3.3 Clever-1 Blockade Modulates the Clever-1 Interactome and Mitochondrial-Associated Protein Complexes in AML Cells

Co-immunoprecipitation followed by mass spectrometry was used to examine whether bexmarilimab treatment altered Clever-1-associated protein complexes in KG-1 cells. Using the anti–Clever-1 antibody 9–11 for pulldown, several proteins showed altered recovery after bexmarilimab treatment compared with isotype-treated controls (III: Fig. 3A; Supplementary Table 1).

Western blot validation of repeated 9–11 pulldowns confirmed reduced recovery of Clever-1, ATAD3, and IMPDH2 after bexmarilimab treatment, while input lysates and isotype pulldowns served as controls (III: Fig. 3B). These findings identified ATAD3 and IMPDH2 as mitochondrial-associated candidates whose recovery with Clever-1 was altered following bexmarilimab exposure.

Reciprocal pulldown experiments yielded a distinct pattern. Biotinylated ATAD3 and IMPDH2 antibodies recovered increased amounts of Clever-1 from bexmarilimab-treated cells relative to controls, with the effect more pronounced in ATAD3 pulldowns and greater variability observed for IMPDH2 (III: Fig. 3C). This opposing pattern is compatible with bexmarilimab modifying the detectable association between Clever-1 and these proteins, potentially through altered complex organisation or altered epitope availability.

Subcellular fractionation further showed that total Clever-1 levels were reduced in whole-cell lysates following bexmarilimab treatment, whereas mitochondrial Clever-1 abundance remained unchanged. Mitochondrial ATAD3 levels were similarly unaffected (III: Fig. 3D). As part of fraction purity/control analyses, western blot validation supported enrichment of mitochondrial fractions and limited contamination from non-mitochondrial compartments, with enrichment of the mitochondrial marker ATAD3A and absence of detectable GAPDH in isolated mitochondria. These blots also included detection of Clever-1 and human IgG/IgG4 to assess possible antibody carryover into the mitochondrial fraction. In this analysis, IgG4/bexmarilimab signal was not detected in isolated mitochondrial fractions, indicating that the mitochondrial-associated Clever-1 findings were not explained by detectable antibody accumulation within the mitochondrial fraction.

Bexmarilimab treatment was therefore associated with reproducible changes in Clever-1-associated protein recovery, including ATAD3 and IMPDH2, without consistent changes in mitochondrial ATAD3 abundance or depletion of the mitochondrial Clever-1 pool (III: Fig. 3A–D; Supplementary Table 1). Together with the microscopy and fractionation data, these findings support the interpretation that Clever-1-associated trafficking intersects with mitochondrial-associated protein complexes in KG-1 cells.

5.3.4 Clever-1 Blockade Reduces Lipoprotein-Derived Lipid Trafficking to Mitochondria in AML Cells

Bexmarilimab reduced scavenger receptor–mediated acLDL uptake in KG-1 cells. Following antibody treatment and pulsing with fluorescent acLDL, whole-cell flow cytometry demonstrated decreased uptake compared with isotype control, although the magnitude varied between experiments (III: Fig. 4A).

The reduction was more pronounced in mitochondria-enriched fractions. acLDL-associated fluorescence in mitochondrial isolates was lower in bexmarilimab-treated cells than in controls, exceeding the relative decrease observed at the whole-cell level and indicating impaired trafficking of lipoprotein-derived material to mitochondria (III: Fig. 4A).

Targeted lipidomic profiling of isolated mitochondria showed preservation of overall lipid class distribution, with phosphatidylcholines and phosphatidylethanolamines remaining predominant in both groups. However, differential analysis identified modest but reproducible reductions in selected mitochondrial phosphatidylcholine and phosphatidylethanolamine species following bexmarilimab treatment (III: Fig. 4B–C; Supplementary Fig. 2). Changes varied between replicates and were not uniform across all detected species.

Mitochondrial mass and receptor availability remained stable under these conditions. MitoView 640 staining did not show consistent alterations in total mitochondrial content, and bexmarilimab did not abolish acLDL surface binding or uniformly reduce surface Clever-1 levels (Supplementary Fig. 3).

5.3.5 Clever-1 Blockade Impairs Mitochondrial Respiratory Capacity in AML Cell Lines with High Baseline Oxidative Metabolism

To assess whether the trafficking- and lipid-associated effects of Clever-1 blockade were accompanied by functional changes in mitochondrial performance, mitochondrial respiration was analysed across AML cell lines with differing baseline metabolic states. Given that the preceding findings indicated altered intracellular routing and mitochondrial-associated phenotypes rather than immediate uniform cytotoxicity, any respiratory consequences were expected to be model-dependent and potentially more pronounced in cell lines with higher baseline oxidative metabolism.

Extracellular flux analysis demonstrated marked heterogeneity in baseline mitochondrial respiration across AML cell lines. Basal oxygen consumption rate (OCR), maximal respiratory capacity, and spare respiratory capacity varied substantially between models (III: Fig. 5A). Given the limited number of cell lines analysed, no firm conclusions could be drawn regarding associations with French–American–British classification, recurrent mutational status, or Clever-1 expression.

Bexmarilimab reduced mitochondrial respiratory parameters in multiple cell lines, with model-dependent magnitude. KG-1 cells showed consistent decreases in basal OCR, FCCP-stimulated maximal respiration, and spare respiratory capacity compared with isotype controls across independent experiments (III: Fig. 5B). HL-60 and other lines with relatively high baseline oxidative metabolism exhibited qualitatively similar but more variable reductions.

Baseline metabolic state related to the magnitude of response. Across cell lines, untreated baseline OCR inversely correlated with the degree of bexmarilimab-induced suppression of maximal respiration, indicating greater reductions in models with higher baseline oxidative activity (III: Fig. 5C). In contrast, cell lines with lower baseline oxidative metabolism displayed smaller or inconsistent changes.

5.3.6 Clever-1 Blockade Alters Mitochondrial Ultrastructure and Increases Mitochondrial Dysfunction Under Metabolic Stress

Transmission electron microscopy revealed treatment-associated alterations in mitochondrial ultrastructure in selected AML cell lines. In HL-60 cells, isotype-treated mitochondria were predominantly elongated with electron-dense matrices and organised cristae, whereas bexmarilimab-treated cells more frequently displayed small, rounded mitochondria with reduced matrix density and disrupted cristae. Concentric multilamellar cristae and vacuolar structures containing mitochondrial remnants were observed selectively following bexmarilimab treatment (III: Fig. 6A).

Quantitative segmentation confirmed these structural changes in HL-60 cells. Bexmarilimab treatment reduced average mitochondrial area and electron-dense (filled) area, indicating altered internal architecture, with variability between individual mitochondria (III: Fig. 6B). In contrast, MOLM-13 and KG-1 cells did not show consistent changes in mitochondrial size or filled area under standard culture conditions (III: Fig. 6C).

Mitochondrial dysfunction under metabolic stress increased following Clever-1 blockade. In KG-1 cells cultured in complete medium, bexmarilimab modestly increased the proportion of mitochondria with reduced membrane potential; this effect was amplified under glucose- and glutamine-restricted conditions and further enhanced in minimal medium supplemented with lipid-depleted serum (III: Fig. 6D).

Total mitochondrial mass remained comparable between treatment groups across conditions, indicating that altered membrane potential reflected functional impairment rather than reduced mitochondrial abundance. Cell viability did not show uniform reductions attributable to treatment within the analysed timeframe.

Overall, these results show that Clever-1 blockade is associated with ultrastructural mitochondrial changes in selected AML models and increased mitochondrial dysfunction under nutrient-restricted and lipid-depleted conditions (III: Fig. 6).

5.1

6 Discussion

6.1 Clever-1 Expression in AML and MDS Reflects Differentiation State, Immune Context, and Disease Conditioning

Clever-1, traditionally described as a marker of specialised endothelial and macrophage compartments, was also detected in malignant myeloid populations in AML and MDS. This expands the relevance of Clever-1 beyond the microenvironment alone and suggests that the receptor may also be present in leukaemic progenitors, blasts, and differentiated myeloid derivatives.

The findings support the interpretation that Clever-1 expression reflects myeloid state rather than a disease-defining feature. AML and MDS develop in a marrow environment shaped by differentiation, immune composition, stromal interactions, and treatment pressure (Lamble et al., 2020; Sallman et al., 2020; Guo et al., 2021). Across cancers, myeloid populations are also increasingly understood as dynamic immunoregulatory states rather than fixed cell types (Dou & Fang, 2021; Locati et al., 2020). In this context, the distribution of Clever-1 in AML and MDS is consistent with differentiation-linked regulation. Surface-detected Clever-1 was higher in monocyte-like populations and lower, more variable, or mainly intracellular in blast populations. Importantly, enrichment in mature myeloid fractions does not necessarily indicate a reactive, non-malignant origin, because genetically abnormal haematopoiesis can extend beyond blasts into differentiated compartments (Fernández et al., 2013; Yokoyama et al., 2018; Hasserjian et al., 2020; Dillon et al., 2021). Clever-1-high monocyte-like cells may therefore include malignant or clonally related progeny that have undergone monocytic differentiation.

This differentiation-linked pattern was also visible at cohort level. Clever-1 was enriched in AML with monocytic differentiation, particularly FAB M4 to M5, compared with less differentiated AML and MDS, although substantial patient-to-patient variability remained. Similar signals in BEAT-AML and TCGA-LAML, together with the report by Yin et al. (2025), support the view that *STAB1* and Clever-1 enrichment is reproducible in monocytic AML, but not exclusive to this lineage. Exploratory associations with mutation status should be interpreted cautiously. Protein-level trends toward higher expression in *FLT3*- or *NPM1*-mutated samples were not

consistently mirrored at the transcript level in public datasets. This is not unexpected, because transcript abundance and protein expression do not always correlate directly in heterogeneous clinical samples. More broadly, transcriptomic approaches can refine AML stratification by capturing disease-state and expression-level information that is not fully represented by recurrent mutation status alone (Docking et al., 2021). Overall, the data argue against a simple mutation-driven model. Instead, Clever-1 expression appears to be shaped by differentiation state, disease stage, prior therapies, supportive medications, cytokine environment, and sampling conditions. Genetic associations should therefore be treated as context-dependent observations that require prospective cohorts with structured clinical annotation.

Immune composition provides a second layer of interpretation. Total Clever-1 expression showed an inverse association with lymphocyte proportion in aspirated marrow, suggesting that Clever-1-high samples tended to be relatively lymphocyte poor, independently of blast percentage. This does not prove immune suppression. Aspirate-derived proportions do not show spatial immune organisation, stromal niches, or functional immune states, and they can be affected by dilution and sampling variability. However, the association is consistent with observations from other Clever-1 blockade settings, where immune effects depend on baseline inflammatory state and multicellular interaction rather than following one uniform pathway across tissues (Rannikko et al., 2024; Rannikko et al., 2025).

A further finding across the thesis is that surface Clever-1 does not necessarily reflect the total receptor pool. In primary samples, surface staining is a practical readout, but it likely captures only the detectable extracellular fraction of the receptor. AML cell-line experiments showed that a substantial intracellular Clever-1 pool can be present even when surface expression and *STAB1* mRNA are low. This is consistent with the known biology of Clever-1 as a receptor that cycles between the plasma membrane and endolysosomal compartments in macrophages (Kzhyshkowska et al., 2004a; Palani et al., 2011). Baseline surface Clever-1 is therefore unlikely to work as a standalone predictive biomarker. It is better interpreted together with cellular state, receptor trafficking, and pharmacodynamic evidence of target engagement.

Functionally, Clever-1 blockade did not produce uniform cytotoxicity in AML and MDS aspirate cultures. The effects were more consistent with modulation of cellular state, including changes in HLA-DR expression in antigen-presenting myeloid compartments and heterogeneous cytokine responses. This supports the interpretation that Clever-1 targeting primarily affects myeloid phenotype and immune-related signalling rather than acting as a direct cytotoxic intervention. In addition, NF-kappaB reporter experiments showed dose-dependent activation that was reduced by a competing recombinant Clever-1 fragment, supporting target-related engagement in at least some AML contexts. Recent AML-focused work has also linked *STAB1* to canonical IKK and NF-kappaB activity and leukaemic-cell behaviour (Yin et al., 2025).

The *ex vivo* drug-combination findings further support a context-dependent interpretation. Clever-1 blockade modified responses to azacitidine and venetoclax in a heterogeneous manner, with effects most evident in selected samples and resistant contexts. These findings should not be interpreted as a uniform sensitising effect. Hypomethylating agents can reshape interferon-linked programmes and marrow immune interactions (Ku et al., 2021; Kogan et al., 2022; Kordella et al., 2021; Daver et al., 2019), and therefore Clever-1-associated readouts are best understood within a therapy-conditioned immune environment rather than as fixed disease traits.

Two limitations are important. First, the analyses were based mainly on aspirate samples and did not show where Clever-1-positive cells were located within intact bone marrow tissue. Second, the monocyte-like cells analysed by flow cytometry could not be definitively classified as malignant or non-malignant. The data therefore support treatment-associated changes in Clever-1-expressing myeloid cells, but they do not define the exact cellular origin of these cells or prove spatial remodelling of the marrow niche.

Taken together, Clever-1 expression in AML and MDS appears to reflect differentiation state, immune composition, and prior therapy rather than baseline surface abundance alone. Clinical interpretation should therefore focus not only on whether Clever-1 is detectable at baseline, but also on whether receptor engagement produces measurable pharmacodynamic changes in myeloid cells and whether the surrounding immune compartment is capable of responding to such modulation. In this setting, target engagement may be demonstrable even when baseline expression does not clearly predict response.

6.2 Clever-1 Blockade Engages the Target and Modulates Myeloid State in AML/MDS, but Clinical Benefit Is Disease- and Immune-Context Dependent

The findings in the clinical cohort extend the expression data discussed in Section 6.1 into an *in vivo* treatment setting. The central questions were whether Clever-1 could be engaged during azacitidine-based therapy, and whether target engagement was accompanied by measurable changes in myeloid phenotype or clinical response.

Clinical activity was heterogeneous and appeared to depend more on disease context than on dose alone. Responses were observed across dose levels without a clear cohort-level dose response gradient. Benefit was most evident in high-risk MDS, including HMA-failed disease, whereas responses in relapsed or refractory AML were limited. Responses in MDS were also observed in patients with adverse molecular features, including *TP53* mutations, a marker of high-risk disease biology in MDS (Bernard et al., 2020), while AML responders did not cluster into a single genetic

subgroup. These findings show that target engagement can be achieved, but clinical benefit is not uniform. They are compatible with the interpretation that disease biology and immune context influence benefit more strongly than baseline target abundance. However, subgroup sizes were small and the study was not powered for disease-stratified comparisons. The apparent enrichment of benefit in MDS, including *TP53*-mutated disease, should therefore be treated as hypothesis-generating and requires validation in larger, prospectively stratified cohorts.

Baseline marrow Clever-1 expression did not correlate with response, and relative marrow expression did not show a consistent on-treatment shift. Clever-1 expression was highest in monocytes and was also detectable in CD34+ blast compartments, particularly in relapsed or refractory AML. However, baseline cellular expression levels did not separate responders from non-responders. This argues against using baseline surface Clever-1 as a standalone predictive biomarker and supports the interpretation in Section 6.1 that surface detectability does not necessarily represent the total receptor pool. By contrast, baseline immune composition appeared more informative. Higher baseline lymphocyte counts were associated with response, whereas blast count was not. This association does not prove causality and may be affected by marrow failure, sampling variability, and disease stage. Nevertheless, it supports the idea that clinical benefit may require an available adaptive immune compartment in addition to target expression.

Target engagement was demonstrated independently of baseline surface expression. Bexmarilimab binding to soluble Clever-1 in blood and bone marrow plasma was detected across dose levels and was sustained at higher doses. This provided an *in vivo* readout of target engagement that did not rely only on flow-cytometric measurement of cellular surface Clever-1. In parallel, receptor occupancy on circulating CD14+ monocytes showed cell-associated target coverage in a disease-relevant myeloid compartment. Together, these findings indicate that Clever-1 engagement was achieved *in vivo* even though baseline cellular expression did not predict response.

Downstream myeloid modulation was detectable but variable, in keeping with the state-linked framework outlined in 6.1. In Manuscript I, *ex vivo* bexmarilimab treatment increased HLA-DR expression in a subset of AML and MDS bone marrow samples, rather than uniformly across the cohort. In Manuscript II, paired marrow analyses during bexmarilimab plus azacitidine treatment also showed variable HLA-DR modulation on monocyte-like myeloid populations. HLA-DR increases were observed in some patients, including patients with MDS, but similar changes were not sufficient to define a reproducible responder threshold. Paired marrow availability was limited and sampling kinetics varied between individuals and dose levels, which constrains interpretation of dose-response relationships, durability, and temporal ordering relative to clinical response.

The biological meaning of HLA-DR modulation should be interpreted cautiously. HLA class II regulation is relevant in AML immune escape and therapeutic response. Relapse after allogeneic transplantation has been linked to *CIITA*-dependent downregulation of HLA class II transcriptional programmes, consistent with immune evasion through impaired antigen presentation (Toffalori et al., 2013). Conversely, pharmacological induction of APC-like programmes in AML models, including LSD1 inhibition, has been associated with *CIITA* and HLA-DR upregulation and with increased immune killing in antigen-specific co-culture assays (Yan et al., 2023). These studies provide a useful reference point for interpreting HLA-DR changes. In the present clinical study, functional antigen-presentation assays were not performed. Therefore, HLA-DR increases should be interpreted as evidence of myeloid state modulation, not as direct proof of improved antigen presentation.

Attribution is also complicated by the azacitidine backbone. Azacitidine can derepress endogenous retroelements, activate interferon-linked programmes, and modulate checkpoint pathways (Ku et al., 2021; Kogan et al., 2022; Kordella et al., 2021; Daver et al., 2019). Immune and myeloid changes during combination therapy therefore likely reflect joint effects of azacitidine and Clever-1 blockade. In this thesis, the pharmacodynamic findings are interpreted as supportive but not response-defining. Exploratory analyses did not identify a single baseline or on-treatment marker that reliably separated responders from non-responders. HLA-DR increases were more frequent among responders but also occurred in some non-responders, and no response-defining threshold emerged. Peripheral blood immune-cell counts also varied without a consistent pattern. In marrow diseases, such counts are shaped by marrow failure, treatment effects, and disease kinetics (Lamble et al., 2020).

This caution is consistent with the broader immune context of azacitidine-treated AML and MDS. Hypomethylating agents can activate interferon-linked and other immune pathways, but they can also induce inhibitory programmes. They should therefore be viewed as bidirectional immunomodulators rather than uniformly activating partners (Wolff et al., 2017; Daver et al., 2018). AML also uses several myeloid-inhibitory pathways beyond Clever-1, including VISTA and LILRB4 (Deng et al., 2018; Pagliuca et al., 2022; Mo et al., 2023; Li & Zhao, 2024). In this setting, it is unlikely that one pharmacodynamic marker would uniformly predict response to Clever-1 blockade. Interpretation should therefore be anchored to direct target engagement, target-expressing myeloid compartments, and disease context rather than to bulk peripheral blood counts alone.

From a safety perspective, the combination was manageable in this early-phase setting. There was no signal for widespread immune-related toxicity, although cohort size and follow-up limit conclusions about rare adverse events and long-term tolerability. This safety profile is relevant in the broader field of macrophage-checkpoint therapeutics. CD47-directed strategies, for example, have been associated with on-target haematological toxicities, especially anaemia and, in some settings,

thrombocytopenia, reflecting broad CD47 expression on normal blood cells. Bexmarilimab plus azacitidine did not show dose-limiting toxicities in this phase 1 study, although immune-related serious adverse events were observed in a small number of patients. These observations do not allow direct comparison across programmes, but they support continued evaluation of Clever-1 blockade as a macrophage-directed immunotherapeutic strategy.

Several limitations affect interpretation. Aspirate-derived measurements do not show spatial niche organisation or functional immune architecture in intact marrow tissue. Paired on-treatment marrow sampling was incomplete and varied between patients. Correlative pharmacodynamic markers do not establish causal order between target engagement, myeloid modulation, and response. In addition, disease phase, prior treatment, and supportive medications can all shape immune tone and cellular composition. These limitations do not negate the observed target engagement or myeloid state changes, but they limit mechanistic and biomarker conclusions.

A restrained clinical interpretation is therefore that Clever-1 blockade achieves measurable target engagement *in vivo* and can produce reproducible but heterogeneous myeloid phenotypic modulation during azacitidine-based therapy. Clinical benefit was disease- and immune-context dependent, with the strongest activity observed in high-risk MDS and limited responses in relapsed or refractory AML. Baseline marrow Clever-1 expression did not stratify response, whereas baseline lymphocyte counts and detectable myeloid state changes appeared to associate with benefit. Larger cohorts with prospective disease stratification and functional immune readouts will be needed to define predictive markers and causal mechanisms in this treatment setting.

6.3 Leukaemia Cell Intrinsic Clever-1 Regulates Trafficking-Linked Lipid Handling and Constrains Mitochondrial Adaptability

In AML models, Clever-1 also appears to function within leukaemic cells. This is important because Clever-1 has traditionally been discussed mainly as a macrophage and endothelial scavenger receptor. The findings in Manuscript III suggest that, in selected AML cells, the same receptor architecture may influence intracellular cargo routing and mitochondrial fitness.

The first requirement for this interpretation is that Clever-1 engagement is not restricted to the cell surface. In KG-1 cells, bexmarilimab was internalised at 37 °C but not at 4 °C, supporting active uptake after antibody binding. This is consistent with Clever-1 functioning as an endocytic trafficking receptor also in AML cells.

The early transcriptional response after bexmarilimab treatment was modest, but pathway analysis showed changes in oxidative phosphorylation and lipid metabolism related signatures. These changes do not prove a direct linear pathway from Clever-1 binding to mitochondrial dysfunction, but they supported further analysis of mitochondrial and lipid-associated phenotypes.

Several findings support a partial association between Clever-1-positive intracellular structures and mitochondria, rather than canonical mitochondrial localisation of Clever-1. Super-resolution imaging showed that a subset of mitochondrial profiles was associated with Clever-1-positive puncta, and immunoelectron microscopy supported mitochondrial-proximal Clever-1 labelling. In parallel, bexmarilimab treatment reduced assembly of respiratory-chain complex IV and its dimeric form, while steady-state levels of individual oxidative phosphorylation subunits were not consistently changed. These findings point to localised changes in mitochondrial organisation rather than global respiratory-chain loss or widespread mitochondrial collapse.

Interaction profiling provided additional support, although it remains correlative. ATAD3 and IMPDH2 were identified among proteins whose association with Clever-1 changed after bexmarilimab exposure. Subcellular fractionation added an important control: total Clever-1 decreased in whole-cell lysates, whereas mitochondrial Clever-1 abundance was maintained, and IgG4/bexmarilimab signal was not detected in isolated mitochondrial fractions. This makes antibody carryover into mitochondria unlikely. The data therefore support a model in which Clever-1 engagement changes protein interaction patterns that include mitochondrial-associated partners, rather than a model in which intact bexmarilimab accumulates in mitochondria.

The lipid-trafficking data are consistent with altered routing of lipoprotein-derived cargo. Bexmarilimab reduced acLDL uptake and caused a stronger reduction of acLDL-associated signal in mitochondria-enriched fractions than at the whole-cell level. Mitochondrial mass was not consistently reduced, and acLDL surface binding was not abolished. These findings argue against mitochondrial loss or complete receptor blockade as the main explanation. Instead, they support altered delivery of lipoprotein-derived material toward mitochondria. Mitochondrial lipidomics showed modest reductions in selected phosphatidylcholine and phosphatidylethanolamine species, while overall lipid-class distribution remained largely comparable. This suggests a focused change in mitochondrial membrane lipid composition rather than broad lipid depletion.

The functional effects were model-specific. AML cell lines differed substantially in baseline respiration, and this variation was not clearly explained by FAB subtype, recurrent mutations, or surface Clever-1 expression. Bexmarilimab most consistently reduced respiration in cells with higher baseline oxidative activity, particularly KG-1, whereas lower-respiring models showed weaker or more variable responses. Thus,

the data support a context-dependent mitochondrial vulnerability rather than uniform metabolic shutdown or acute cytotoxicity across AML models.

Structural readouts also showed model dependence. HL-60 cells displayed mitochondrial ultrastructural changes after bexmarilimab exposure, including smaller and more rounded mitochondria with altered internal architecture. In contrast, MOLM-13 and KG-1 cells did not show consistent ultrastructural changes under nutrient-replete conditions. This indicates that the morphological phenotype is not universal across AML models. The previously reported sensitivity of HL-60 mitochondria to mitochondrial stress provides a possible context for why this cell line showed the clearest ultrastructural response (Mondet et al., 2021).

Nutrient and serum context further supported a stress-dependent phenotype rather than constitutive mitochondrial failure. In KG-1 cells, bexmarilimab produced only modest changes in complete medium, whereas nutrient restriction increased the proportion of mitochondria with reduced membrane potential, particularly under conditions using human serum or lipid-depleted human serum. Mitochondrial mass remained largely unchanged, indicating impaired mitochondrial function rather than loss of mitochondrial content.

This stress-dependent phenotype is relevant to the marrow niche, where lipid availability is shaped by stromal and adipocyte interactions rather than by a neutral culture environment. Bone marrow adipocytes regulate haematopoiesis and leukaemic survival, AML blasts can promote adipocyte lipolysis, and adipocyte-rich environments can support fatty-acid oxidation linked survival programmes (Cuminetti & Arranz, 2019; Shafat et al., 2017; Tabe et al., 2018; Matsushita et al., 2022). In such settings, altered routing of lipoprotein-derived cargo and selective changes in mitochondrial membrane lipids could influence cellular fitness, although direct *in vivo* relevance remains to be demonstrated.

A direct biochemical route from Clever-1 trafficking to respiratory dysfunction was not established. Cholesterol handling therefore remains a plausible but unproven mechanism. Mitochondrial cholesterol accumulation can impair respiratory efficiency in other systems (Marí et al., 2006; Fernández et al., 2009; Torres et al., 2017), but mitochondrial cholesterol was not directly quantified in Manuscript III. Therefore, cholesterol-mediated effects cannot be claimed as causal. More cautiously, the combined findings support the possibility that altered lipid routing contributes to changes in mitochondrial organisation and function.

Ihe interpretation is also limited by the experimental system. Monoculture models do not reproduce spatial lipid gradients, stromal interactions, or adipocyte–blast crosstalk *in vivo*. In addition, steady-state lipidomics does not measure lipid flux or define enzymatic causality. The data therefore show altered mitochondrial

vulnerability under controlled experimental conditions, but they do not establish quantitative lipid utilisation or cholesterol trafficking *in vivo*.

Across this thesis, Clever-1 emerges as a state-linked myeloid receptor with relevance in both non-malignant and malignant compartments. In patient material, Clever-1 blockade achieved target engagement and was associated with variable myeloid phenotypic modulation during azacitidine-based therapy. In AML cell models, Clever-1 engagement intersected with intracellular trafficking of lipoprotein-derived cargo and with selected aspects of mitochondrial organisation and stress-adaptive performance. Taken together, these findings support a model in which Clever-1 contributes to immune restraint in the myeloid compartment and to metabolic adaptability in leukaemic cells. This provides a framework for understanding how Clever-1 targeting may affect both immune regulation and metabolic vulnerability in myeloid malignancies, as summarised in Figure 5.

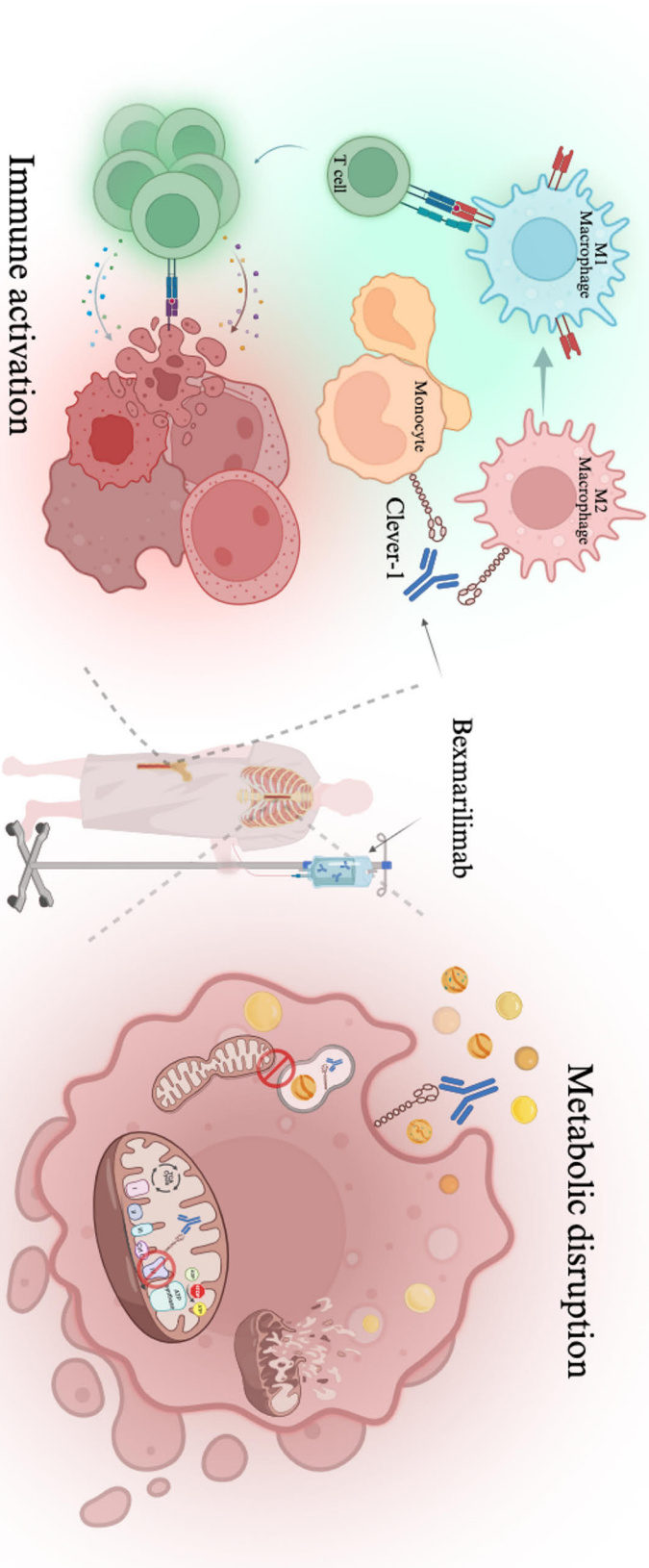
Immune activation
T cell
M1 Macrophage
Monocyte
M2 Macrophage
Clever-1
Bexmarilimab
Metabolic disruption

Figure 5. Proposed working model of the dual effects of Clever-1 inhibition in myeloid malignancies. Clever-1 blockade is proposed to act through two complementary, context-dependent mechanisms. In immunoregulatory myeloid cells, Clever-1 inhibition can promote a shift toward a more inflammatory and antigen-presentation-associated phenotype, supporting adaptive immune activation. In leukaemic cells, Clever-1 targeting affects intracellular trafficking pathways linked to lipid handling and mitochondrial organisation. These effects are most evident under metabolic stress conditions and may expose mitochondrial vulnerabilities in selected AML contexts. Illustration created with BioRender.

7 Summary

Acute myeloid leukaemia (AML) and myelodysplastic syndromes (MDS) are characterised by therapy resistance and relapse risk, reflecting immune dysfunction within the bone-marrow niche and the metabolic adaptability of malignant myeloid cells. This thesis establishes the biological and clinical relevance of the scavenger receptor Clever-1 (*STAB1*) in myeloid malignancies and evaluates therapeutic targeting with the anti–Clever-1 antibody bexmarilimab.

Clever-1 was consistently detected in malignant myeloid populations in AML cell lines and primary AML/MDS samples, including leukaemic blasts and CD34+ progenitors, with marked inter-patient heterogeneity. Expression was enriched in AML with monocytic differentiation (FAB M4–M5) compared with less differentiated AML and MDS, a pattern reproduced in independent transcriptomic cohorts.

Ex vivo Clever-1 blockade did not induce uniform cytotoxicity but promoted myeloid phenotypic modulation, most notably HLA-DR upregulation in antigen-presenting monocyte-like populations, and modified responsiveness to azacitidine and venetoclax in selected resistant settings. In a phase I/II clinical study with bexmarilimab treatment combined with azacitidine, the regimen demonstrated a manageable safety profile without dose-limiting toxicities and achieved sustained *in vivo* target engagement, evidenced by high receptor occupancy on circulating CD14+ monocytes and shifts away from an immunoregulatory phenotype. Clinical responses occurred across dose levels in high-risk MDS and relapsed/refractory AML, with activity associated with baseline immune composition rather than blast burden.

Mechanistically, we identify a previously unrecognised intracellular trafficking axis whereby AML cell–intrinsic Clever-1 translocates from the cell surface to mitochondrial compartments and regulates delivery of modified lipoprotein-derived cargo. Disruption of this pathway reduced mitochondrial lipid incorporation, impaired complex IV assembly, and diminished respiratory capacity, particularly in models reliant on mitochondrial energy metabolism and under lipid-restricted conditions. Collectively, this PhD thesis establishes Clever-1 as a context-dependent immunometabolic regulator in malignant myeloid cells and justifies continued clinical development of Clever-1–targeted therapy in myeloid malignancies.

Acknowledgements

This dissertation was conducted in MediCity Research Laboratories, at the Institute of Biomedicine, Faculty of Medicine, University of Turku, during the years 2021–2026. I wish to acknowledge the University of Turku, the Faculty of Medicine, the Institute of Biomedicine, the Molecular Biomedicine Research Track, and the Turku Doctoral Programme of Molecular Medicine for providing a supportive environment in which to learn and grow as a scientist. The research track and the opportunity to complete a laboratory rotation were decisive in leading me to the Hollmén laboratory.

I also wish to thank the InFLAMES Flagship and its doctoral module for broadening my doctoral training through courses, methodological education, visiting professors, mentoring, networking, and travel support. I am especially grateful to Professor of Practice Timo Veromaa, who kindly agreed to serve as my mentor and to offer guidance beyond the immediate scientific work of this thesis. Your out-of-the-box perspectives, encouragement, and practical guidance have helped me stay on track during these years and see things from a broader perspective. These opportunities, together with the services and support provided by Turku Bioscience Centre, were important for the scientific work presented in this thesis.

Special thanks go to Outi Irjala, chief academic officer of doctoral training at the University of Turku, whose help and guidance have been invaluable in finalizing my doctoral education and the thesis process. For the pre-examination of this thesis, my sincere gratitude goes to Docent Markus Vähä-Koskela, PhD, and Mikko Myllymäki, MD, PhD, who provided a thorough and insightful examination of the thesis. Their comments helped shape this work into a more refined form. I also wish to thank Professor Jukka Westermarck for serving on my PhD follow-up committee. His objective perspective and inspiring example provided many valuable insights along the way.

The work presented here was supported by grants from the Sigrid Jusélius Foundation, Turku University Foundation, Emil Aaltonen Foundation, Finnish Medical Foundation, Orion Research Foundation, Paulo Foundation, Uulo Arhio Foundation, and the University of Turku. Travel for education and for presenting scientific results internationally was additionally supported by the Turku Doctoral Programme of

Molecular Medicine, InFLAMES Flagship, Turku Foundation for Microbiologists, the Scandinavian Societies for Immunology, the International Union of Immunological Societies, the European Hematology Association, and Cancer Foundation Finland.

I am deeply grateful to my supervisor, Docent Maija Hollmén, who welcomed me as a summer trainee in 2019, when I had just completed my first year of medical school and had only minimal laboratory experience. Thank you for the trust you placed in me from the very beginning, for encouraging me to grow as a scientist, and for teaching me to troubleshoot, think creatively, develop hypotheses, and approach scientific questions with an open mind. I am also grateful for the flexibility that allowed me to continue in research and complete my MD thesis the following year. I will never forget our meeting in early spring 2021, when we discussed the project that would later become my PhD thesis; the confidence you showed in my ability to take on such a project has stayed with me throughout this thesis journey. You have been an inspiring role model as a principal investigator, building your own laboratory while creating a culture of high-quality science, open collaboration, and thoughtful discussion in our weekly meetings.

I also wish to thank my other supervisor, Academician Sirpa Jalkanen, MD, PhD. It has been a privilege to witness your leadership at MediCity over the past seven years. Your ability to bring together several research groups into a larger scientific community has created an environment where science can be discussed openly and from many different perspectives. You have also shown the importance of celebrating achievements and finding joy in hard work. It has been remarkable to follow your continuous drive to develop ambitious initiatives, including the InFLAMES Flagship, and to see how scientific discoveries can mature over decades toward clinical application. I am grateful for your direct comments, wise advice, and practical perspective on how scientific findings can be developed further.

I wish to thank the supervisor of my MD thesis, Reetta Virtakoivu, who was working as an enthusiastic postdoc in the Hollmén laboratory when I first started in 2019. You had the patience to teach me the foundations of scientific work and showed me how to approach science with excitement and endless curiosity. You also showed me what a privilege it can be to do scientific work for a living.

I also wish to thank another alumnus of the Hollmén laboratory, Rogerio de Figueiredo, one of the most talented and dedicated scientists I have had the pleasure to work with. You provided a true example of what one can accomplish through hard work and the pursuit of excellence.

I want to thank Sina Tadayon, the first PhD graduate I witnessed from the group, for creating such a joyful working atmosphere and for approaching science with humour, playfulness, and openness. I thank Miro Viitala and Jenna Rannikko for the valuable example you set as senior PhD students and for raising the bar for

independent scientific work. I am also grateful to Milja Hakoniemi, whom I had the privilege to supervise during her Master's thesis project and from whom I also learned a great deal. Your hard work in the laboratory allowed me to continue my studies knowing that the project was in good hands, and this work would not have been possible without you. I also wish to thank the next generation of PhD students in the group, Jesper Mickos, Mahalakshmi Karthikeyan, and Reshmi Suresh, for continuing the work with dedication and an inspiring work ethic.

Special thanks go to Stuart Prince, whose exceptional technical expertise, scientific enthusiasm, and sharp insight were central to the experimental work in my thesis. Your contribution was important in the laboratory and in the many scientific discussions that helped refine ideas, generate hypotheses, and give direction to the experiments. I also wish to extend my gratitude to the co-authors outside the Hollmén laboratory, especially Sofia Aakko and Mika Kontro, the first authors of two of the publications, for their leadership, perseverance, and hard work in bringing these articles to publication.

I wish to thank the laboratory technicians Riikka Sjöroos, Maritta Pohjansalo, Sari Mäki, Mari Parsama, and Teija Kanasuo for their endless support. Your expertise and help made my work, and the work of many others, possible. I am thankful for your patience in teaching me practical laboratory work and the importance of good day-to-day working habits.

From the Friday meeting community, including former and current members of the Jalkanen, Salmi, and Takeda groups, I want to thank Gennadi Egutkin, Karolina Losenkova Mingeaud, Dominik Eichin, Akira Takeda, Sadaf Fazeli, Rita Turpin, Nora Alnusairat, Dinghao Zheng, and Samuel Svärd for the wonderful working community. I look forward to seeing all that you will achieve in the future.

A special note of gratitude goes to Diana Lehotina, who joined the laboratory as a fellow PhD student four years ago. We quickly became close friends through lunches, spontaneous coffee breaks, and time spent together outside the laboratory. Sharing the thoughts, challenges, and occasional struggles of PhD work — as well as travels to a summer school in Sardinia, a conference in Cape Town, and many other memorable places — made this journey far more enjoyable. I am especially grateful for our shared courage to say yes to opportunities beyond our comfort zones, to enter unfamiliar scientific settings with more determination than certainty, and to realize how often the most rewarding experiences begin with simply daring to show up. Your friendship has brought laughter, perspective, and much-needed lightness to this journey, often exactly when I needed them most.

This PhD degree would not have been accomplished without my dear friends and family. To my friends from Pori, whose friendship goes all the way back to our early teenage years, thank you for being a constant reminder of true friendship. Although our lives have taken different paths, every time we meet it feels as though we

continue from where we left off. You never fail to remind me how to enjoy life without always striving for the next accomplishment, and I always leave with less stress and deep happiness for having you in my life.

I am also grateful to my friends from medical school for all the fun times and for making the years of studying more enjoyable. To Noora Tikkanen, I owe more than words can express. Your support over many years brought light to the darkest moments and gave me strength to continue toward this and other goals in life. For this I am forever grateful, and I would not be defending this thesis without you.

For my family, I am grateful to my three siblings: my brother Arttu and my sisters Anna and Assi. Each of you has taught me a great deal about life through your example, and by challenging and supporting your little brother in equal measure. I owe special thanks to Assi and Arttu for their final polish and artistic vision in shaping the cover image of this thesis. To my parents, Antti and Kirsi, who have always prioritized supporting their children and providing the best possible environment for growth, I remain deeply indebted. You have taught me the value of persistence, responsibility, and optimism, not through grand words, but through everyday example. Thank you for showing me that no goal needs to sound too ambitious or too difficult to manage, and that where there is a will, there is a way.

I am also lucky and grateful to have a large and close extended family, which has brought me much happiness throughout these years. I want to thank my late grandmother Anna-Leena, whose love, warmth, and support remain an important part of my earliest memories. Finally, I wish to thank my grandfather Kale, to whom I have dedicated this book, in honour of his truly inspiring life and all the life lessons I have received from him from my early childhood until today. His is the kind of full life I can only aspire to live.

Turku, May 2026
Arno Ville Verneri Ylitalo

References

Adachi, H., & Tsujimoto, M. Adaptor protein sorting nexin 17 interacts with the scavenger receptor FEEL-1/stabilin-1 and modulates its expression on the cell surface. Biochimica et Biophysica Acta (Molecular Cell Research), 2010; 1803(5): 553-563, 2010; 1803(5). https://doi.org/10.1016/j.bbamcr.2010.02.011

Adès L, Itzykson R, Fenaux P. Myelodysplastic syndromes. Lancet, 2014; 383(9936): 2239–2252. https://doi.org/10.1016/S0140-6736(13)61901-7

Akira S; Uematsu S; Takeuchi O. Pathogen recognition and innate immunity. Cell, 2006; 124.(4): 783–801. https://doi.org/10.1016/j.cell.2006.02.015

Alfinito F, Sica M, Luciano L, Della Pepa R, Palladino C, Ferrara I, Giani U, Ruggiero G, Terrazzano G. Immune dysregulation and dyserythropoiesis in the myelodysplastic syndromes. British Journal of Haematology, 2010; 148(1): 90-98, 2010; 148(1): 1365–2141. https://doi.org/10.1111/j.1365-2141.2009.07921.x

Alloatti A, Kotsias F, Pauwels A-M, et al. Toll-like Receptor 4 Engagement on Dendritic Cells Restrains Phago-Lysosome Fusion and Promotes Cross-Presentation of Antigens. Immunity, 2015. https://doi.org/10.1016/j.immuni.2015.11.006

Andersen J-P, Zhang J, Sun H, Liu X, Liu J, Nie J, Shi Y. Aster-B coordinates with Arf1 to regulate mitochondrial cholesterol transport. Molecular Metabolism, 2020; 42: 101055, 2020. https://doi.org/10.1016/j.molmet.2020.101055

Arber DA, Orazi A, Hasserjian RP, et al. International Consensus Classification of Myeloid Neoplasms and Acute Leukemias: integrating morphologic, clinical, and genomic data. Blood, 2022; 140(11): 1200–1228. https://doi.org/10.1182/blood.2022015850

Arellano-Ballestero H, Sabry M, Lowdell MW. A Killer Disarmed: Natural Killer Cell Impairment in Myelodysplastic Syndrome. Cells, 2023; 12(4): 633. https://doi.org/10.3390/cells12040633

Baccin C, Al-Sabah J, Velten L, et al. Combined single-cell and spatial transcriptomics reveal the molecular, cellular and spatial bone marrow niche organization. Nature Cell Biology, 2020; 22(1): 38–48. https://doi.org/10.1038/s41556-019-0439-6

Bachmann C, Ochsenbein A. Immune checkpoints regulate acute myeloid leukemia stem cells. *Leukemia*, 2025; 39(6): 1277–1293. https://doi.org/10.1038/s41375-025-02566-x

Ballabio A, Bonifacino JS. Lysosomes as dynamic regulators of cell and organismal homeostasis. Nature Reviews Molecular Cell Biology, 2020. https://doi.org/10.1038/s41580-019-0185-4

Banker DE; Mayer SJ; Li HY; Willman CL; Appelbaum FR; Zager RA. Cholesterol synthesis and import contribute to protective cholesterol increments in acute myeloid leukemia cells. Blood, 2004; 104(6): 2004–01. https://doi.org/10.1182/blood-2004-01-0395

Barakos GP; Hatzimichael E. Microenvironmental Features Driving Immune Evasion in Myelodysplastic Syndromes and Acute Myeloid Leukemia. Diseases, 2022; 10(2): 33. https://doi.org/10.3390/diseases10020033

Barakos Barbero-Camps, E.; Fernandez, A.; Baulies, A.; Martinez, L.; Fernandez-Checa, J. C.; Colell, A. Endoplasmic Reticulum Stress Mediates Amyloid β Neurotoxicity via Mitochondrial Cholesterol Trafficking. The American Journal of Pathology, 2014; 184, 2066-2081. https://doi.org/10.1016/j.ajpath.2014.03.014

Barton GM, Kagan JC. A cell biological view of Toll-like receptor function: regulation through compartmentalization. Nature Reviews Immunology, 2009; 9(8): 535-542, 2009; 9(8). https://doi.org/10.1038/nri2587

Bauer M, Vaxevanis C, Al-Ali HK, Jaekel N, Naumann CLH, Schaffrath J, Rau A, Seliger B, Wickenhauser C. Altered Spatial Composition of the Immune Cell Repertoire in Association to CD34+ Blasts in Myelodysplastic Syndromes and Secondary Acute Myeloid Leukemia. Cancers (Basel). 2021 Jan 7;13(2):186. https://doi.org/10.3390/cancers13020186

Bernard E, Nannya Y, Hasserjian RP, et al. Implications of TP53 allelic state for genome stability, clinical presentation and outcomes in myelodysplastic syndromes. Nature Medicine, 2020; 26: 1549–1556. https://doi.org/10.1038/s41591-020-1008-z

Bernard E, Tuechler H, Greenberg PL, et al. Molecular International Prognostic Scoring System for myelodysplastic syndromes. NEJM Evidence, 2022; 1(7): EVIDoa2200008. https://doi.org/10.1056/EVIDoa2200008

Bhatt S, Pioso MS, Olesinski EA, et al. Reduced mitochondrial apoptotic priming drives resistance to BH3 mimetics in acute myeloid leukemia. Cancer Cell, 2020; 38(6): 872–890.e6. https://doi.org/10.1016/j.ccell.2020.10.010

Bizymi N, Bjelica S, Kittang AO, et al. Myeloid-Derived Suppressor Cells in Hematologic Diseases: Promising Biomarkers and Treatment Targets. HemaSphere, 2019; 3(1): e168. https://doi.org/10.1097/HS9.0000000000000168

Blander JM. Regulation of the Cell Biology of Antigen Cross-Presentation. Annual Review of Immunology, 2018; 36: 717–753. https://doi.org/10.1146/annurev-immunol-041015-055523

Boada-Romero E, Martinez J, Heckmann BL, Green DR. The clearance of dead cells by efferocytosis. Nature Reviews Molecular Cell Biology, 2020. https://doi.org/10.1038/s41580-020-0232-1

Bonnet D, Dick JE. Human acute myeloid leukemia is organized as a hierarchy that originates from a primitive hematopoietic cell. Nature Medicine, 1997; 3(7): 730–737. https://doi.org/10.1038/nm0797-730

Bonifacino JS, Rojas R. Retrograde transport from endosomes to the trans-Golgi network. Nature Reviews Molecular Cell Biology, 2006;7(8):568-579, 2006; 7(8). https://doi.org/10.1038/nrm1985

Borchers AC, Langemeyer L, Ungermann C. Who's in control? Regulation of Rab GTPases by their GEFs and GAPs. Small GTPases, 2021; 12 (2): 107-114, 2021; 12(2). https://doi.org/10.1080/21541248.2019.1685496

Borchers A-C, Langemeyer L, Ungermann C. Who's in control? Principles of Rab GTPase activation in endolysosomal membrane trafficking and beyond. Journal of Cell Biology, 2021. https://doi.org/10.1083/jcb.202105120

Borrego F. The CD300 molecules: an emerging family of regulators of the immune system. Blood, 2013; 121(11): 2012–09. https://doi.org/10.1182/blood-2012-09-435057

Boström MM, Irjala H, Mirtti T, Taimen P, Kauko T, Ålgars A, Jalkanen S, Boström PJ. Tumor-Associated Macrophages Provide Significant Prognostic Information in Urothelial Bladder Cancer. PLOS ONE, 2015; 10(7): e0133552. https://doi.org/10.1371/journal.pone.0133552

Boy M, Bisio V, Zhao LP, et al. Myelodysplastic syndrome associated TET2 mutations affect NK cell function and genome methylation. Nature Communications, 2023; 14(1): 588. https://doi.org/10.1038/s41467-023-36193-w

Brown MS, Goldstein JL. Regulated intramembrane proteolysis: a control mechanism conserved from bacteria to humans. Cell, 2000; 100(4):391–398. https://doi.org/10.1016/S0092-8674(00)80675-3

Brück O, Dufva O, Hohtari H, Blom S, Turkki R, Ilander M, Kovanen PE, Pallaud C, Marques Ramos P, Lähteenmäki H, Välimäki K, El Missiry M, Ribeiro A, Kallioniemi O, Porkka K, Pellinen T, Mustjoki S. Immune profiles in acute myeloid leukemia bone marrow associate with patient age, T-cell receptor clonality, and survival. Blood Advances, 2020; 4(2): 274–286. https://doi.org/10.1182/bloodadvances.2019000792

Böttinger L, Horvath SE, Kleinschroth T, Hunte C, Daum G, Pfanner N, Becker T. Phosphatidylethanolamine and Cardiolipin Differentially Affect the Stability of Mitochondrial Respiratory Chain Supercomplexes. Journal of Molecular Biology, 2012. https://doi.org/10.1016/j.jmb.2012.09.001

Calvi LM; Link DC. The hematopoietic stem cell niche in homeostasis and disease. Blood, 2015; 126(22): 2443–2451. https://doi.org/10.1182/blood-2015-07-533588

Cao G, Zhang H, Huang L, Wang S, Gu R, Deng Q. Menin inhibitors from monotherapies to combination therapies: clinical trial updates from 2024 ASH annual meeting. Journal of Hematology & Oncology, 2025; 18: 82. https://doi.org/10.1186/s13045-025-01718-x

Canton J, Neculai D, Grinstein S. Scavenger receptors in homeostasis and immunity. Nature Reviews Immunology, 2013; 13: 621–634. https://doi.org/10.1038/nri3515

Castellino F; Germain RN. Extensive trafficking of MHC class II–invariant chain complexes in the endocytic pathway and appearance of peptide-loaded class II in multiple compartments. Immunity, 1995; 2(1): 73–88. https://doi.org/10.1016/1074-7613(95)90080-2

Cencini E, Fabbri A, Sicuranza A, Gozzetti A, Bocchia M. The cellular composition and function of the bone marrow niche after allogeneic hematopoietic cell transplantation. International Journal of Hematology, 2022; 115(5): 635–644. https://doi.org/10.1007/s12185-022-03301-4

Chang Z, Zhong C, Xu S, Zhang Y, Guo X, Yu J, Xu Z, Han S, Han B, Lv C, Tian Y. Multi-modal integration of histopathology and transcriptomics reveals STAB1^{+} macrophage-associated efferocytosis as a suppressive immune mechanism in colon adenocarcinoma. Journal of Translational Medicine, 2025. https://doi.org/10.1186/s12967-025-07348-8

Chandra DJ, Alber B, Saultz JN. The Immune Resistance Signature of Acute Myeloid Leukemia and Current Immunotherapy Strategies. Cancers, 2024; 16(15): 2615. https://doi.org/10.3390/cancers16152615

Chao MP, Alizadeh AA, Tang C, Myklebust JH, Varghese B, Gill S, Jan M, Cha AC, Chan CKF, Tan BT, Park CY, Zhao F, Kohrt HEK, Malumbres R, Briones J, Gascoyne RD, Lossos IS, Levy R, Weissman IL, Majeti R. Anti-CD47 antibody synergizes with rituximab to promote phagocytosis and eradicate non-Hodgkin lymphoma. Cell, 142(5), 699–713. https://doi.org/10.1016/j.cell.2010.07.044

Chao MP, Takimoto CH, Feng DD, McKenna K, Gip P. The CD47-SIRPα immune checkpoint. Immunological Reviews, 2020; 295(1): 106–123. https://doi.org/10.1111/imr.12884

Chao MP, Takimoto CH, Feng DD, McKenna K, Gip P, Liu J, Volkmer J-P, Weissman IL, Majeti R. Therapeutic Targeting of the Macrophage Immune Checkpoint CD47 in Myeloid Malignancies. Frontiers in Oncology, 2020; 9: 1380. https://doi.org/10.3389/fonc.2019.01380

Christiansson L, Söderlund S, Svensson E, Mustjoki S, Bengtsson M, Simonsson B, Olsson-Strömberg U, Loskog ASI. Increased Level of Myeloid-Derived Suppressor Cells, Programmed Death Receptor Ligand 1/Programmed Death Receptor 1, and Soluble CD25 in Sokal High Risk Chronic Myeloid Leukemia. PLOS ONE, 2013; 8(1): e55818. https://doi.org/10.1371/journal.pone.0055818

Ciantra Z, Paraskevopoulou V, Aifantis I. The rewired immune microenvironment in leukemia. Nature Immunology, 2025; 26(3): 351–365. https://doi.org/10.1038/s41590-025-02096-9

Cogliati S, Cabrera-Alarcón JL, Enriquez JA. Regulation and functional role of the electron transport chain supercomplexes. Biochemical Society Transactions, 2021; 49(6): 2655–2668. https://doi.org/10.1042/BST20210460

Coll O, Colell A, García-Ruiz C, Kaplowitz N, Fernández-Checa JC. Sensitivity of the 2-oxoglutarate carrier to alcohol intake contributes to mitochondrial glutathione depletion. Journal of Hepatology, 2003; 38: 692–702. https://doi.org/10.1053/jhep.2003.50351

Comazzetto S, Shen B, Morrison SJ. Niches that regulate stem cells and hematopoiesis in adult bone marrow. Developmental Cell, 2021; 56(13): 1848–1860. https://doi.org/10.1016/j.devcel.2021.05.018

Cooper RA; Thomas E; Sozanska AM; Pescia C; Royston DJ. Spatial transcriptomic approaches for characterising the bone marrow landscape: pitfalls and potential. Leukemia, 2025; 39 (2): 291–295. https://doi.org/10.1038/s41375-024-02480-8

Corradi G, Bassani B, Simonetti G, et al. Release of IFNγ by Acute Myeloid Leukemia Cells Remodels Bone Marrow Immune Microenvironment by Inducing Regulatory T Cells. Clinical Cancer Research, 2022; 28 (14): 3141–3155. https://doi.org/10.1158/1078-0432.CCR-21-3594

Crocker, P. R.; Paulson, J. C.; Varki, A, Siglecs and their roles in the immune system. Nature Reviews Immunology 2007; 7 (4). https://doi.org/10.1038/nri2056

Cullen PJ, Steinberg F. To degrade or not to degrade: mechanisms and significance of endocytic recycling. Nature Reviews Molecular Cell Biology, 2018; 19 (11): 679–696. https://doi.org/10.1038/s41580-018-0053-7

Daëron M, Jaeger S, Du Pasquier L, Vivier E. Immunoreceptor tyrosine-based inhibition motifs: a quest in the past and future. Immunological Reviews, 2008; 224: 11-43, 2008; : 1600–065. https://doi.org/10.1111/j.1600-065X.2008.00666.x

Dasdemir E, Veletic I, Ly CP, et al. Integrative spatial multi-omics reveal niche-specific inflammatory signaling and differentiation hierarchies in AML. *iScience*, 2026; 29(1): 114289. https://doi.org/10.1016/j.isci.2025.114289

Daver N; Boddu P; Garcia-Manero G; Yadav SS; Sharma P; Allison J; Kantarjian H. Hypomethylating agents in combination with immune checkpoint inhibitors in acute myeloid leukemia and myelodysplastic syndromes. Leukemia, 2018; 32 (5): 1094–1105. https://doi.org/10.1038/s41375-018-0070-8

Daver, N., Garcia-Manero, G., Basu, S., Boddu, P.C., Alfayez, M., Cortes, J.E., Konopleva, M., Ravandi-Kashani, F., Jabbour, E., Kadia, T., DiNardo, C.D., Pemmaraju, N., Kornblau, S.M., Bose, P., Ohanian, M., Pierce, S., Borthakur, G., Andreeff, M., Kantarjian, H.M. & Ravandi, F. (2019). Efficacy, safety, and biomarkers of response to azacitidine and nivolumab in relapsed/refractory acute myeloid leukemia: a nonrandomized, open-label, phase II study. Cancer Discovery, 9(3), 370–383. https://doi.org/10.1158/2159-8290.CD-18-0774

de Beauchamp L, Himonas E, Helgason GV. Mitochondrial metabolism as a potential therapeutic target in myeloid leukaemia. Leukemia, 2022; 36(1):1–12. https://doi.org/10.1038/s41375-021-01416-w

de Jong MME, Chen L, Raaijmakers MHGP, Cupedo T. Bone marrow inflammation in haematological malignancies. *Nature Reviews Immunology*, 2024; 24(8): 543–558. https://doi.org/10.1038/s41577-024-01003-x

Dembitz, V., Lawson, H., Philippe, C., Burt, R.J., James, S., Magee, A.S.M., et al. Stearoyl-CoA desaturase inhibition is toxic to acute myeloid leukemia displaying high levels of the de novo fatty acid biosynthesis and desaturation. Leukemia, 2024 38, 2395–2409. https://doi.org/10.1038/s41375-024-02390-9

Dembitz V., James, S.C. & Gallipoli, P. Targeting lipid metabolism in acute myeloid leukemia: biological insights and therapeutic opportunities. Leukemia 39, 1814–1823 (2025). https://doi.org/10.1038/s41375-025-02645-z

Docking TR, Parker JDK, Jädersten M, et al. A clinical transcriptome approach to patient stratification and therapy selection in acute myeloid leukemia. Nature Communications, 2021; 12: 2474. https://doi.org/10.1038/s41467-021-22625-y

Dolgalev I, Tikhonova AN. Connecting the dots: resolving the bone marrow niche heterogeneity. Frontiers in Cell and Developmental Biology, 2021;9:622519, 2021; 9 (622519). https://doi.org/10.3389/fcell.2021.622519

Dou A, Fang J. Heterogeneous Myeloid Cells in Tumors. Cancers (Basel), 2021; 13 (15): 3772. https://doi.org/10.3390/cancers13153772

Dufva O, Pölönen P, Brück O, et al. Immunogenomic landscape of hematological malignancies. *Cancer Cell*, 2020; 38: 380–399.e13. https://doi.org/10.1016/j.ccell.2020.06.002

Döhner H; Estey E; Grimwade D; Amadori S; Appelbaum FR; Büchner T; Dombret H; Ebert BL; Fenaux P; Larson RA; Levine RL; Lo-Coco F; Naoe T; Niederwieser D; Ossenkoppele GJ; Sanz

M; Sierra J; Tallman MS; Tien H-F; Wei AH; Löwenberg B. Diagnosis and management of AML in adults: 2017 ELN recommendations from an international expert panel. Blood, 2017; 129 (4): 424–447. https://doi.org/10.1182/blood-2016-08-733196

Döhner H; Wei AH; Appelbaum FR; Craddock C; DiNardo CD; Dombret H; Ebert BL; Fenaux P; Godley LA; Hasserjian RP; Larson RA; Levine RL; Miyazaki Y; Niederwieser D; Ossenkoppele G; Röllig C; Sierra J; Stein EM; Tallman MS; Tien H-F; Wang J; Wierzbowska A; Löwenberg B. Diagnosis and management of AML in adults: 2022 recommendations from an international expert panel on behalf of the ELN. Blood, 2022; 140 (12): 1345–1377. https://doi.org/10.1182/blood.2022016867

Egan, G. & Schimmer, A. D, Contribution of metabolic abnormalities to acute myeloid leukemia pathogenesis. Trends in Cell Biology, 2022; 33, 455-462.https://doi.org/10.1016/j.tcb.2022.11.004

Elorbany S, Berlato C, Carnevalli LS, Maniati E, Barry ST, Wang J, Manchanda R, Kzhyshkowska J, Balkwill F. Immunotherapy that improves response to chemotherapy in high-grade serous ovarian cancer. Nature Communications 15, 10144 (2024). https://doi.org/10.1038/s41467-024-54295-x

Ennis S, Ó Dálaigh M, Verga JU, Ó Broin P, Szegezdi E. Cell-cell interactome of the hematopoietic niche and its changes in acute myeloid leukemia. *iScience*, 2023; 26(6): 106943. https://doi.org/10.1016/j.isci.2023.106943

Farge T, Saland E, de Toni F, et al. Chemotherapy-resistant human acute myeloid leukemia cells are not enriched for leukemic stem cells but require oxidative metabolism. Cancer Discovery, 2017; 7 (7): 716–735. https://doi.org/10.1158/2159-8290.CD-16-0441

Fernández, A.; Llacuna, L.; Fernández-Checa, J. C.; Colell, A. Mitochondrial cholesterol loading exacerbates amyloid beta peptide-induced inflammation and neurotoxicity, Journal of Neuroscience, 2009; 29 (20) 6394-6405. https://doi.org/10.1523/JNEUROSCI.4909-08.2009

Fleming BD, Mosser DM. Regulatory macrophages: setting the threshold for therapy. European Journal of Immunology, 2011; 41(9): 2498–2502. https://doi.org/10.1002/eji.201141717

Forgac M. Vacuolar ATPases: rotary proton pumps in physiology and pathophysiology. Nature Reviews Molecular Cell Biology, 2007; 8 (11): 917–929. https://doi.org/10.1038/nrm2272

Frenz-Wiessner S, Fairley SD, Buser M, et al. Generation of complex bone marrow organoids from human induced pluripotent stem cells. Nature Methods, 2024; 21(5): 868–881. https://doi.org/10.1038/s41592-024-02172-2

Fu H, Xie X, Zhai L, et al. CX43-mediated mitochondrial transfer maintains stemness of KG-1a leukemia stem cells through metabolic remodeling. Stem Cell Research & Therapy, 2024; 15: 460, 2024; : 13287–024. https://doi.org/10.1186/s13287-024-04079-3

Galli S, Zlobec I, Schürch C, Perren A, Ochsenbein AF, Banz Y. CD47 protein expression in acute myeloid leukemia: A tissue microarray-based analysis. Leukemia Research, 2015; 39 (7): 749–756. https://doi.org/10.1016/j.leukres.2015.04.007

García-Ruiz C, Conde de la Rosa L, Ribas V, Fernández-Checa JC. Mitochondrial cholesterol and cancer. Seminars in Cancer Biology, 2021; 73: 76–85. https://doi.org/10.1016/j.semcancer.2020.07.014

Goicoechea L, Conde de la Rosa L, Torres S, García-Ruiz C, Fernández-Checa JC. Mitochondrial cholesterol: Metabolism and impact on redox biology and disease. *Redox Biology*, 2023; 61: 102643. https://doi.org/10.1016/j.redox.2023.102643

Gopaldass N, Chen K-E, Collins B, Mayer A. Assembly and fission of tubular carriers mediating protein sorting in endosomes. Nature Reviews Molecular Cell Biology, 2024; 25: 765–783. https://doi.org/10.1038/s41580-024-00746-8

Gordon S; Martinez FO. Alternative Activation of Macrophages: Mechanism and Functions. Immunity, 2010; 32 (5): 593–604. https://doi.org/10.1016/j.immuni.2010.05.007

Guo R, Lü M, Cao F, et al. Single-cell map of diverse immune phenotypes in the acute myeloid leukemia microenvironment. Biomarker Research, 2021; 9(1):15, 2021; 9 (1): 40364–021. https://doi.org/10.1186/s40364-021-00265-0

Gurung, J.L.; Tamang, R.L.; Madduri, L.; Bennett, R.G.; Harris, E.N.; Denton, P.W.; McVicker, B. Stabilin-1 in Tumor-Associated Macrophages: A Potential Therapeutic Target in Cancer Immunotherapy. Biology 2025, 14, 1198. https://doi.org/10.3390/biology14091198

Haddad, F. & Daver, N. An update on immune based therapies in acute myeloid leukemia: 2021 and beyond! In A. Naing & J. Hajjar (Eds.), Immunotherapy. Advances in Experimental Medicine and Biology, 2021; 1342, 273–295. Springer, Cham. https://doi.org/10.1007/978-3-030-79308-1_9

Harding, C.V. & Geuze, H.J. Class II MHC molecules are present in macrophage lysosomes and phagolysosomes that function in the phagocytic processing of Listeria monocytogenes for presentation to T cells. Journal of Cell Biology, 1992; 119(3), 531–542. https://doi.org/10.1083/jcb.119.3.531

Heckmann BL, Boada-Romero E, Cunha LD, Magne J, Green DR. LC3-associated phagocytosis and inflammation. Journal of Molecular Biology, 2017; 429(23): 3561-3576, 2017; 429(23). https://doi.org/10.1016/j.jmb.2017.08.012

Hellström-Lindberg ES, Kröger N. Clinical decision-making and treatment of myelodysplastic syndromes. Blood, 2023; 142(26): 2268–2281. https://doi.org/10.1182/blood.2023020079

Herber DL, Cao W, Nefedova Y, Novitskiy SV, Nagaraj S, Tyurin VA, Corzo A, Cho HI, Celis E, Lennox B, Knight SC, Padhya T, McCaffrey TV, McCaffrey JC, Antonia S, Fishman M, Ferris RL, Kagan VE, Gabrilovich DI. Lipid accumulation and dendritic cell dysfunction in cancer. Nature Medicine, 2010; 16 (8): 2010; 16 (8). https://doi.org/10.1038/nm.2172

Hopfner KP, Hornung V. Molecular mechanisms and cellular functions of cGAS-STING signalling. Nature Reviews Molecular Cell Biology, 2020; 21(9): 501-521, 2020; 21 (9): 41580–020. https://doi.org/10.1038/s41580-020-0244-x

Hossain F, Al-Khami AA, Wyczechowska D, Hernández C, Zheng L, Reiss K, Del Valle L, Trillo-Tinoco J, Maj T, Zou W, Rodriguez PC, Ochoa AC. Inhibition of Fatty Acid Oxidation Modulates Immunosuppressive Functions of Myeloid-Derived Suppressor Cells and Enhances Cancer Therapies. Cancer Immunology Research, 2015; 3 (11): 1236-1247, 2015; 3 (11): 2326–6066. https://doi.org/10.1158/2326-6066.CIR-15-0036

Hou D, Wang B, You R, et al. Stromal cells promote chemoresistance of acute myeloid leukemia cells via activation of the IL-6/STAT3/OXPHOS axis. Annals of Translational Medicine, 2020; 8 (21): 1346, 2020; 8 (21): 20–3191. https://doi.org/10.21037/atm-20-3191

Hsu C-L; Lin W; Seshasayee D; et al. Equilibrative nucleoside transporter 3 deficiency perturbs lysosome function and macrophage homeostasis. Science, 2012; 335 (6064): 89–92. https://doi.org/10.1126/science.1213682

Huber V, Vallentin B, Di Tacchio M, Hofer TP, Huber HJ, Trattnig S, et al. Spatially resolved single-cell analysis of the bone marrow microenvironment in acute myeloid leukemia. Leukemia, 2023; 37 (8): 1675–1687. https://doi.org/10.1038/s41375-023-01908-3

Huotari J, Helenius A. Endosome maturation. EMBO Journal, 2011; 30 (17): 3481-3500, 2011; 30 (17). https://doi.org/10.1038/emboj.2011.286

Iaea DB, Maxfield FR. Cholesterol trafficking and distribution. Essays in Biochemistry, 2015; 57: 43-55, 2015. https://doi.org/10.1042/bse0570043

Ikonen E. Cellular cholesterol trafficking and compartmentalization. Nature Reviews Molecular Cell Biology, 2008; 9 (2): 125–138. https://doi.org/10.1038/nrm2336

Itzykson R, Solary E. Chronic myelomonocytic leukemia: myelodysplastic or myeloproliferative? Best Practice & Research Clinical Haematology, 2013; 26(4): 387–400. https://doi.org/10.1016/j.beha.2013.09.006

Jacobsen SEW, Nerlov C. Haematopoiesis in the era of advanced single-cell technologies. Nature Cell Biology, 2019; 21(1): 2–8. https://doi.org/10.1038/s41556-018-0227-8

Jädersten M, Saft L, Smith A, et al. TP53 mutations in low-risk myelodysplastic syndromes with del(5q) predict disease progression. Journal of Clinical Oncology, 2011; 29(15): 1971–1979. https://doi.org/10.1200/JCO.2010.31.8576

Karikoski M, Irjala H, Maksimow M, Miiluniemi M, Granfors K, Hernesniemi S, Elima K, Moldenhauer G, Schledzewski K, Kzhyshkowska J, Goerdt S, Salmi M, Jalkanen S. Clever-1/Stabilin-1

regulates lymphocyte migration within lymphatics and leukocyte entrance to sites of inflammation. European Journal of Immunology, 2009; 39 (12): 3477-3487, 2009; 39 (12). https://doi.org/10.1002/eji.200939896

Karthikeyan M, Mickos J, Hollmén M. Clinical optimization of bexmarilimab as a myeloid checkpoint therapy. Immunotherapy, 2026. https://doi.org/10.1080/1750743X.2026.2617035

Khaldoyanidi S, Nagorsen D, Stein A, Ossenkoppele G, Subklewe M. Immune Biology of Acute Myeloid Leukemia: Implications for Immunotherapy. Journal of Clinical Oncology, 2021; 39(5): 419–432. https://doi.org/10.1200/JCO.20.00475

Kaur H, et al. Management of myelodysplastic syndromes in older adults. Blood Reviews, 2021; 45: 100694. https://doi.org/10.1016/j.blre.2020.100694

Kelley SM, Ravichandran KS. Putting the brakes on phagocytosis: don't-eat-me signaling in physiology and disease. EMBO Reports, 2021; 22(6): e52564, 2021; 22 (6): e52564.https://doi.org/10.15252/embr.202152564

Kikushige Y, Shima T, Takayanagi SI, et al. TIM-3 is a promising target to selectively kill acute myeloid leukemia stem cells. Cell Stem Cell, 2010; 7(6): 708–717. https://doi.org/10.1016/j.stem.2010.11.014

Kiyoi H, Issa GC, Altman JK. Menin inhibitors in the treatment of acute myeloid leukemia. Blood, 2025; 145(6): 561–570. https://doi.org/10.1182/blood.2024025335

Kinchen, J.M., Doukoumetzidis, K., Almendinger, J., Stergiou, L., Tosello-Trampont, A., Sifri, C.D., Hengartner, M.O. & Ravichandran, K.S. A pathway for phagosome maturation during engulfment of apoptotic cells. *Nature Cell Biology,* 2008; 10(5), 556–566. https://doi.org/10.1038/ncb1718

Kinchen JM, Ravichandran KS. Phagosome maturation: going through the acid test. Nature Reviews Molecular Cell Biology, 2008; 9(10): 781–795. https://doi.org/10.1038/nrm2515

Kittang AO; Kordasti S; Sand KE; Costantini B; Kramer AM; Perezabellan P; Seidl T; Rye KP; Hagen KM; Kulasekararaj A; Bruserud Ø; Mufti GJ. Expansion of myeloid derived suppressor cells correlates with number of T regulatory cells and disease progression in myelodysplastic syndrome. OncoImmunology, 2016; 5(2): e1062208. https://doi.org/10.1080/2162402X.2015.1062208

Kokkaliaris KD, Scadden DT. Cell interactions in the bone marrow microenvironment affecting myeloid malignancies. Blood Advances, 2020; 4(15): 3795–3803. https://doi.org/10.1182/bloodadvances.2020002127

Koedijk JB, van der Werf I, Calkoen FG, Nierkens S, Kaspers GJL, Zwaan CM, Heidenreich O. Paving the Way for Immunotherapy in Pediatric Acute Myeloid Leukemia: Current Knowledge and the Way Forward. Cancers (Basel), 2021; 13(17): 4364. https://doi.org/10.3390/cancers13174364

Koedijk J, Swierstra J, de Vries IJM, Schreibelt G. Targeting the CD47-SIRPα axis in cancer: advances and challenges. Immunotherapy Advances, 2021; 1 (1): ltab003, 2021; 1(1). https://doi.org/10.1093/immadv/ltab003

Kordasti SY; Ingram W; Hayden J; et al. CD4+CD25high Foxp3+ regulatory T cells in myelodysplastic syndrome (MDS). Blood, 2007; 110(3): 847–850. https://doi.org/10.1182/blood-2007-01-067546

Korbecki J, Bosiacki M, Kupnicka P, et al. CXCR4 as a therapeutic target in acute myeloid leukemia. Leukemia, 2024; 38: 2303–2317. https://doi.org/10.1038/s41375-024-02326-3

Kouroukli O; Symeonidis A; Foukas P; Maragkou M-K; Kourea EP. Bone Marrow Immune Microenvironment in Myelodysplastic Syndromes. Cancers (Basel), 2022; 14(22): 5656. https://doi.org/10.3390/cancers14225656

Krevvata M; Shan X; Zhou C; Dos Santos C; Habineza Ndikuyeze G; Secreto A; Glover J; Trotman W; Brake-Silla G; Nunez-Cruz S; Wertheim G; Ra H-J; Griffiths E; Papachristou C; Danet-Desnoyers G; Carroll M. Cytokines increase engraftment of human acute myeloid leukemia cells in immunocompromised mice but not engraftment of human myelodysplastic syndrome cells. Haematologica, 2018; 103(6): 959–971. https://doi.org/10.3324/haematol.2017.183202

Kwon M, Yeo SC, Lee JS, Park JJ. Not CD68 but stabilin-1 expression is associated with the risk of recurrence in patients with oral cavity squamous cell carcinoma. Head & Neck, 2019; 41(7): 2058–2064. https://doi.org/10.1002/hed.25654

Kzhyshkowska J; Krusell L. Cross-talk between endocytic clearance and secretion in macrophages. Immunobiology, 2009; 214(7): 576–593. https://doi.org/10.1016/j.imbio.2009.03.007

Kzhyshkowska J. Multifunctional receptor stabilin-1 in homeostasis and disease. TheScientific-WorldJournal, 2010; 10.0: 2039–2053. https://doi.org/10.1100/tsw.2010.189

Kzhyshkowska J, Gratchev A, Goerdt S. Stabilin-1, a homeostatic scavenger receptor with multiple functions. Journal of Cellular and Molecular Medicine, 2012; 16 (2): 246-255, 2012; 16(2): 1582–4934. https://doi.org/10.1111/j.1582-4934.2011.01386.x

Kzhyshkowska J, Gratchev A, Goerdt S. Stabilin-1, a homeostatic scavenger receptor with multiple functions. Journal of Cellular and Molecular Medicine, 2005; 10(3): 635-649, 2005; 10(3): 1582–4934. https://doi.org/10.1111/j.1582-4934.2006.tb00432.x

Kzhyshkowska J, Gratchev A, Martens JH, et al. Stabilin-1 localizes to endosomes and the trans-Golgi network in human macrophages and interacts with GGA adaptors. Journal of Leukocyte Biology, 2004; . https://doi.org/10.1189/jlb.0504300

Kzhyshkowska, J., Workman, G., Card--Vila, M., et al. Novel function of alternatively activated macrophages: stabilin-1-mediated clearance of SPARC. Journal of Immunology, 2006; 176(10): 5825-5832, 2006; 176(10). https://doi.org/10.4049/jimmunol.176.10.5825

Lagadinou P, et al. BCL-2 inhibition targets oxidative phosphorylation and selectively eradicates quiescent human leukemia stem cells. Cell Stem Cell, 2013; 12(3): 329–341. https://doi.org/10.1016/j.stem.2012.12.013

Lamble AJ, Kosaka Y, Laderas T, et al. Reversible suppression of T cell function in the bone marrow microenvironment of acute myeloid leukemia. Proceedings of the National Academy of Sciences of the United States of America, 2020; 117 (25): 14331-14341, 2020; 117(25). https://doi.org/10.1073/pnas.1916206117

Lancet JE, Uy GL, Cortes JE, et al. CPX-351 (cytarabine and daunorubicin) Liposome for Injection Versus Conventional Cytarabine Plus Daunorubicin in Older Patients With Newly Diagnosed Secondary Acute Myeloid Leukemia. Journal of Clinical Oncology, 2018; 36(26): 2684-2692, 2018; 36(26): 2017–0603. https://doi.org/10.1200/JCO.2017.77.6112

Langemeyer L, et al. Rab GTPase Function in Endosome and Lysosome Biogenesis. Trends in Cell Biology, 2018; 28(11): 957–970. https://doi.org/10.1016/j.tcb.2018.06.007

Ledderose C, Bromberger S, Slubowski CJ, Sueyoshi K, Junger WG. Frontline Science: P2Y11 receptors support T cell activation by directing mitochondrial trafficking to the immune synapse. Journal of Leukocyte Biology, 2021; 109(3): 497–508. https://doi.org/10.1002/JLB.2HI0520-191R

Lecoultre C, Antoniewicz L, et al. LC3-associated phagocytosis controls STING-dependent innate immune responses. Nature Communications, 2020; 11: 5673, 2020; : 41467–020. https://doi.org/10.1038/s41467-020-19567-1

Li Z, Philip, M. & Ferrell, P.B. (2020). Alterations of T cell mediated immunity in acute myeloid leukemia. Oncogene, 39, 3611–3619. https://doi.org/10.1038/s41388-020-1239-y

Li J, Bolyard C, Xin G, Li Z. Targeting Metabolic Pathways of Myeloid Cells Improves Cancer Immunotherapy. Frontiers in Cell and Developmental Biology, 2021; 9: 747863. https://doi.org/10.3389/fcell.2021.747863

Lind NA, Rael VE, Pestal K, Liu B, Barton GM. Regulation of the nucleic acid-sensing Toll-like receptors. Nature Reviews Immunology, 2022; 22(4): 224-235, 2022; 22(4): 41577–021. https://doi.org/10.1038/s41577-021-00577-0

Liu X, Qu X, Chen Y, Liao L, Cheng K, Shao C, Zenke M, Keating A, Zhao RCH. Mesenchymal stem/stromal cells induce the generation of novel IL-10-dependent regulatory dendritic cells by SOCS3 activation. Journal of Immunology, 2012; 189(3): 1182-1192, 2012; 189(3). https://doi.org/10.4049/jimmunol.1102996

Luciano M, Krenn PW, Horejs-Hoeck J. The cytokine network in acute myeloid leukemia. Frontiers in Immunology, 2022; 13: 1000996. https://doi.org/10.3389/fimmu.2022.1000996

Luzio JP, Pryor PR, Bright NA. Lysosomes: fusion and function. Nature Reviews Molecular Cell Biology, 2007; 8 (8): 622-632, 2007; 8(8). https://doi.org/10.1038/nrm2217

Lévesque J-P, Summers KM, Millard SM, Bisht K, Winkler IG, Pettit AR. Role of macrophages and phagocytes in orchestrating normal and pathologic hematopoietic niches. Experimental Hematology, 2021; 100.0: 12–31.e1. https://doi.org/10.1016/j.exphem.2021.07.001

Lévesque SA, Paré A, Mailhot B, Bellver-Landete V, Kébir H, Lécuyer MA, Alvarez JI, Prat A, de Rivero Vaccari JP, Keane RW, Lacroix S. Myeloid cell transmigration across the CNS vasculature triggers IL-1-driven neuroinflammation during autoimmune encephalomyelitis. Journal of Experimental Medicine, 2021; 218(4): e20201537. https://doi.org/10.1084/jem.20201537

Ly CP, Veletic I, Pacheco CD, et al. Multimodal spatial proteomic profiling in acute myeloid leukemia. npj Precision Oncology, 2025; 9: 148. https://doi.org/10.1038/s41698-025-00897-7

Machado JAL, Steimle V. The MHC class II transactivator CIITA: not (quite) the odd-one-out anymore among NLR proteins. International Journal of Molecular Sciences, 2021; 22(3): 1074. https://doi.org/10.3390/ijms22031074

Majeti R, Chao MP, Alizadeh AA, et al. CD47 is an adverse prognostic factor and therapeutic antibody target on human acute myeloid leukemia stem cells. Cell, 2009; 138(2): 286–299. https://doi.org/10.1016/j.cell.2009.05.045

Malcovati L, Tuechler H, Bowen D, et al. Diagnosis and classification of myelodysplastic syndromes. Blood, 2023; 142(26): 2247–2261. https://doi.org/10.1182/blood.2022015852

Maher SG, Romero-Weaver AL, Scarzello AJ, Gamero AM. Interleukin-10 and TGF-a suppress dendritic cell maturation and function in the tumor microenvironment. Frontiers in Immunology, 2021; 12: 642125, 2021; . https://doi.org/10.3389/fimmu.2021.642125

Mantovani A., Allavena P., Marchesi F. Macrophages as tools and targets in cancer therapy. Nature Reviews Drug Discovery, 2022; 21 (11): 799-820, 2022; https://doi.org/10.1038/s41573-022-00520-5

Maranzana E, Barbero G, Falasca AI, Lenaz G, Genova ML. Mitochondrial respiratory supercomplex association limits production of reactive oxygen species from complex I. Antioxidants & Redox Signaling, 2013; 19(13): 1469–1480. https://doi.org/10.1089/ars.2012.4845

Marí M, Morales A, Colell A, García-Ruiz C, Fernández-Checa JC. Mitochondrial glutathione, a key survival antioxidant. Antioxidants & Redox Signaling, 2009; 11(11): 2685–2700. https://doi.org/10.1089/ARS.2009.2695

Marí M, Caballero F, Colell A, Morales A, Caballeria J, Fernández A, Enrich C, Fernández-Checa JC, García-Ruiz C. Mitochondrial free cholesterol loading sensitizes to TNF- and Fas-mediated steatohepatitis. Cell Metabolism, 2006; 4(3): 185–198. https://doi.org/10.1016/j.cmet.2006.07.006

Marí M, Morales A, Colell A, Garcia-Ruiz C, Fernandez-Checa JC. Mitochondrial cholesterol accumulation in alcoholic liver disease: Role of ASMase and endoplasmic reticulum stress. Redox Biology, 2014; 3: 100-108, 2014; . https://doi.org/10.1016/j.redox.2014.09.005

Marí M, Morales A, Colell A, Garcia-Ruiz C, Kaplowitz N, Ferandez-Checa JC. Mitochondrial glutathione: features, regulation and role in disease. Biochimica et Biophysica Acta, 2013; 1830 (5): 3317-3328, 2013; 1830(5). https://doi.org/10.1016/j.bbagen.2012.10.018

Matozaki T, Murata Y, Okazawa H, Ohnishi H. Functions and molecular mechanisms of the CD47–SIRPα signalling pathway. Trends in Cell Biology, 2009; 19(2): 72–80. https://doi.org/10.1016/j.tcb.2008.12.001

Matlung HL, Szilagyi K, Barclay NA, van den Berg TK. The CD47-SIRPα signaling axis as an innate immune checkpoint in cancer. Immunological Reviews, 2017; 276(1): 145–164. https://doi.org/10.1111/imr.12527

Maynard RS, Hellmich C, Bowles KM, Rushworth SA. Acute Myeloid Leukaemia Drives Metabolic Changes in the Bone Marrow Niche. Frontiers in Oncology, 2022; 12: 924567. https://doi.org/10.3389/fonc.2022.924567

Maxfield FR, McGraw TE. Endocytic recycling. Nature Reviews Molecular Cell Biology, 2004; 5 (2): 121-132, 2004; 5(2). https://doi.org/10.1038/nrm1315

McMahon HT, Boucrot E. Molecular mechanism and physiological functions of clathrin-mediated endocytosis. Nature Reviews Molecular Cell Biology, 2011;12(8):517-533, 2011; 12(8). https://doi.org/10.1038/nrm3151

McNally KE, Cullen PJ. Endosomal Retrieval of Cargo: Retromer Is Not Alone. Trends in Cell Biology, 2018; 28(10): 807–822. https://doi.org/10.1016/j.tcb.2018.06.005

Mei Y, Ren K, Liu Y, Ma A, Xia Z, Han X, Li E, Tariq H, Bao H, Xie X, Zou C, Zhang D, Li Z, Dong L, Verma A, Lu X, Abaza Y, Altman JK, Sukhanova M, Yang J, Ji P. Bone marrow-confined IL-6 signaling mediates the progression of myelodysplastic syndromes to acute myeloid leukemia. Journal of Clinical Investigation, 2022;132(17):e152673, 2022; 132(17): e152673. https://doi.org/10.1172/JCI152673

Meng Y, Heybrock S, Neculai D, Saftig P. Cholesterol Handling in Lysosomes and Beyond. Trends in Cell Biology, 2020; 30(6): 452–466. https://doi.org/10.1016/j.tcb.2020.02.007

Mian, Steven Ngo, Dominique Bonnet. Is the bone marrow microenvironment the hidden catalyst in malignant haematopoiesis? Leukemia, 2025; 39(7): 1589-1592. https://doi.org/10.1038/s41375-025-02630-6

Miller PG, Sperling AS, Brea EJ, et al. Aberrant activation of TCL1A promotes stem cell expansion in clonal haematopoiesis. Nature, 2023; 616(7958): 755–763. https://doi.org/10.1038/s41586-023-05806-1

Mitchell E, Spencer Chapman M, Williams N, et al. Clonal dynamics of haematopoiesis across the human lifespan. Nature, 2022; 606(7913): 343–350. https://doi.org/10.1038/s41586-022-04786-y

Miari KE, Guzman ML, Wheadon H, Williams MTS. Macrophages in Acute Myeloid Leukaemia: Significant Players in Therapy Resistance and Patient Outcomes. Frontiers in Cell and Developmental Biology, 2021; 9.0: 692800. https://doi.org/10.3389/fcell.2021.692800

Mishra SK; Millman SE; Zhang L. Metabolism in acute myeloid leukemia: mechanistic insights and therapeutic targets. Blood, 2023; 141(10): 1119–1135. https://doi.org/10.1182/blood.2022018092

Mosser, D. M., & Edwards, J. P Exploring the full spectrum of macrophage activation. Nat Rev Immunol 8, 958–969 (2008). https://doi.org/10.1038/nri2448

Moschoi R, Imbert V, Nebout M, et al. Protective mitochondrial transfer from bone marrow stromal cells to acute myeloid leukemic cells during chemotherapy. Blood, 2016; 128(2): 253–264. https://doi.org/10.1182/blood-2015-07-655860

Mózes FE, Tzika E, Holyoake TL, et al. Myelodysplastic Syndromes and Metabolism. Cancers, 2021; 13(19): 4989. https://doi.org/10.3390/cancers13194989

Mussai F; De Santo C; Abu-Dayyeh I; et al. Acute myeloid leukemia creates an arginase-dependent immunosuppressive microenvironment. Blood, 2013; 122(5): 749–758. https://doi.org/10.1182/blood-2013-01-480129

Méndez-Ferrer S, Bonnet D, Steensma DP, Hasserjian RP, Ghobrial IM, Gribben JG, Andreeff M, Krause DS. Bone marrow niches in haematological malignancies. Nature Reviews Cancer, 2020; 20(5): 285-298, 2020; 20(5): 41568–020. https://doi.org/10.1038/s41568-020-0245-2

Mulherkar N, Scadden DT. What is the role of the bone marrow microenvironment in AML? Best Practice & Research Clinical Haematology, 2021; 34(4): 101328. https://doi.org/10.1016/j.beha.2021.101328

Muntjewerff EM, Meesters LD, van den Bogaart G. Antigen Cross-Presentation by Macrophages. Frontiers in Immunology, 2020; 11: 1276. https://doi.org/10.3389/fimmu.2020.01276

Nabrega-Pereira S, Caiado F, Carvalho T, et al. VEGFR2-Mediated Reprogramming of Mitochondrial Metabolism Regulates the Sensitivity of Acute Myeloid Leukemia to Chemotherapy. Cancer Research, 2018;78(3):731-741, 2018; 78(3): 0008–5472. https://doi.org/10.1158/0008-5472.CAN-17-1166

Navada SC, Silverman LR. The safety and efficacy of rigosertib in the treatment of myelodysplastic syndromes. Expert Review of Anticancer Therapy, 2016; 16(8): 805–810. https://doi.org/10.1080/14737140.2016.1209413

Neefjes J, Jongsma MLM, Paul P, Bakke O. Towards a systems understanding of MHC class I and MHC class II antigen presentation. Nature Reviews Immunology, 2011; 11(12): 823–836. https://doi.org/10.1038/nri3084

Nelde A, Schuster H, Heitmann JS, et al. Immune surveillance of acute myeloid leukemia is mediated by HLA-presented antigens on leukemia progenitor cells. Blood Cancer Discovery, 2023; 4(6): 468–489. https://doi.org/10.1158/2643-3230.BCD-23-0020

Newell LF, Cook RJ. Acute myeloid leukaemia. Lancet, 2023; 401(10370): 151–166. https://doi.org/10.1016/S0140-6736(23)00108-3

Nimmerjahn, F.; Ravetch, J. V. Fcγ receptors as regulators of immune responses, 2008; 8(1). https://doi.org/10.1038/nri2206

Noviello M, Manfredi F, Ruggiero E, Perini T, Oliveira G, Cortesi F, et al. Bone marrow central memory and memory stem T-cell exhaustion in AML patients relapsing after HSCT. Nature Communications, 2019; 10.0: 1065. https://doi.org/10.1038/s41467-019-08871-1

Nwosu GO, Ross DM, Powell JA, Pitson SM. Venetoclax therapy and emerging resistance mechanisms in acute myeloid leukaemia. Cell Death & Disease, 2024; 15: 413. https://doi.org/10.1038/s41419-024-06810-7

Ogawa S. Genetics of MDS. Blood, 2019; 133(10): 1049–1059. https://doi.org/10.1182/blood-2018-10-844621

Orkin SH, Zon LI. Hematopoiesis: an evolving paradigm for stem cell biology. Cell, 2008; 132(4): 631–644. https://doi.org/10.1016/j.cell.2008.01.025

Owen DJ, Collins BM, Evans PR. Adaptors for clathrin coats: structure and function. Annual Review of Cell and Developmental Biology, 2004;20:153-191, 2004; 20(153). https://doi.org/10.1146/annurev.cellbio.20.010403.104543

Palani, S., Elima, K., Ekholm, E., Jalkanen, S. & Salmi, M. (2016). Monocyte stabilin-1 suppresses the activation of Th1 lymphocytes. The Journal of Immunology, 196(1), 115–123. https://doi.org/10.4049/jimmunol.1500257

Panuzzo C, Jovanovski A, Pergolizzi B, et al. Mitochondria: A Galaxy in the Hematopoietic and Leukemic Stem Cell Universe. International Journal of Molecular Sciences, 2020; 21(11): 3928, 2020; 21(11). https://doi.org/10.3390/ijms21113928

Paradies G, Paradies V, Ruggiero FM, Petrosillo G. Oxidative stress, cardiolipin and mitochondrial dysfunction in nonalcoholic fatty liver disease. World Journal of Gastroenterology, 2014; 20(39): 14205–14218. https://doi.org/10.3748/wjg.v20.i39.14205

Park, S.-Y.; Jung, M.-Y.; Lee, S.-J.; Kang, K.-B.; Gratchev, A.; Riabov, V.; Kzhyshkowska, J.; Kim, I.-S. Stabilin-1 mediates phosphatidylserine-dependent clearance of cell corpses in alternatively activated macrophages. Journal of Cell Science, 2009; 122 (18): 3365-3373, 2009; 122(18). https://doi.org/10.1242/jcs.049569

Patnaik MM, Tefferi A. Chronic myelomonocytic leukemia: 2018 update on diagnosis, risk stratification and management. American Journal of Hematology, 2018; 93(6): 824–840. https://doi.org/10.1002/ajh.25104

Patnaik MM, Tefferi A. Chronic myelomonocytic leukemia: molecular pathogenesis and therapeutic innovations. Haematologica, 2025; 110(1). https://doi.org/10.3324/haematol.2024.286061

Pei S, Pollyea DA, Gustafson A, et al. Monocytic Subclones Confer Resistance to Venetoclax-Based Therapy in Patients with Acute Myeloid Leukemia. Cancer Discovery, 2020;10(4):536-551, 2020; 10(4): 2159–8290. https://doi.org/10.1158/2159-8290.CD-19-0710

Pellin D, Loperfido M, Baricordi C, Wolock SL, Montepeloso A, Weinberg OK, et al; Biasco L. A comprehensive single cell transcriptional landscape of human hematopoietic progenitors. Nature Communications, 2019; 10.0: 2395. https://doi.org/10.1038/s41467-019-10291-0

Perzolli A, Koedijk JB, Zwaan CM, Heidenreich O. Targeting the innate immune system in pediatric and adult AML. *Leukemia*, 2024; 38(6): 1191–1201. https://doi.org/10.1038/s41375-024-02217-7

Pinho, S., & Frenette, P. S. Haematopoietic stem cell activity and interactions with the niche, Nat Rev Mol Cell Biol, 2019; 20(5): 41580–019. https://doi.org/10.1038/s41580-019-0103-9

Politz, O., Gratchev, A., McCourt, P. A. G., Schledzewski, K., Guillot, P., Johansson, S., et al. Stabilin-1 and −2 constitute a novel family of fasciclin-like hyaluronan receptor homologues. Biochem J 2002; 362 (1): 155–164 https://doi.org/10.1042/0264-6021:3620155

Pollyea DA, Stevens BM, Jones CL, et al. Venetoclax with azacitidine disrupts energy metabolism and targets leukemia stem cells in patients with acute myeloid leukemia. *Nature Medicine*, 2018; 24(12): 1859–1866. https://doi.org/10.1038/s41591-018-0233-1

Poscablo DM, Worthington AK, Smith-Berdan S, et al. An age-progressive platelet differentiation path from hematopoietic stem cells causes exacerbated thrombosis. *Cell*, 2024; 187(12): 3090–3107.e21. https://doi.org/10.1016/j.cell.2024.04.018

Prevo, R., Banerji, S., Ni, J., & Jackson, D. G. Rapid plasma membrane-endosomal trafficking of the lymph node sinus and high endothelial venule scavenger receptor/homing receptor stabilin-1 (FEEL-1/CLEVER-1), 2004; 279(50). https://doi.org/10.1074/jbc.M406897200

Prince S; Viitala M; Sjöroos R; et al. Secreted Clever-1 modulates T cell responses and impacts cancer immunotherapy efficacy. Theranostics, 2025; 15(15): 7501–7527. https://doi.org/10.7150/thno.110544

Pyzer AR; Stroopinsky D; Rajabi H; et al. MUC1-mediated induction of myeloid-derived suppressor cells in patients with acute myeloid leukemia. Blood, 2017; 129(13): 1791–1801. https://doi.org/10.1182/blood-2016-07-730614

Rantakari, P.; Patten, D. A.; Valtonen, J.; Karikoski, M.; Gerke, H.; Dawes, H.; Laurila, J.; Ohlmeier, S.; Elima, K.; Hübscher, S. G.; Weston, C, Stabilin-1 expression defines a subset of macrophages that mediate tissue homeostasis and prevent fibrosis in chronic liver injury, Proc. Natl. Acad. Sci. U.S.A. 2016; 113 (33) 9298-9303 https://doi.org/10.1073/pnas.1604780113

Ramachandra, L., Song, R. & Harding, C.V. Phagosomes are fully competent antigen-processing organelles that mediate the formation of peptide:class II MHC complexes. (1999). The Journal of Immunology, 162(6), 3263–3272. https://doi.org/10.4049/jimmunol.162.6.3263

Rath JA, Bajwa G, Carreres B, et al. Single-cell transcriptomics identifies multiple pathways underlying antitumor function of TCR- and CD8αβ-engineered human $CD4^+$ T cells. Science Advances, 2020; 6(27): eaaz7809. https://doi.org/10.1126/sciadv.aaz7809

Rattigan KM, Brabcova Z, Sarnello D, et al. Pyruvate anaplerosis is a targetable vulnerability in persistent leukaemic stem cells. Nature Communications, 2023; 14 (1): 4634, 2023; 14(1): 41467–023. https://doi.org/10.1038/s41467-023-40222-z

Rattigan YI, Patel BB, Helgeson BE, et al. Targeting chemoresistance and mitochondria-dependent metabolic reprogramming in acute myeloid leukemia. *Cancer Drug Resistance*, 2023; 6: 760–780. https://doi.org/10.20517/cdr.2023.18

Raud B, Roy DG, Divakaruni AS, et al. Etomoxir Actions on Regulatory and Memory T Cells Are Independent of Cpt1a-Mediated Fatty Acid Oxidation. Cell Metabolism, 2018;28(3):504-515.e7, 2018; 28(3). https://doi.org/10.1016/j.cmet.2018.06.002

Ravetch JV; Lanier LL. Immune inhibitory receptors. Science, 2000; 290(5489): 84–89. https://doi.org/10.1126/science.290.5489.84

Ribas, V., García-Ruiz, C. and Fernández-Checa, J.C. (2016), Mitochondria, cholesterol and cancer cell metabolism. Clin Trans Med, 5: e22. https://doi.org/10.1186/s40169-016-0106-5

Roche P.A., Furuta K. The ins and outs of MHC class II-mediated antigen processing and presentation. Nature Reviews Immunology, 2015; 15(4): 203–216. https://doi.org/10.1038/nri3818

Roche, P.A., Teletski, C.L., Stang, E., Bakke, O. & Long, E.O. Cell surface HLA-DR–invariant chain complexes are targeted to endosomes by rapid internalization. Proceedings of the National Academy of Sciences of the United States of America, 1993; 90(18), 8581–8585. https://doi.org/10.1073/pnas.90.18.8581

Rodriguez-Sevilla JJ, Ganan-Gomez I, Kumar B, et al. Natural killer cells' functional impairment drives the immune escape of pre-malignant clones in early-stage myelodysplastic syndromes. *Nature Communications*, 2025; 16: 3450. https://doi.org/10.1038/s41467-025-58662-0

Saito K, Zhang Q, Yang H, et al. Exogenous mitochondrial transfer and endogenous mitochondrial fission facilitate AML resistance to OxPhos inhibition. Blood Advances, 2021; 5(20): 4233–4255. https://doi.org/10.1182/bloodadvances.2020003661

Sallman DA; McLemore AF; Aldrich AL; et al. TP53 mutations in myelodysplastic syndromes and secondary AML confer an immunosuppressive phenotype. Blood, 2020; 136(24): 2812–2823. https://doi.org/10.1182/blood.2020006158

Salmi M; Koskinen K; Henttinen T; Elima K; Jalkanen S. CLEVER-1 mediates lymphocyte transmigration through vascular and lymphatic endothelium. Blood, 2004; 104(13): 3849–3857. https://doi.org/10.1182/blood-2004-01-0222

Schoufour TAW, Voogd L, Franken KLMC, Ottenhoff THM, Wijdeven RHM, Joosten SA. Conformation of HLA-E/peptide complex guides interaction with two novel HLA-E receptors: Stabilin 1 and 2. PLOS ONE, 2025; 20(10): e0334543 https://doi.org/10.1371/journal.pone.0334543

Schmalbrock LK, Dolnik A, Cocciardi S, et al. Clonal evolution of acute myeloid leukemia with FLT3-ITD mutation under treatment with midostaurin and intensive chemotherapy. Blood, 2021; 137(22): 3093–3104. https://doi.org/10.1182/blood.2020007626

Schuurhuis GJ, Heuser M, Freeman S, et al. Minimal/measurable residual disease in AML: a consensus document from the European LeukemiaNet MRD Working Party. *Blood*, 2018; 131(12): 1275–1291. https://doi.org/10.1182/blood-2017-09-801498

Siebeler, R.; de Winther, M. P. J.; Hoeksema, M. A. The regulatory landscape of macrophage interferon signaling in inflammation. Journal of Allergy and Clinical Immunology. 2023;152(1):20–32. https://doi.org/10.1016/j.jaci.2023.04.022.

Serrano-Lopez J, Hegde S, Kumar S, Serrano J, Fang J, Wellendorf AM, Roche PA, Rangel Y, Carrington LJ, Geiger H, Grimes HL, Luther S, Maillard I, Sanchez-Garcia J, Starczynowski DT, Cancelas JA. Inflammation rapidly recruits mammalian GMP and MDP from bone marrow into regional lymphatics. eLife, 2021;10:e66190, 2021; : e66190. https://doi.org/10.7554/eLife.66190

Settembre C, Fraldi A, Medina DL, Ballabio A. Signals from the lysosome: a control centre for cellular clearance and energy metabolism. *Nature Reviews Molecular Cell Biology*, 2013; 14(5): 283–296. https://doi.org/10.1038/nrm3565

Shafat MS, Gnaneswaran B, Bowles KM, Rushworth SA. The bone marrow microenvironment – Home of the leukemic blasts. *Blood Reviews*, 2017; 31(5): 277–286. https://doi.org/10.1016/j.blre.2017.03.004

Shlush LI, Mitchell A, Heisler L, et al. Tracing the origins of relapse in acute myeloid leukaemia to stem cells. *Nature*, 2017; 547(7661): 104–108. https://doi.org/10.1038/nature22993

Shetty S, Weston CJ, Oo YH, Westerlund N, Stamataki Z, Youster J, Hubscher SG, Salmi M, Jalkanen S, Lalor PF, Adams DH. Common Lymphatic Endothelial and Vascular Endothelial Receptor-1 Mediates the Transmigration of Regulatory T Cells across Human Hepatic Sinusoidal Endothelium. The Journal of Immunology, 2011; 186(7): 4147-4155, 2011; 186(7). https://doi.org/10.4049/jimmunol.1002961

Shukron O, Vainstein V, Kündgen A, Germing U, Agur Z. Analyzing transformation of myelodysplastic syndrome to secondary acute myeloid leukemia using a large patient database. American Journal of Hematology, 2012;87(9):853-860, 2012; 87(9). https://doi.org/10.1002/ajh.23257

Solsona-Vilarrasa E, Fucho R, Torres S, Núñez S, Nuüo-Lombarri N, Enrich C, Garcia-Ruiz C, Fernandez-Checa JC. Cholesterol enrichment in liver mitochondria impairs oxidative phosphorylation and disrupts the assembly of respiratory supercomplexes. Redox Biology, 2019; 24: 101214, 2019; 101214(PubMed). https://doi.org/10.1016/j.redox.2019.101214

Smith CC, Levis MJ, Perl AE, et al. Molecular profile of FLT3-mutated relapsed/refractory patients with AML in the phase 3 ADMIRAL study of gilteritinib. *Blood Advances*, 2022; 6(7): 2144–2155. https://doi.org/10.1182/bloodadvances.2021006489

Sperling AS, Gibson CJ, Ebert BL. The genetics of myelodysplastic syndrome: from clonal haematopoiesis to secondary acute myeloid leukaemia. *Nature Reviews Cancer*, 2017; 17(1): 5–19. https://doi.org/10.1038/nrc.2016.112

Steensma DP, Bejar R, Jaiswal S, Lindsley RC, Sekeres MA, Hasserjian RP, Ebert BL. Clonal hematopoiesis of indeterminate potential and its distinction from myelodysplastic syndromes. *Blood*, 2015; 126(1): 9–16. https://doi.org/10.1182/blood-2015-03-631747

Sternadt D, Pereira-Martins DA, Chatzikyriakou P, et al. Metformin induces ferroptosis associated with lipidomic remodeling in AML. *Blood Advances*, 2026. https://doi.org/10.1182/bloodadvances.2025016155

Straube J, Janardhanan Y, Haldar R, Bywater MJ. Immune control in acute myeloid leukemia. *Experimental Hematology*, 2024; 138: 104256. https://doi.org/10.1016/j.exphem.2024.104256

Sun Z, Zhang L, Liu L. Reprogramming the lipid metabolism of dendritic cells in tumor immunomodulation and immunotherapy. Biomedicine & Pharmacotherapy, 2023; 167: 115574, 2023; . https://doi.org/10.1016/j.biopha.2023.115574

Swatler J; Turos-Korgul L; Kozlowska E; Piwocka K. Immunosuppressive Cell Subsets and Factors in Myeloid Leukemias. Cancers (Basel), 2021; 13(6): 1203. https://doi.org/10.3390/cancers13061203

Symeonidi A, Harris WJ, Taoudi S. Aging and clonal behavior of hematopoietic stem cells. *International Journal of Molecular Sciences*, 2022; 23(4): 1948. https://doi.org/10.3390/ijms23041948

Tabe Y, Konopleva M, Andreeff M. Fatty Acid Metabolism, Bone Marrow Adipocytes, and AML. Frontiers in Oncology, 2020;10:155, 2020; 77(6): 0008–5472. https://doi.org/10.3389/fonc.2020.00155

Tadayon S, Dunkel J, Takeda A, Eichin D, Virtakoivu R, Elima K, Jalkanen S, Hollmén M. Lymphatic Endothelial Cell Activation and Dendritic Cell Transmigration Is Modified by Genetic Deletion of Clever-1. Frontiers in Immunology, 2021; 12: 602122, 2021;https://doi.org/10.3389/fimmu.2021.602122

Tan J, Yu Z, Huang J, et al. Increased PD-1+Tim-3+ exhausted T cells in bone marrow may influence the clinical outcome of patients with AML. Biomarker Research, 2020;8:6, 2020; 16(3): 40364–020. https://doi.org/10.1186/s40364-020-0185-8

Tatsuta T, Scharwey M, Langer T. Mitochondrial lipid trafficking. Trends in Cell Biology, 2014; 24 (1): 44-52, 2014; 24(1). https://doi.org/10.1016/j.tcb.2013.07.011

Tervahartiala M, Taimen P, Mirtti T, Koskinen I, Ecke T, Jalkanen S, Boström PJ. Immunological tumor status may predict response to neoadjuvant chemotherapy and outcome after radical cystectomy in bladder cancer. Scientific Reports, 2017; 7(1): 12682. https://doi.org/10.1038/s41598-017-12892-5

Tettamanti S, Pievani A, Biondi A, Dotti G, Serafini M. Catch me if you can: how AML and its niche escape immunotherapy. *Leukemia*, 2022; 36: 13–22. https://doi.org/10.1038/s41375-021-01350-x

Toffalori C, Zito L, Gambacorta V, et al. Immune signature drives leukemia escape and relapse after hematopoietic cell transplantation. Nature Medicine, 2019; 25: 603–611. https://doi.org/10.1038/s41591-019-0400-z

Timperi E, Gueguen P, Molgora M, et al. Lipid-associated macrophages are induced by cancer-associated fibroblasts and mediate immune suppression in breast cancer. Cancer Research, 2022; 82(18): 3291–3306. https://doi.org/10.1158/0008-5472.CAN-22-1427

Torres S, Matías N, Baulies A, Nuñez S, Alarcon-Vila C, Martinez L, et al. Mitochondrial GSH replenishment as a potential therapeutic approach for Niemann Pick type C disease. Redox Biology, 2017; 11.0: 60–72. https://doi.org/10.1016/j.redox.2016.11.010

Townsend A, Öhlén C, Bastin J, Ljunggren H-G, Foster L, Kärre K. Association of class I major histocompatibility heavy and light chains induced by viral peptides. Nature, 1989; 340(6233): 443–448. https://doi.org/10.1038/340443a0

Tremblay D, Rippel N, Feld J, El Jamal SM, Mascarenhas J. Contemporary Risk Stratification and Treatment of Chronic Myelomonocytic Leukemia. *The Oncologist*, 2021; 26(5): 406–421. https://doi.org/10.1002/onco.13769

Trinh MN, Brown MS, Seemann J, Vale G, McDonald JG, Goldstein JL, Lu F. Interplay between Asters/GRAMD1s and phosphatidylserine in intermembrane transport of LDL cholesterol.

Proceedings of the National Academy of Sciences of the United States of America, 2022; 119 (2): e2120411119, 2022; 119(2): e2120411119. https://doi.org/10.1073/pnas.2120411119

Triana S, Vonficht D, Jopp-Saile L, et al. Single-cell proteo-genomic reference maps of the hematopoietic system enable the purification and massive profiling of precisely defined cell states. *Nature Immunology*, 2021; 22(12): 1577–1589. https://doi.org/10.1038/s41590-021-01059-0

Trombetta ES, Mellman I. Cell biology of antigen processing in vitro and in vivo. Annual Review of Immunology, 2005; 23: 975-1028, 2005; . https://doi.org/10.1146/annurev.immunol.22.012703.104538

Tu Y, Seaman MNJ. Navigating the Controversies of Retromer-Mediated Endosomal Protein Sorting. Frontiers in Cell and Developmental Biology, 2021; 9:658741, 2021; 9(658741). https://doi.org/10.3389/fcell.2021.658741

Ugolini A, Tyurin VA, Tyurina YY, et al. Polymorphonuclear myeloid-derived suppressor cells limit antigen cross-presentation by dendritic cells in cancer. *JCI Insight*, 2020; 5(15): e138581. https://doi.org/10.1172/jci.insight.138581

Unger S, Nuñez N, Becher B, Kreutmair S. Next-generation immune profiling – beyond blood cancer cells. Trends in Molecular Medicine, 2025; 31(12): 1140–1153. https://doi.org/10.1016/j.molmed.2025.06.004

Vadakekolathu J, Rutella S. Immune dysregulation in myelodysplastic syndromes and acute myeloid leukemia. Frontiers in Immunology, 2024; 15: 1324567, 2024; . https://doi.org/10.3389/fimmu.2024.1324567

Vadakekolathu J, Rutella S. Escape from T-cell–targeting immunotherapies in acute myeloid leukemia. Blood, 2024; 143(26): 2689–2700. https://doi.org/10.1182/blood.2023019961

Vago L, Gojo I. Immune escape and immunotherapy of acute myeloid leukemia. Journal of Clinical Investigation, 2020; 130(4): 1552-1564, 2020; 130(4). https://doi.org/10.1172/JCI129204

Veillette A, Chen J. SIRPα-CD47 Immune Checkpoint Blockade in Anticancer Therapy. *Trends in Immunology*, 2018; 39(3): 173–184. https://doi.org/10.1016/j.it.2017.12.005

Vasanthakumar T, Rubinstein JL. Structure and Roles of V-type ATPases. Trends in Biochemical Sciences, 2020; 45 (4): 295-307, 2020; 45(4). https://doi.org/10.1016/j.tibs.2019.12.007

Vegivinti CTR, Keesari PR, Veeraballi S, et al. Role of innate immunological/inflammatory pathways in myelodysplastic syndromes and AML: a narrative review. Experimental Hematology & Oncology, 2023; 12 (1): 60, 2023; 12(1): 40164–023. https://doi.org/10.1186/s40164-023-00422-1

Veglia F, Sanseviero E, Gabrilovich DI. Myeloid-derived suppressor cells in the era of increasing myeloid cell diversity. Nature Reviews Immunology, 2021; 21 (8): 485-498, 2021; 21(8): 41577–020.https://doi.org/10.1038/s41577-020-00490-y

Verovskaya E, Dellorusso PV, Passegué E. Aging of hematopoietic stem cells: DNA damage and mutations? Cell Stem Cell, 2019; 25(2): 185–197. https://doi.org/10.1016/j.stem.2019.06.005

Viitala M, Virtakoivu R, Tadayon S, Rannikko J, Jalkanen S, Hollmén M. Immunotherapeutic Blockade of Macrophage Clever-1 Reactivates the CD8+ T-cell Response against Immunosuppressive Tumors. Clinical Cancer Research, 2019;25(11):3289-3303, 2019; 25(11): 3289–3303. https://doi.org/10.1158/1078-0432.CCR-18-3016

Virtakoivu R, Rannikko JH, Viitala M, et al. Systemic blockade of Clever-1 elicits lymphocyte activation alongside checkpoint molecule downregulation in patients with solid tumors: results from a phase I/II clinical trial. Clinical Cancer Research, 2021; 27(15): 4205–4220. https://doi.org/10.1158/1078-0432.CCR-20-4862

Wang X, Li J, Dong K, et al. Interleukin-10 inhibits the differentiation and function of human dendritic cells by suppressing antigen presentation and T-cell activation. Cellular Immunology, 2013; 281(2): 92-100, 2013; 281(2): 92–100. https://doi.org/10.1016/j.cellimm.2013.01.004

Wang B, Huang H, Yang M, Yang W, Liu Z, Hou W, Zeng H, He Z, Lin T, Huang J. Microlocalization and clinical significance of stabilin-1+ macrophages in treatment-naïve patients with urothelial carcinoma of the bladder. World Journal of Urology, 2020; 38(3): 709-716, 2020; 38(3): 709–716. https://doi.org/10.1007/s00345-019-02853-0

Watson CJ, Papula AL, Poon GYP, et al. The longitudinal dynamics and natural history of clonal haematopoiesis. *Nature*, 2022; 606(7913): 335–342. https://doi.org/10.1038/s41586-022-04785-z

Weinhäuser I, Pereira-Martins DA, Almeida LY, et al. M2 macrophages drive leukemic transformation by imposing resistance to phagocytosis and improving mitochondrial metabolism. Science Advances, 2023; 9(15): eadf8522. https://doi.org/10.1126/sciadv.adf8522

Weeks LD, Marinac CR, Redd R, et al. Age-related diseases of inflammation in myelodysplastic syndrome and chronic myelomonocytic leukemia. *Blood*, 2022; 139(8): 1246–1250. https://doi.org/10.1182/blood.2021014418

Xu Z-J, Gu Y, Wang C-Z, et al. The M2 macrophage marker CD206: a novel prognostic indicator for acute myeloid leukemia. OncoImmunology, 2020; 9(1): 1683347. https://doi.org/10.1080/2162402X.2019.1683347

Yan D, Adeshakin AO, Xu M, et al. Lipid Metabolic Pathways Confer the Immunosuppressive Function of Myeloid-Derived Suppressor Cells in Tumor. Frontiers in Immunology, 2019;10:1399, 2019; 10(1399). https://doi.org/10.3389/fimmu.2019.01399

Ye H, Adane B, Khan N, et al. Leukemic Stem Cells Evade Chemotherapy by Metabolic Adaptation to an Adipose Tissue Niche. Cell Stem Cell, 2016;19(1):23-37, 2016; 19(1). https://doi.org/10.1016/j.stem.2016.06.001

Yin J, Luo J, Wang L, Liu L, Liu L. STAB1 Promotes Acute Myeloid Leukemia Progression by Activating the IKK/NF-κB Pathway and Increasing M2 Macrophage Polarization. Cancer Science, 2025; 116(6): 1508–1521. https://doi.org/10.1111/cas.70044

Yin S-P, Gao Y, Xie X-S, Xu D-D, Riabov V, Du W-D. Accumulation of stabilin-1 positive macrophages in the early stage of gastric cancer is associated with short cumulative survival. Oncology Letters, 2020; 19(3): 2404–2412. https://doi.org/10.3892/ol.2020.11310

Yue X, Kong Y, Zhang Y, et al. SREBF2-STARD4 axis confers sorafenib resistance in hepatocellular carcinoma by regulating mitochondrial cholesterol homeostasis. Cancer Science, 2023; 114 (2): 477-489, 2023; 114(2). https://doi.org/10.1111/cas.15449

Zalmaï L, Viailly P-J, Biichlé S, et al. Plasmacytoid dendritic cells proliferation associated with acute myeloid leukemia: phenotype profile and mutation landscape. Haematologica, 2021; . https://doi.org/10.3324/haematol.2020.276410

Zeng AGX, Iacobucci I, Shah S, et al. Single-cell Transcriptional Atlas of Human Hematopoiesis Reveals Genetic and Hierarchy-Based Determinants of Aberrant AML Differentiation. Blood Cancer Discovery, 2025; 6(4): 307–324. https://doi.org/10.1158/2643-3230.BCD-24-0342

Zhang H-B, Sun Z-K, Zhong F-M, Yao F-Y, Liu J, Zhang J, Zhang N, Lin J, Li S-Q, Li M-Y, Jiang J-Y, Cheng Y, Xu S, Cheng X-X, Huang B, Wang X-Z. A novel fatty acid metabolism-related signature identifies features of the tumor microenvironment and predicts clinical outcome in acute myeloid leukemia. Lipids in Health and Disease, 2022; 21(1):79, 2022; 21(1): 12944–022. https://doi.org/10.1186/s12944-022-01687-x

Zhang, J., Gratchev, A., Riabov, V., Mamidi, S., Schmuttermaier, C., Krusell, L., Kremmer, E., Workman, G., Sage, E. H., Jalkanen, S., Goerdt, S., & Kzhyshkowska, J. A novel GGA-binding site is required for intracellular sorting mediated by stabilin-1, 2009; 29(22): 00505–09. https://doi.org/10.1128/MCB.00505-09

Ålgars A, Irjala H, Vaittinen S, Huhtinen H, Sundström J, Salmi M, Ristamäki R, Jalkanen S. Type and location of tumor-infiltrating macrophages and lymphatic vessels predict survival of colorectal cancer patients. International Journal of Cancer, 2012; 131(4): 864–873. https://doi.org/10.1002/ijc.26457

TURUN
YLIOPISTO
UNIVERSITY
OF TURKU

Painosalama, Turku, Finland 2026

ISBN 978-952-02-0703-8 (PRINT)
ISBN 978-952-02-0704-5 (PDF)
ISSN 0355-9483 (Print)
ISSN 2343-3213 (Online)